1991

Synthesis and characterization of reduced tungsten sulfide cluster complexes

Xiang Zhang
Iowa State University

Order Number 9202412

Synthesis and characterization of reduced tungsten sulfide cluster complexes

Zhang, Xiang, Ph.D.

Iowa State University, 1991

U·M·I
300 N. Zeeb Rd.
Ann Arbor, MI 48106

Synthesis and characterization of reduced tungsten sulfide cluster complexes

by

Xiang Zhang

A Dissertation Submitted to the
Graduate Faculty in Partial Fulfillment of the
Requirements for the Degree of
DOCTOR OF PHILOSOPHY

Department: Chemistry
Major: Inorganic Chemistry

Approved:

Signature was redacted for privacy.

In Charge of Major Work

Signature was redacted for privacy.

For the Major Department

Signature was redacted for privacy.

For the Graduate College

Iowa State University
Ames, Iowa
1991

TABLE OF CONTENTS

LIST OF TABLES

LIST OF FIGURES

GENERAL INTRODUCTION

Statement of the Problem

The chemstry of hexanuclear metal clusters has been extensively studied for both molybdenum and tungsten. The existence of these clusters in both molybdenum(II) and tungsten(II) halides and their derivatives has been well established [1,2]. The hexanuclear molybdenum clusters are also known to exist in the ternary and binary molybdenum chalcogenides, $M_xMo_6Y_8$ and Mo_6Y_8 (M = ternary metal cation; Y = chalcogenide), which are also known as Chevrel phases [3,4]. Many Chevrel phase compounds have been found to have superconductivity [5], catalytic activity [6] and ionic conductivity [7].

The rich chemistry of the Chevrel phases raises considerable interest in finding the tungsten analogues of these phases. However, no such analogue has ever been synthesized, although the Chevrel phases are usually prepared directly from elements at high temperatures over 1000°C. The absence of the tungsten analogues may be caused by their thermodynamic instability at such high temperatures. Thus it might be neccessary to avoid high-temperature synthetic procedures in order to establish the ternary and binary tungsten chalcogenides.

Despite the difference of the overall structures between the Chevrel phases and

the molybdenum(II)/tungsten(II) halides, there remains a great similarity that both classes of compounds contain hexanuclear metal cluster units, as shown in Figure 1. In the former class, the cluster unit is Mo_6Y_8, an octahedron of six molybdenum atoms with each face capped by a chalcogen atom. In the latter case, the cluster unit is Mo_6X_8 or W_6X_8, an octahedron of six molybdenum or tungsten atoms with each face capped by a halogen ligand. These bridging ligands are noted by Schäfer as "*i*" for "inner". Additionally, a set of six ligands, which are noted as "*a*" for "ausser", occupies the terminal positions found at each vertex of the octahedron. In the solid state structures of these two classes, the hexametal clusters combine in different ways by adopting different styles of ligand sharing. The ligands are shared as *a*-*i*[1] in the Chevrel phases, and *a*-*a* in the α-molybdenum/tungsten(II) halides, respectively, as shown in Figure 2. The similarity and difference in the structures of these two classes of compounds has led to the investigation of many mixed halide-chacogenide hexamolybdenum clusters with structures related to the Chevrel phases [8–11], as well as the investigation of a series of molecular complexes of mixed halide-chalcogenide hexamolybdenum clusters [12–16].

The first molecular Mo_6X_8 cluster compound with mixed bridging ligands, $(pyH)_3[(Mo_6Cl_7S)Cl_6]$, was reported by Michel and McCarley [12]. This mixed halide-chalcogenide molecular cluster was established by substituting one chlorine ligand in the cluster unit Mo_6Cl_8 of α-molybdenum(II) chloride with a sulfur ligand. Additional substitutions have led to the discovery of molecular pyridine complexes of $Mo_6S_xCl_{8-x}$ (x = 5, 6, and 7) [13], as well as molecular pyridine, n-propylamine,

[1] An *a*-*i* designation, by Schäfer's terminology, denotes a ligand in the terminal position of one cluster which is shared through a bridging position of another cluster.

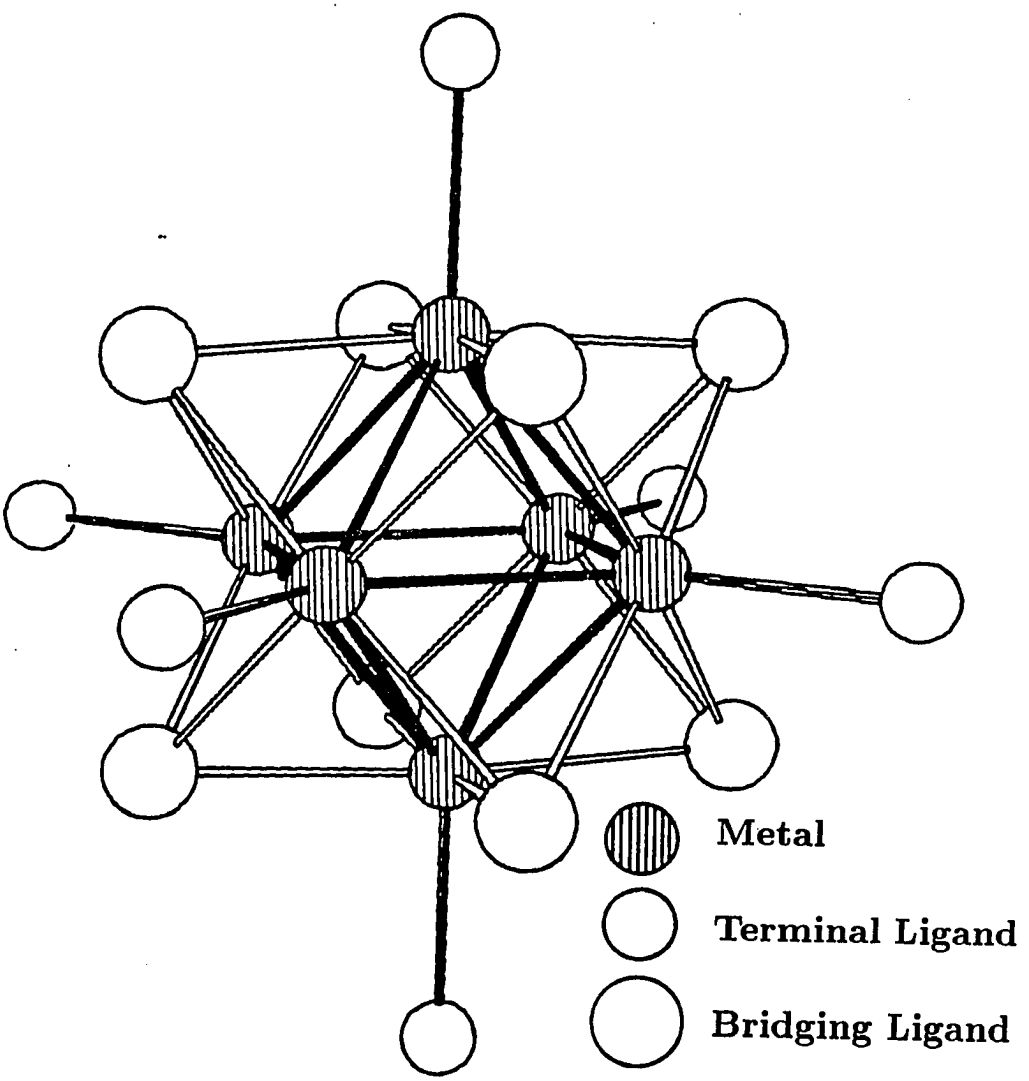

Figure 1: Structure of the $M_6X^i{}_8L^a{}_6$ cluster

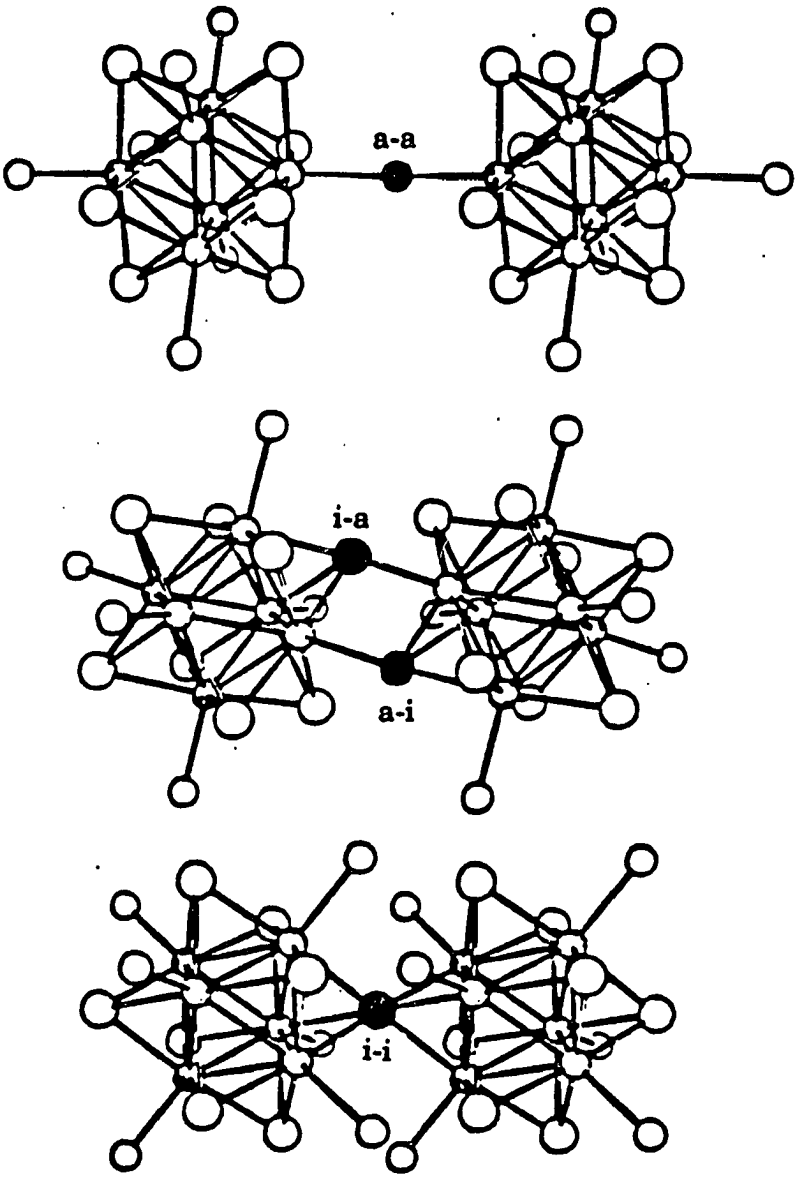

Figure 2: Possible ways that ligands can be shared between two $M_6X^i{}_8L^a{}_6$ clusters

and triethylphosphine complexes of other members of $Mo_6S_xCl_{8-x}$ where x varies from 3 to 8 [14-18]. The results of these studies suggested that the products of these attempted preparations were not single stoichiometric clusters, but rather, were mixtures of cluster products which had a range of values of x. Because of this, these complexes are usually less characterized, except those of the end member Mo_6S_8. Pyridine, n-propylamine, triethylphosphine, and tetrahydrothiophene derivatives of Mo_6S_8 have been well established. Among these the triethylphosphine and tetrahydrothiophene adducts have been structured by x-ray diffraction of single crystals [15–18]. Almost at the same time, the triethylphosphine complex of the Mo_6S_8 cluster was also established through an unrelated synthetic procedure [19,20].

The success of converting α-molybdenum(II) chloride into molecular complexes of the hexamolybdenum sulfide cluster Mo_6S_8 through substitution of sulfur ligands for chlorine ligands in Mo_6Cl_8 suggests an approach to the synthesis of novel molecular model complexes of the hexatungsten cluster W_6S_8. The same similarity exists between the cluster unit W_6Cl_8 in α-tungsten(II) chloride and the ideal W_6S_8 cluster. So substitution of sulfur ligands for chlorine ligands in W_6Cl_8 could lead to the ideal model complexes of W_6S_8. Such progress would not only uncover the new chemistry of molecular W_6S_8 clusters , but also provide opportunities to approach the still unknown "tungsten Chevrel phases" *via* molecular precursors.

Towards the overall goal of the ideal "tungsten Chevrel phases", the investigations of the substitution of sulfur ligands for chlorine ligands in the W_6Cl_8 cluster unit of α-tungsten(II) chloride, the establishment of molecular complexes of W_6S_8 cluster unit, and the removal of coordinated ligands from the W_6S_8 cluster were undertaken in this work. Also, investigations to find a more efficient and convenient

synthetic route for α-tungsten(II) chloride, which was chosen as the starting material for this work, were conducted.

Review of Previous Work

Chevrel phases

The first ternary molybdenum sulfides were reported by Chevrel and Sergent in 1971 [21]. Since then, a huge family of ternary molybdenum chalcogenides with the general formula $M_xMo_6Y_8$ (M = ternary metal cation, Y = chalcogen) have been discovered, as well as the binary phases Mo_6Y_8 [4]. Almost all of these compounds were synthesized directly from elements of ternary metal, chalcogen, and molybdenum (or molybdenum binary chalcogenides) at temperatures between 800°C and 1100°C. One notable exception is Mo_6S_8, which could only be prepared through indirect routes [22,23].

The structures of these phases have been determined by x-ray diffraction analysis of data from single crystals. Nearly all these compounds crystallize in a hexagonal-rhombohedral ($R\bar{3}$) unit cell. All of them contain three dimensional nets of interlinked Mo_6Y_8 clusters. The cluster unit is an octahedron of molybdenum atoms with each face capped by one chalcogen ligand, as shown in Figure 1. The clusters are linked together in such a way that each of the six bridging chalcogen ligands not along the three-fold axis (in $R\bar{3}$) serves as a terminal ligand for one of the six neighboring clusters. The connectivity in these compounds can be written as $(Mo_6Y^i{}_2Y^{i-a}{}_{6/2})Y^{a-i}{}_{6/2}$, as each cluster is linked with six other clusters as shown in Figure 3. Because of this strong linkage evidenced by the short intercluster $Mo-Y$ distance (as short as the intracluster $Mo-Y$ distance), the clusters are brought close

enough together to result in a direct intercluster molybdenum-molybdenum interaction. For example, in $PbMo_6S_8$, 3.262 Å is the shortest intercluster $Mo - Mo$ distance.

The only difference of the overall structures for the binary and ternary phases is that, for the ternary phases additional ternary metal cations occupy the cavities or channels which exist in the network of three dimensional chains of Mo_6Y_8 clusters. Thus the ternary phases are formally derived from the binary phases by insertion of metal cations into the binary lattice. Actually, some of them can be prepared by thermal or electrochemical insertion of ternary metal cations into a binary Chevrel phase. Schöllhorn *et al.* have used such methods to obtain the alkali metal derivatives of Mo_6S_8 which were not previously prepared by direct reactions of the elements [24]. This synthesis can be illustrated in equation 1:

$$xM + Mo_6S_8 \longrightarrow M_xMo_6S_8 \qquad (1)$$

$$(M = Li, Na; 0 < x < 3.6)$$

The ternary metal cations in the ternary phases are also mobile as many of them are good ionic conductors [7]. Also, the cations can be replaced by other metal cations through cation exchange reactions [25]:

$$M' + MMo_6S_8 \longrightarrow M'Mo_6S_8 + M \qquad (2)$$

The addition of ternary metal cations affected many chemical aspects like the bonding, properties and cluster distortions of the Chevrel phases, which have been

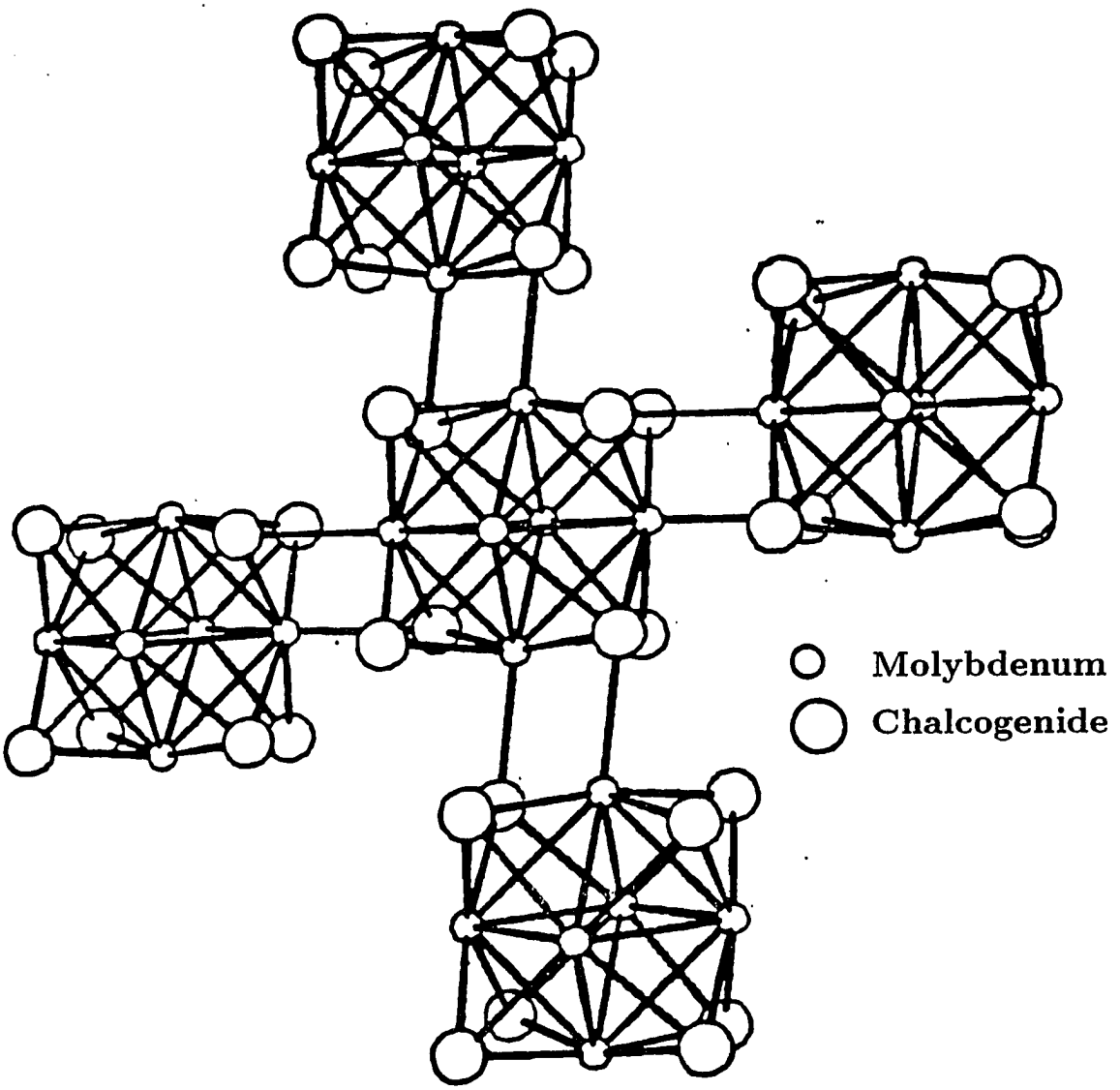

Figure 3: Structure of the Chevrel phases showing four of the six neighboring clusters

explained by band structure calculations accordingly. The first band structure calculation was reported by Anderson *et al.* [26]. They used the linearized muffin-tin orbital approach and the atomic sphere approximation. Other researchers have used more complicated models but achieved basically the same results [27–30]. Among the results of these calculations are that the p orbitals of the chacogenides are fully occupied, there are twelve $Mo - Mo$ bonding orbitals, and the conduction band is primarily of E_g character and located just below the 24 electron gap.

Based on the results of the band calculations, the chalcogenides could be assigned as Y^{2-} so there is 20 electrons available in each cluster for metal-metal bonding in the binary phases. The addition of ternary metal cations in the ternary phases contributes more electrons to the cluster for metal-metal bonding through charge transfer. So the average intracluster $Mo - Mo$ distance decreases as the number of electrons donated by the ternary metal cation increases. This trend has been observed in the Chevrel phases experimentally [4]. For example, the average intracluster $Mo - Mo$ distances are 2.705 Å and 2.780 Å, respectively, in $PbMo_6S_8$ and Mo_6S_8. The number of electrons through charge transfer can not exceed four as the electrons are donated to the conduction band of primarily E_g character, which is also recognized experimentally.

Because there are twelve $Mo - Mo$ bonding orbitals for each octahedral cluster which has just twelve edges, each edge corresponds to an average of one bonding orbital. So for a 24 electron cluster, the average metal-metal distance should be about a single bond distance. For clusters with less than 24 electrons the average metal-metal bond distance could be estimated based on the single bond distance and the bond order which is the number of total electrons divided by 24, by using the

Pauling bond order equation [31]. But if the average intracluster $Mo-Mo$ distances of the Chevrel phases are examined more carefully, one can notice that these distances are a little longer than the values calculated. The reason for this is that the atomic orbitals that give rise to these twelve $Mo-Mo$ bonding orbitals are also involved in the intercluster interactions, and thus the $Mo-Mo$ bonding can not be simply treated as twelve bonding orbitals localized completely in the octahedral cluster. For example, the intercluster $Mo-Mo$ distance is 3.08 Å in Mo_6S_8, short enough to reflect significant metal-metal bonding. By comparison of structural data from a variety of Chevrel phases, Yvon has shown that the intercluster $Mo-Mo$ distances increase as the number of electrons through the charge transfer increases [3]. This may be explained by the fact that the conduction band of E_g character has little involvement in intercluster interactions, and the addition of electrons to this band just increases the strength of intracluster bonding, and thus contraction of clusters with concommitant lengthing of the intercluster $Mo-Mo$ distance. The intercluster metal-chalcogenide distance also increases when the clusters are pushed apart, but this is also related to steric factors by the insertion of ternary metal cations.

The addition of ternary metal cations also affect the cluster distortion in these phases. Generally speaking, Mo_6X_8 clusters in Chevrel phases are not regular octahedra, but rather, distorted with expansion along the three-fold axis (in $R\bar{3}$) so the $Mo-Mo$ distances in the triangles perpendicular to the axis are shorter than those between them. This trigonal distortion is most severe in 20 electron clusters, and as more electrons are donated to the cluster by charge transfer the clusters become more and more regular. This trend is the same as the lengthing of the intercluster $Mo-Mo$ distances.

All of the Chevrel phases are metallic conductors, even for those binary compounds where there are only 20 electrons for metal-metal bonding. This is explained by the finding that the conduction band is of primary but not pure E_g character. The E_g band also contains some p character of chalcogenides and thus is not completely empty. If the total electrons for metal-metal bonding is 24, the material is expected to be an insulator or semiconductor. For the ternary molybdenum chalcogenides there is no example of exact 24 electrons for metal-metal bonding. But the mixed metal phases $Re_4Mo_2Y_8$ ($Y = S, Se$), which are formally derived from the binary phases by substituting four molybdenum atoms with four rhenium atoms, have the same structure as (and are also often referred to as) Chevrel phases. They are indeed semiconductors as expected of 24 electrons clusters [32]. Many of the Chevrel phases are superconductors. The superconductivities of these phases are a sensitive function of the bonding between clusters [3]. Particularly the shape of the conduction band is an important factor in the superconducting behavior of compounds with less than 24 electrons.

There are also mixed halide-chalcogenide hexamolybdenum clusters which are often referred to as Chevrel phases [11]. Compounds $Mo_6S_6X_2(X = Br, I)$ are formally derived from Mo_6S_8 by replacing two of the sulfur atoms with halogen atoms. The structure is described as $(Mo_6S^{i-a}{}_{6/2}Br^i{}_2)S^{a-i}{}_{6/2}$ for $Mo_6S_6Br_2$. This compound is a cluster with 22 electrons and an intercluster $Mo-Mo$ distance of 3.255 Å, slightly shorter than 3.267 Å of $PbMo_6S_8$ but much longer than 3.084 Å in the binary Mo_6S_8 with 20 cluster electrons. The lengthing of the intercluster $Mo-Mo$ distance in this compound supports the idea that intercluster $Mo-Mo$ bonding is affected through the electron charge transfer rather than the steric factors for the

ternary molybdenum chacogenide phases. The superconducting critical temperatures for the two mixed ligand cluster compounds are 13.8K and 14.0K, very close to 14K of $PbMo_6S_8$. More chalcogenides can be formally replaced by halides, and the resulting compounds have related but different structures and properties [8–10,33,34].

α-Molybdenum(II)/tungsten(II) halides and related phases

Molybdenum(II) and tungsten(II) halides and their derivatives have been extensively studied for a long time. The chemistry of these hexametal clusters has been developed in parallel. As early as 1916, Hill reported reduction of tungsten(VI) chloride with sodium amalgam and subsequent extraction of the reduction product into hydrochloric acid to prepare a chloroacid which he formulated as $W_6Cl_{12} \cdot 2HCl \cdot 9H_2O$ on the basis of analytical data [35]. Several years later Lindner prepared additional haloacids of molybdenum and tungsten although he formulated them as trimeric clusters, $H(Mo_3Cl_7 \cdot H_2O)$, $H(Mo_3Cl_4Br_3 \cdot H_2O)$, $H(W_3Cl_7 \cdot H_2O)$ and $H(W_3Br_4Cl_3 \cdot H_2O)$ [36,37]. By adding a cation to these acidic solutions, Lindner and coworkers found they could precipitate salts such as $(PyH)^+(Mo_3Cl_7 \cdot H_2O)^-$ and $(PyH)^+(Mo_3Br_7)^-$ [38,39], which gave molecular weights in nitrobenzene supporting the trimeric formulation [40].

Sheldon prepared an entire series of anionic compounds of molybdenum clusters that are derivatives of the acid hydrates [41-44]. More importantly he correctly formulated them on the basis of molecular data as $M'_2[(Mo_6X_8)X'_6]$, where $M' = M(I)^+, H_3O^+, PyH^+, (C_6H_5)_3PH^+, NH_4^+$ or R_4N^+; $X = Cl, Br, I$; $X' = Cl, Br, I, OH$. Other members of the above series have been prepared and verified by Mackay [45], Cotton [46], Clark [47], Hartley and Ware [48], and Opalovskii and

Samoilov [49]. The series of salts of tungsten clusters having the general formula $R_2[(W_6X_8)X'_6]$, $(X, X' = Cl, Br, I)$, was prepared by Hogue and McCarley later [2,50].

Thermal decomposition of the acid hydrate salts mentioned above produced a new series of anhydrous compounds, $(M_6X_8)X'_4$. Sheldon [42,44], Mackay [45] and Mattes [51] prepared the series where $M = Mo; X = Cl, Br, I; X' = Cl, Br, I, OH$. Hogue and McCarley have published a study of the tungsten series [2].

Many physical measurements have been recorded for both molybdenum and tungsten compounds of these series. The most important one was probably x-ray structure studies. A limited number of x-ray single crystal studies had been complemented with powder diffraction studies to elucidate the hexanuclear molecular structure of the clusters. Brosset analyzed single crystals of $(Mo_3Cl_4)(OH)_2 \cdot 8H_2O$ and $(Mo_3Cl_4)Cl_2 \cdot 4H_2O$, and found both contained $(Mo_6Cl_8)X_6$ groups (X = chloride or the oxygen of hydroxide or water) as shown in Figure 1 [52,53]. The inner Mo_6Cl_8 cluster consists of a regular octahedron of molybdenum atoms with an average single bond distance, while a chlorine atom is symmetrically located above each of the trianglular faces of the octahedron with μ_3 bridge bonding. Single crystal studies led Schäfer to formulate molybdenum(II) chloride as $(Mo_6Cl_8)Cl_{4/2}Cl_2$ with a cluster core of $Mo_6Cl_8{}^{4+}$ [54]. For the tungsten case, a single crystal x-ray study of the oxidized bromide cluster W_6Br_{16} was performed by Siepmann and Schnering [55]. The structural formula $(W_6Br_8)Br_4(Br_4)_{2/2}$ indicates a cluster core of $W_6Br_8{}^{6+}$. Powder data by Brown [56], Schäfer [54], Murray [57] and Clark [47] shows that all of the dichlorides, dibromides and diiodides of molybdenum and tungsten are isostructural, having the general formula $(M_6X_8)X_{4/2}X_2$. Isomorphous

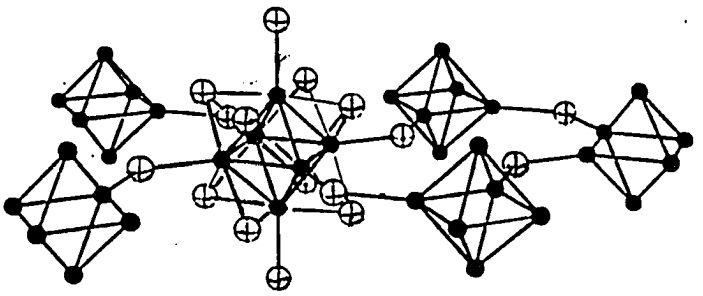

Figure 4: Structure of α-molybdenum(II)/tungsten(II) halides

stuctures were found for other series of compounds for molybdenum and tungsten by Sheldon [44], Mackay [45], Clark [47]. The structural information had been extented to similar clusters with far infrared and Raman spectral studies by Mackay [45], Cotton [46], Clark [47], Hartley and Ware [48], Mattes [51], Walton and Edwards [58], and Hogue and McCarley [2,50].

The structure of $(M_6X_8)X_{4/2}X_2$ is shown in Figure 4. Four of the terminal halides are bridged between neighboring clusters to form a layered structure, and each of these halides serves as a terminal ligand for both of the bridged clusters. This cluster sharing pattern of *a-a* is compared to that of *a-i* in the Chevrel phases in Figure 2. The difference of the cluster connection in the halides from that of the Chevrel phases shows that the halide clusters are well-separated from each other and are virtually isolated. In fact they can be easily extracted to form $(M_6X_8)X_4L_2$ and $R_2[(M_6X_8)Y_6]$. All of these cluster compounds are insulators, and are diamagnetic.

The Xα calculations of Cotton and Stanley [59] showed that the highest occupied metal-metal bonding orbital is of E_g character, which is in agreement with the earlier more simple calculations. The cluster can be viewed as having 24 electrons (4 from each metal atom), in twelve orbitals of primarily metal-metal bonding character. Thus the metal-metal bonding within the cluster can be described as twelve single bonds, one along each of the edges of the octahedron. For example, the average $Mo-Mo$ distance in Mo_6Cl_{12} is 2.613 Å [54], which is almost identical to the estimated single bond value 2.614 Å based upen the distances in bcc metallic molybdenum [60].

The terminal and bridging halides of the clusters can be replaced by other halides. The terminal chlorides of $(Mo_6Cl_8)Cl_4$ and $(W_6Cl_8)Cl_4$ are replaced by bromides and iodides in reactions with hydrohalic acids [41,42,50]. The displacement of the bridging chlorides also can be achieved with molten lithium salts at high temperature [44,50,61]. The displacement of terminal chlorides by hydroxide, methoxide and alkyl groups are also known for the molybdenum case [42,62–64], as well as the displacement of the bridging chlorides by sulfides, which led to the discovery of molecular complexes of hexamolybdenum mixed chloride-sulfide clusters and hexamolybdenum sulfide clusters.

Molecular complexes of hexamolybdenum chalcogenides/chalcohalides

The molecular complexes of the cluster unit found in the Chevrel phases had not been known until very recently [17–20], and the chemistry of these cluster complexes is still much limited. In 1988, Saito *et al.* reported the crystal structure of $Mo_6S_8(PEt_3)_6$, which was obtained in 30% yield from reductive dimerization of trimeric cuboidal Mo_3S_4 clusters [19]. This reaction was interpreted by Holm as

shown in the following equation [65]:

$$2[Mo_3S_4Cl_4(PEt_3)_4(MeOH)] + 2Mg \longrightarrow Mo_6S_8(PEt_3)_6 + 2MgCl_2 + 2Et_3PCl_2 + 2MeOH \quad (3)$$

Later Saito and coworkers also achieved $Mo_6Se_8(PEt_3)_6$ by using similar procedure, and obtained $[PPN][Mo_6Y_8(PEt_3)_6]$ ($Y = S, Se$; $PPN = (Ph_3P)_2N$) by one electron reduction with sodium amalgam [20].

Almost at the same time, McCarley *et al.* established a series of molecular complexes of Mo_6S_8 cluster unit through a totally unrelated procedure. Pyridine, propylamine, triethylphosphine and tetrahydrothiophene adducts were synthesized [17,18]. Among them phosphine and thiophene complexes are structurally characterized. The same structure and bonding were found by both sets of workers for $Mo_6S_8(PEt_3)_6$. The synthetic route McCarley *et al.* chose was to substitute sulfide for chloride in the bridging positions of α-molybdenum(II) chloride, in which advantage was taken of the stability of the metal cluster during the substitution process. By reacting sodium hydrosulfide with α-molybdenum chloride, in the presence of sodium n-butoxide and pyridine, they found eventually that completely substituted clusters could be formed as pyridine adducts:

$$Mo_6Cl_{12} + 8NaSH + 4NaOBu^n + py \longrightarrow Mo_6S_8(py)_n + 4HOBu^n + 12NaCl + 2H_2 \quad (4)$$

The reaction with the above stoichiometry could not directly produce the completely sulfided cluster, but rather, produced a mixture of mixed sulfide-chloride

clusters with average formula of $Mo_6S_6Cl_2$ as pyridine complexes. $Mo_6S_8(py)_n$ was finally obtained by subsequent sulfidation with excess sodium hydrosulfide. It was found later that the completely sulfided cluster adduct with pyridine could also be prepared in one step by using an excess amount of sodium hydrosulfide and sodium n-butoxide [66].

The advantage of the stability of the hexamolybdenum cluster is obvious in that little cluster decomposition, if any at all, occurs during the substitution process. The yield was usually close to quantitative. The completely sulfided cluster Mo_6S_8 is stabilized by the coordination of pyridine ligands. By ligand exchange reactions, the Mo_6S_8 cluster also could be stabilized in the molecular complexes of triethylphosphine, propylamine and tetrahydrothiophene:

$$Mo_6S_8(py)_n + 6PEt_3 \longrightarrow Mo_6S_8(PEt_3)_6 + py \quad (5)$$

$$Mo_6S_8(py)_n + 6PrNH_2 \longrightarrow Mo_6S_8(PrNH_2)_6 + py \quad (6)$$

$$Mo_6S_8(PrNH_2)_6 + 6THT \longrightarrow Mo_6S_8(THT)_6 + 6PrNH_2 \quad (7)$$

Structures of only the triethylphosphine and the tetrahydrothiophene complexes have been established. The Mo_6S_8 clusters are found to be isolated from each other with no intercluster interactions. The average $Mo-Mo$ distance is 2.6672 Å in $Mo_6S_8(PEt_3)_6$, which agrees well with the value 2.662 Å estimated for a 20 electron octahedral cluster based on the Pauling bond order equation [31].

Prior to the establishment of the molecular complexes of Mo_6S_8, McCarley *et al.* had found the molecular complexes of mixed sulfide-chloride clusters. The first report of a molecular chalcohalide hexamolybdenum cluster was made by Michel and Mc-

Carley [12]. The Mo_6SCl_7 cluster was found as the product of the reaction between two moles of sodium hydrosulfide and one mole of Mo_6Cl_{12} cluster. It was isolated in the structures $(pyH)_3[(Mo_6SCl_7)Cl_6]$ and $(pyH)_3[(Mo_6SCl_7)Cl_6] \cdot 3pyHCl$. The sulfur and chlorine positions were indistinguishable by x-ray diffraction. X-ray photoelectron spectroscopy confirmed that the sulfide occupies a bridging position of the cluster and not a terminal position. The $Mo-Mo$ distances were found to be 2.606 Å and 2.610 Å in these two structures, which are in good agreement with the values observed for the isoelectronic $Mo_6Cl_8{}^{4+}$ clusters of Mo_6Cl_{12} and $Hg[(Mo_6Cl_8)Cl_6]$, and the isoelectric $Mo_6Cl_7Se^{3+}$ cluster of $Mo_6Cl_{10}Se$. All of these clusters have 24 electrons for $Mo-Mo$ bonding, and thus the average $Mo-Mo$ distances are close to 2.614 Å of the estimated single bond value.

The crystal structure of a compound whose composition was thought to be $Mo_6S_6Cl_2(py)_6$ was also reported by Michel [13]. Again, structure data provided no evidence for ordering of the sulfides and chlorides in the cluster. The average $Mo-Mo$ distance was found to be 2.634 Å, close to the value estimated for a 22 electron cluster from the Pauling bond order equation. Compounds with the compositions $Mo_6S_5Cl_3(py)_3$ and $Mo_6S_7Cl(py)_5$ were also found, and gave the same or almost same x-ray powder patterns as $Mo_6S_6Cl_2(py)_6$. Other studies of substitution of sulfide for chloride in Mo_6Cl_{12} led to less well characterized species [14-16].

Explanation of Dissertation Format

This dissertation consists of three parts. Each part is formatted for publication in a technical journal. The references cited are found at the end of the dissertation.

PART I.

NEW SYNTHETIC METHOD FOR PREPARATION OF α-TUNGSTEN(II) CHLORIDE

INTRODUCTION

The chemistry of hexatungsten halides has grown together with that of hexamolybdenum halides. But unlike the molybdenum cases, one of the problems still remaining is lack of convenient and high-yield synthetic routes for the preparation of these tungsten(II) halide clusters. Traditionally a variety of methods have been used to synthesize these lower oxidation states of tungsten halides. Higher oxidation state tungsten halides had been reduced thermally and with metals and hydrogen, whereas halides of intermediate oxidation state have been disproportionated.

Preparations of tungsten(II) chloride and bromide had been achieved by reduction of tungsten(VI) chloride and tungsten(V) bromide with hydrogen gas [67]. Reduction of tungsten(VI) chloride with sodium amalgam resulted in the first preparation of the tungsten(II) cluster [35]. Metals like lead, zinc or magnesium were also used to reduce the tungsten(VI) chloride. But all these early preparations suffered from low yields of product. Aluminum was demonstrated by Lindner and Kohler to produce higher yields of the dichloride when reducing the hexachloride [38], and reduction with aluminum in a temperature gradient furnace was once used as a synthetic route to prepare both tungsten dichloride and dibromide from hexachloride and pentabromide respectively [56,57]. However, in the case of preparing tungsten dichloride, the vapor pressure of the aluminum chloride produced rises steeply as a function of temperature and explosions were frequent whenever the cooler temperature was raised high enough (225°C) to sustain rapid reactions [56]. A modified method, which employed use of sodium tetrachloroaluminate melts as solvent when reducing the tungsten(VI) chloride with aluminum, was studied by Dorman and McCarley [68], and was only partially succesful as the produced tungsten(II) dichloride

cluster was found to be unstable in the molten salts.

The method of disproportionation of tungsten(IV) chloride was reliable [69] and widely used. The reaction was performed in a temperature gradient furnace with very pure tungsten dichloride well separated from by-product tungsten(V) chloride. The shortcoming of this synthetic route is low efficiency although the yield is high. As illustrated in the following equation, three moles of tungsten(IV) chloride yield only one mole of dichloride:

$$3WCl_4(s) = WCl_2(s) + 2WCl_5(g) \quad (8)$$

The most efficient conversion from tungsten(VI) chloride to tungsten dichloride is reduction with tungsten metal [56,70], as illustrated in the following equation:

$$WCl_6(g) + 2W(s) \longrightarrow 3WCl_2(s) \quad (9)$$

This synthetic method has been widely used since the report by Schäfer in the early seventies [70]. The reaction was operated in a two-zone furnace with the temperatures set at 750°C and 550°C, respectively, for the hot zone and the cooler zone. The reaction occurred in the hot end where tungsten metal was located. But the reduction with tungsten metal was very slow and took more than a week, as tungsten metal is more stable and kinetically inert compared to molybdenum metal. The high chance of explosion caused by the high pressure of tungsten pentachloride or hexachloride at the high temperature (550°C) neccesary to sustain the reaction is a constant hazard.

In this dissertation α-tungsten(II) chloride was chosen as the starting material for further synthetic work. As large quantities of α-tungsten(II) chloride were needed, it became essential to find a convenient and relatively high-yield preparation. The work reported here concerns the development of a new synthetic method for α-tungsten(II) chloride.

EXPERIMENTAL

Materials

All syntheses, of starting materials and products, were carried out in either evacuated Pyrex/Vycor glass systems or inert gas atmosphere. All air sensitive reactants and products were stored in a dry box.

Tungsten metal, as 200 mesh powder, 99.9% pure, was obtained from General Electric Co. It was used either directly or processed with a stream of hydrogen gas at 1000°C before use. Iron metal, as powder, was used as received. Tungsten(VI) chloride was obtained from Pressure Chemical Company, and was purified by sublimation. Tungsten hexacarbonyl was used as received.

Chlorobenzene was purified by refluxing with CaH_2, followed by vacuum distillation onto 4Å molecular sieves for storage.

Analytical Procedures

Chlorine analysis was carried out by a potentiometric titration with standard silver nitrate solution in an acidic medium. Samples were first decomposed and oxidized in strongly basic hydrogen peroxide solution. These solutions were then carefully acidified with nitric acid to a pH of 5-6. Finally the solutions were titrated potentiometrically using a standard calomel electrode versus a silver/silver chloride electrode.

Analysis for tungsten metal was performed by the standard gravimetric method whereby the tungsten is weighed as the oxide, WO_3. Samples were placed in tared crucibles and wetted with a few milliliters of acetone or just water. The crucibles

were suspended above a hot plate on a porcelain desiccator tray. A small volume of concentrated nitric acid was added and as the samples were oxidized a red gas was given off. The process was continued until the solids in the crucible turned white or light yellow. All the moisture was removed while the samples were yet above the hot plate. The crucibles were then heated in a muffle furnace at 800°C until the solid was completely converted to WO_3, usually in several hours.

Physical Measurements

Infrared spectroscopy

Infrared spectra (4000–200 cm^{-1}) were obtained from an IR/98 Fourier Transform Infrared Spectrometer made by IBM Instruments, Inc. The sample chamber was constantly purged with nitrogen gas. Samples were prepared as Nujol mulls. Data were collected for the mulls which were pressed between CsI plates, while the nitrogen atmosphere was used as reference. Mid-infrared (4000–400 cm^{-1}), and far-infrared (600–200 cm^{-1}) spectra were recorded separately.

X-ray powder diffraction

An Enraf Nonius Delft FR552 Guinier camera was used to obtain x-ray powder patterns. A General Electric XRD-5 generator with a Philips normal focus tube and a copper target was used to generate the x-rays. Air sensitive samples were ground thoroughly and then mounted between strips of cellophane tape in the drybox. Powdered NBS silicon was used as an internal standard.

Synthetic Procedures

Tungsten(VI) chloride, as received, was not pure and contained impurities like

tungsten oxochlorides. It was necessary to effect purification before use otherwise poor yields would be obtained. Fortunately the oxochlorides are more volatile than the hexachloride and thus can vaporize at lower temperature. A typical purification process is described below. About 40 grams of unprocessed WCl_6 was put into a pyrex tube fitted with a standard ball joint in the dry box. The tube and contents were attached to the vacuum line, evacuated to 10^{-5} torr and then sealed with a gas torch. The tube was then put into a furnace in the horizontal position with one end of the tube protruding outside of the furnace. Slowly the temperature was raised at the center of the furnace where the WCl_6 was located. A thermocouple was used to moniter the temperature. As the temperature rose to over 100°C, red gas was seen coming out to the cooler end and depositing as crystalline needles. The temperature was kept at 160°C overnight. Both red and yellow materials were collected at the cooler end while black-blue shining powder was clearly separated from them. The tube was broken in the dry box and the black-blue powder was collected and stored.

Preparation of tungsten(IV) chloride

A typical synthesis is like the following. 7.1 grams $W(CO)_6$ (0.020 moles), and 17.3 grams WCl_6 (0.044 moles) were loaded into a 250-mL reaction flask which was equipped with Schlenk condenser in the dry box. The reaction flask was then attached to the vacuum line. About 100 mL chlorobenzene was syringed in under nitrogen gas flow so minimum contamination by air was achieved. The mixture was brought to boiling by raising the temperature and refluxed under a nitrogen atmosphere. Gas evolution was observed while the reaction was in progress. The reaction was completed in several hours after gas evolution stopped. At the same time, the color

of the solid turned into gray from the initial brown. After cooling the mixture this gray solid was filtered and separated from the dark brown solution. It was extracted with filtrate solvent and then dryed under vacuum.

This solid was then taken into the dry box and reloaded into a Pyrex tube with a standard ball joint. The tube was attached to the vacuum line in a horizontal position and evacuated. Most of the tube was wrapped with heating tapes and fitted with a thermocouple fitted at the end of the tube where the solid was located. The temperature was raised slowly to 250°C, where it was held while the solid was heated under dynamic vacuum overnight. Unreacted WCl_6 as well as some tungsten oxochloride was sublimed away to leave a pure gray-green product. The final product weighed 17.3 grams. Infrared spectra and analytical data were obtained for the product. Anal. Calc. Cl, 43.6; W, 56.4. Found: Cl, 43.6; W, 56.5; $Cl/W = 4.00$.

Reduction of tungsten(IV) chloride with tungsten

A mixture of 5.8 grams WCl_4 (0.018 moles) and 4.1 grams W (0.022 moles) was put into a Vycor tube in the dry box. The tube was attached to the vacuum line and sealed carefully under vacuum. The tube was then put into a two-zone furnace in the horizontal position such that each end of the tube was located in the center of one zone. The temperatures were manipulated carefully as shown in Table 1. First the temperatures in both zones were raised simultaneously to 550°C. Then the temperature for the particular end of the tube where the reaction mixture was located was raised further, at the rate of 50°C per hour, to 750°C. This temperature setting was then kept constant throughout the reaction period of 8 days.

After the reaction was finished and the tube was cooled down, most of the

Table 1: Time/temperature setting for reduction of tungsten(IV) chloride with tungsten

Temp(1)[a] (°C)	Temp(2)[b] (°C)	Duration (hours)
200	200	1
300	300	1
400	400	1
450	450	1
500	500	1
550	550	12
600	550	1
650	550	1
700	550	1
750	550	192

[a]Temperature of the hot end, where the reaction mixture was initially located.
[b]Temperature of the cooler end.

mixture was located at the other end of the tube where the temperature was kept at 550°C during the reaction, while some unreacted tungsten powder was left at the hotter end. Next, the temperature for the cooler end was raised slowly to 530°C and kept constant overnight to sublime away impurities like tungsten oxochlorides and unreacted WCl_4. Finally the tube was broken in air and the pale gray solid at the cooler end was collected.

Reduction of tungsten(IV) chloride with iron

A sample of 7.3 grams WCl_4 (0.022 moles) and 1.26 grams Fe (0.023 moles) was loaded into a Pyrex tube equipped with a standard ball joint. The tube was attached to the vacuum line for evacuation and sealing. Then it was put into a furnace in horizontal position. Thereupon the temperature was raised slowly to 500°C and kept constant for 3 days. After the reaction was completed and the tube was cooled down, one end of the tube (containing product) was reheated to 450°C as the other end was placed outside of the furnace to sublime away materials with higher vapor pressure for several hours. A good yield of α-WCl_2 was reflected by the presence of a pale yellow powder as the product, where the initial reaction mixture was located. Again the tube was broken in air, and the pale yellow solid was collected.

Reduction of tungsten(IV) chloride with other metals

A sample of 1.0 gram WCl_4 (0.003 moles) and 0.5 grams Sn (0.004 moles) was loaded into a Pyrex tube equipped with a standard ball joint. The tube was attached to the vacuum line for evacuation and sealing. Then it was put into a furnace in horizontal position. The temperature was raised slowly to 510°C and kept constant for 3 days. After the reaction was completed and cooled down, the tube was reheated

to 450°C with one end placed out side of the furnace to sublime away lower vapor pressure materials for several hours. Then the tube was broken in air, and the solid was collected. The same reaction setup and procedures were used for reductions of tungsten(IV) chloride with stoichiometric amounts of zinc and manganese.

Isolation of tungsten(II) chloride

The reaction product W_6Cl_{12} from the reductions of tungsten(IV) chloride was present in a solid mixture. Crystallization from acidic aqueous solution as $(H_3O)_2W_6Cl_{14} \cdot 6H_2O$ was used to purify the material by the literature method [70]. The product mixture was ground in a mortar and carefully poured into 200 mL of freshly made 6N HCl solution with addition of a small volume of ethanol. A stirring bar was placed in the solution and the contents were stirred for about one hour. The solution was then filtered and the residue was washed with a little more HCl. The filtrate was usually greenish yellow and was gentally heated on a hot plate. As the solution evaporated to reduce the volume, solids began separating from solution. At this time concentrated HCl was added to the solution so as to approximately triple the volume. The solution was cooled in a ice bath and yellow crystalline needles deposited out of solution. These crystalline needles were separated by filtering through a medium porosity sintered glass frit by aspirator vacuum and washed with cold concentrated HCl. They were left on the frit until dried by the aspirator suction.

The yellow acid hydrate was put into a tube and attached to the vacuum. It was heated to 325°C overnight in *vacuo* to produce a pale yellow powder of the final product anhydrous W_6Cl_{12}. Infrared spectra and analytical data were obtained for the

product. Anal. Calc. for W_6Cl_{12}: $W, 72.2; Cl$, 27.8. Found: $W, 70.1; Cl, 27.6; Cl/W$ = 2.04.

RESULTS AND DISCUSSION

The early synthetic routes in the literature for preparation of W_6Cl_{12} (α-WCl_2) were reduction of WCl_6 with hydrogen gas, sodium amalgam or metals like lead, zinc, magnesium, aluminum and tungsten. Usually either the yields were very low, or the reactions were explosion-hazards and very difficult to control, or the reactions were too slow to give useful results. The disproportionation of WCl_4 is a relatively reliable and convenient preparation for α-WCl_2. However, the actual conversion percentage was low as 3 moles of WCl_4 produced only 1 mole of WCl_2 if the reaction was 100% complete:

$$3WCl_4(s) \longrightarrow WCl_2(s) + 2WCl_5(g)$$

Most of the traditional preparations of tungsten(II) chloride use tungsten(VI) chloride as starting material. The reduction of WCl_6 to α-WCl_2 is known to be indirect and WCl_4 is formed as an intermediate reduction product which can be isolated [56]. It is possible that involvement of intermediate WCl_4 complicates the synthesis, and thus results in poor yields of α-WCl_2. If so, by choosing reaction conditions adjusted to WCl_4 as starting material some of the problems might be overcome. At least it might reduce the reaction time and possibly enhance the yields. As the generally used preparations of WCl_4 had also been difficult, this synthetic route had never been tested previously. With the development of a new synthetic route for WCl_4, the reductions starting from WCl_4 were investigated.

Tungsten(IV) Chloride

Traditionally preparation of WCl_4 was complicated by its disproportionation and instability to oxidation. A new synthetic route was developed by M. Schaefer in this group earlier which employed tungsten hexacarbonyl reduction of either WCl_5 or WCl_6 in refluxing chlorobenzene [71]. The reduction of WCl_6 with the tungsten hexacarbonyl was extremely convenient as the reaction was quick, the conditions were moderate and the starting material was readily available. Although this reaction was originally thought to give about 50% yield of WCl_4, it was found in this work that the yield was near quantitative if pure WCl_6 was used in slight excess:

$$2WCl_6 + W(CO)_6 \longrightarrow 3WCl_4 + 6CO \qquad (10)$$

The reaction was quick and relatively easy, as it usually was completed within several hours in refluxing chlorobenzene. The separation of product was also easy as WCl_4 is not soluble in chlorobenzene, thus the product was filtered under nitrogen and dried under vacuum. The product also contained impurities of some tungsten oxochlorides as well as the excess tungsten(VI) chloride used. Pure WCl_4 was obtained by removal of these impurities by sublimation at 250°C in *vacuo*. The infrared spectra indicated an absence of chlorobenzene in the final product. The purity of the product, which was found to be very important in subsequently obtaining a high-yield synthesis of α-tungsten(II) chloride, was also confirmed by the results of analytical work.

Reduction of Tungsten(IV) Chloride with Tungsten

Reduction of WCl_4 with tungsten powder in a temperature gradient furnace

is a modification of the method used by Schäfer [70]. The mixture was put into a Vycor tube and outgassed under dynamic vacuum before sealing of the tube. The temperatures had to be carefully controlled during the reaction, especially in the early stage of raising the temperature, in order to avoid a sharp temperature rise which could cause a potential explosion. A good yield of about 50% was obtained based upon the following equation:

$$WCl_4 + W \longrightarrow 2WCl_2 \tag{11}$$

The mechanism of the reduction was thought to be:

$$\begin{aligned} 3WCl_4(s) &\longrightarrow WCl_2(s) + 2WCl_5(g) \\ 4WCl_5(g) + W(s) &\longrightarrow 5WCl_4(g) \\ 3WCl_4(s) &\longrightarrow WCl_2(s) + 2WCl_5(g) \end{aligned} \tag{12}$$

The disproportionation of WCl_4 occurred at the cooler end which was set at 550°C. WCl_2 was deposited as the solid, while WCl_5 remained in the vapor phase and diffused back to the hot end. Reduction of WCl_5 occurred at the hot end where the temperature was 750°C. Because of the high pressure of WCl_5 at 550°C, the danger of potential explosions still existed. If a lower temperature for the cooler end was employed, the yield decreased sharply. Apparently the reduction of WCl_5 with tungsten metal is very slow and needs a sufficiently high vapor pressure of WCl_5 to proceed. The reaction time was still as long as a week. The chance of explosion could not be strictly excluded. Considering these shortcomings as well as the necessity

to handle Vycor glass tubing, the practical application of this reduction method is unfavorable even though high theoretical conversion of one mole WCl_4 to two moles WCl_2 is possible.

Reduction of Tungsten(IV) Chloride with Iron

The reduction of WCl_4 with iron metal was run at 500°C. Unlike the tungsten reduction, the reaction was pursued in a sealed Pyrex tube because of the relatively low reaction temperature. The stoichiometric amount of metal calculated for formation of iron(II) chloride was used and the reaction was allowed to proceed for 2 days. This reduction method gave a yield of about 60%. The reaction was repeated many times and proved to be consistent with the completion of reduction usually in 2 to 3 days. The reaction is represented by the following equation:

$$WCl_4(g,s) + Fe(s) \longrightarrow WCl_2(s) + FeCl_2(s) \qquad (13)$$

Like the case of reduction with tungsten, the mechanism is thought to involve the disproportionation of WCl_4, followed by reduction of WCl_5 with iron metal, which proceeds readily at 500°C. At this temperature the vapor pressure of neither WCl_5 nor $FeCl_2$ threatens to cause any explosion. This method is so far the most convenient one, as it makes use of inexpensive and more easily sealed Pyrex tubing, employs a lower reaction temperature and requires a relatively short period of time.

Reductions of tungsten(IV) chloride with other metals were also tested under similar reaction conditions to those of iron reduction in the hope of finding still another convenient and high-yield preparation. All of these trials gave poor or no

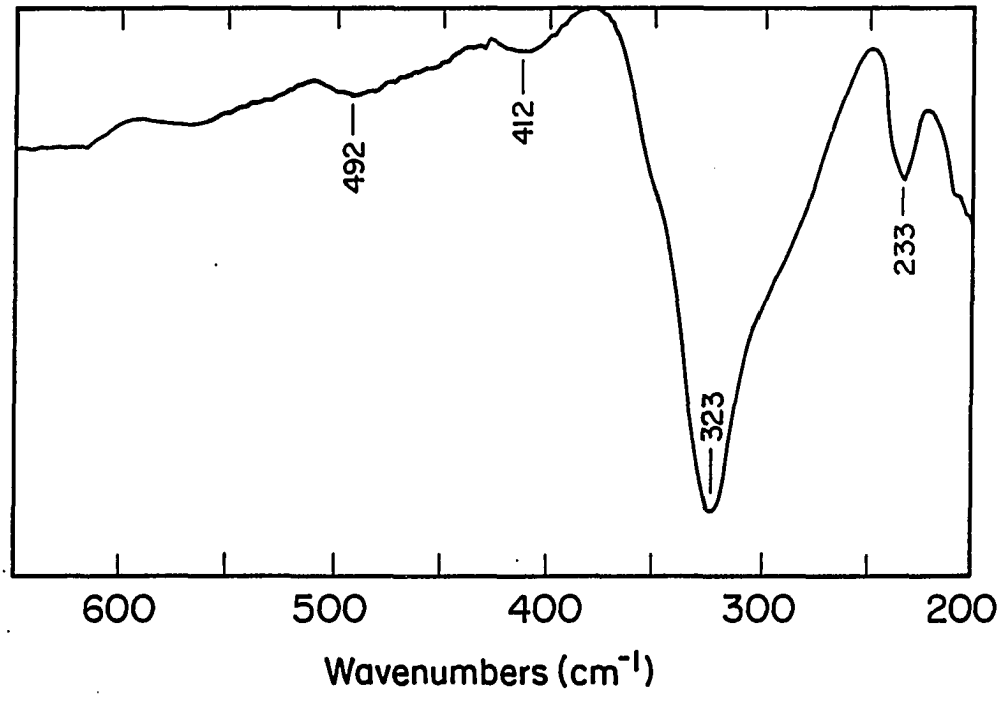

Figure 5: Far-infrared spectrum of α-tungsten(II) chloride

yield of α-tungsten(II) chloride. The reduction with tin gave a yield of 29%, which is about the theoretical yield for disproportination of tungsten(IV) chloride. Reductions with zinc and manganese gave virtually no product.

Tungsten(II) chloride prepared from these reactions was not pure and was always purified before further use by recrystallization of the chloroacid, $(H_3O)_2[(W_6Cl_8)Cl_6]\cdot 6H_2O$ from hydrochloric acid. The bright yellow crystals of chloroacid faded to pale yellow during thermal decomposition under dynamic vacuum. The decomposition temperature of at least 325°C must be maintained to obtain pure α-tungsten(II)

chloride. Decomposition at lower temperatures yields the hydrate, $W_6Cl_{12} \cdot 2H_2O$ [50]. Anhydrous tungsten(II) chloride prepared by thermal decomposition of the chloroacid was pyrophoric and amorphous to x-rays. The final product gave broad, poorly resolved bands in the far infrared spectrum, as shown in Figure 5, and no bands in the mid-infrared spectrum. These results agreed well with those found previously [50].

CONCLUSIONS

The synthesis of tungsten(IV) chloride through the reduction of tungsten(VI) chloride with tungsten carbonyl, which was discovered by Shaefer earlier and reported to give 50% yield, proved to be an efficient and quantitative method in this work. This synthesis made it feasible and relatively easy to study the reduction of tungsten(IV) chloride with metals towards the goal of finding an easier and more efficient synthesis of α-tungsten(II) chloride.

The reduction of tungsten(IV) with tungsten metal is developed and found to be efficient, but without exclusion of the danger of potential explosions. It is also relatively slow, and high temperature conditions as well as Vycor reaction tubes have to be used. On the contrary, the reduction of tungsten(IV) chloride with iron metal proved to be relatively easy (500°C reaction temperature and use of inexpensive Pyrex tubes) and short (usually in two or three days). It has proved to be the most convenient and reliable synthesis of α-tungsten(II) chloride, with a good yield about 60%.

PART II.

PREPARATION AND CHARACTERIZATION OF MOLECULAR CLUSTER COMPLEXES WITH GENERAL FORMULA $W_6S_8L_6$

INTRODUCTION

The Chevrel phases $M_xMo_6Y_8$ ($Y = S, Se, Te$) have been thoroughly investigated since their discovery in the early 1970s [3,4]. They are usually prepared directly from elements at high temperatures around 1000°C, and are known to have very rich physical and chemical properties. For example, many of them are superconducters [5]. In addition, these materials are also hydrodesulfurization catalysts [6], and good ionic conductors [7]. These properties are directly related to the structure of these phases, which cornsists of Mo_6Y_8 cluster units interlinked in three dimensions by intercluster $Mo-Mo$ and $Mo-Y$ bonds to form a framework. In this three dimensional network sites are available to accommodate the ternary metal cations M^{n+}.

However, no tungsten analogue of these phases has ever been synthesized. One possible explanation is that the "tungsten Chevrel phases" are not thermodynamically stable at high temperatures where the Chevrel phases are usually synthesized. Thus, it may be necessary to employ a low temperature approach to the synthesis of the "tungsten Chevrel phases". In recent years the preparation of metastable compounds *via* molecular precursors has received a good deal of attention. But even the molecular model compounds $W_6S_8L_6$ (L is an organic donar ligand) had not been known before the start of this study.

As a first step towards synthesis of the "tungsten Chevrel phases" *via* a low temperature approach, synthesis of the molecular model compounds $W_6S_8L_6$ has been chosen as an intermediate goal. The α-tungsten(II) chloride $(W_6Cl_8)Cl_4$ was chosen as starting material, because it is structurally similar to the Chevrel phases, in that it also has octahedral cluster units of W_6Cl_8. Substitution of sulfide for chloride in W_6Cl_8, if it can be done successfully without decomposition of the cluster, could

be an efficient synthesis of $W_6S_8L_6$.

Prior to this work, substitution of sulfide for chloride in Mo_6Cl_8 had led to the discovery of molecular complexes of hexamolybdenum sulfide and hexamolybdenum mixed chloride-sulfide clusters. Incomplete substitutions were known to lead to Mo_6Cl_7S [12], and $Mo_6S_6Cl_2$ [13]. Complete substitution was also established later in a similar way [17].

EXPERIMENTAL

Materials

Unless otherwise indicated all materials and reaction mixtures were handled under dry inert atmospheres or on a high vacuum manifold. Solids were carefully handled in vials, water-cooled condenser-equipped reflux reaction flasks, and extractors. Solvents were generally vacuum- distilled or syringed under a blanket of nitrogen or argon gas.

Pyridine and toluene were dried by refluxing with CaH_2, distilled and stored under nitrogen over outgassed 4Å molecular sieves. Methanol was dried over sodium methoxide, followed by vacuum distillation onto outgassed 3Å molecular sieves for storage. n-Butanol was dried over sodium n-butoxide and then distilled onto outgassed 4Å molecular sieves. Dichloromethane was dried by refluxing with phosphorous(V) oxide, followed by vacuum distillation onto outgassed 3Å molecular sieves.

Triethylphosphine was used as received from Aldrich Chemical Co. and stored under nitrogen. Anhydrous sodium hydrosulfide was prepared by reaction of hydrogen sulfide with sodium ethoxide by using the procedure described by Brauer [72]. Sodium n-butoxide was prepared by reaction of n-butanol with sodium metal, and was used as solid. Early on in this work W_6Cl_{12} was prepared by a literature method [70]. Then it was prepared through a vastly improved method which is described in detail in Part 1 of this dissertation.

Analytical Procedures

Chlorine was determined by potentiometric titration of neutralized solutions with

standard $AgNO_3$ solution using a $Ag/AgCl$ electrode *versus* a standard calomel electrode. Samples were first decomposed and oxidized in $NaOH$ solutions with H_2O_2, and then the solutions were neutralized with HNO_3. The end point was determined by the second derivative method.

Tungsten was determined by conventional gravimetric analyses. Samples were either decomposed and oxidized directly by concentrated HNO_3, or treated with NH_4OH and H_2O_2 first, and then oxidized with concentrated HNO_3 in tared porcelain crucibles. Following ignition in a muffle furnace at 800°C for about 4 hours, the resulting WO_3 was weighed. This method usually gave good results, except for the materials containing phosphine.

Additional microanalyses for sulfur, carbon and hydrogen were obtained from Galbraith Laboratories [73].

Physical Measurements

Infrared spectroscopy

Infrared spectra (4000–200 cm^{-1}) were obtained from an IR/98 Fourier Transform Infrared Spectrometer made by IBM Instruments, Inc. Samples were prepared as Nujol mulls. Data were collected for the mulls which were pressed between CsI plates, while the dry atmosphere was used as reference. The sample chamber was constantly purged with nitrogen. Mid-infrared (4000–400 cm^{-1}), and far-infrared (600–200 cm^{-1}) spectra were recorded separately.

Nuclear magnetic resonance spectroscopy

Proton decoupled ^{31}P NMR spectra were collected on WM-200 or WM-300 instruments by Bruker. The instruments were equipped with deuterium lock. Chemical

shifts for each sample were referenced to 85% phosphoric acid contained in a capillary within the sample tubes. Samples were put into 10 mm tubes in the drybox and deuterated solvents, $C_6D_5CD_3$ or $C_2D_2Cl_2$, were syringed into the sample tubes. In the sample preparation, exposure to air was minimized but not strictly avoided.

X-ray powder diffraction

An Enraf Nonius Delft FR552 Guinier camera was used to obtain x-ray powder patterns. A General Electric XRD-5 generator with a Philips normal focus tube and a copper target was used to generate the x-rays. Air sensitive samples were ground thoroughly and then mounted between strips of cellophane tape in the drybox. Powdered NBS silicon was added to each sample as an internal standard.

Magnetic susceptibility

The magnetic susceptibility data were carried out on solid samples with a SQUID magnetosusceptometer. Samples were taken out in vials from the drybox and put into sample tubes followed by immediate measurement. Exposure to air was minimized but not strictly avoided. Corrections for diamagnetism of the sample tubes were made.

Synthetic Procedures

The strategy employed in this research was to substitute sulfur into the already formed octahedral cluster unit of W_6Cl_8 in α-tungsten(II) chloride. Past studies for reactions of $(Mo_6Cl_8)Cl_4$ with $NaSH$ in pyridine at reflux under nitrogen or at 200°C in sealed tubes had demonstrated partial substitution of sulfide for chloride in Mo_6Cl_8 [12,13], and the extent of substitution had been shown to be increased

with the addition of $NaOBu^n$ [14]. In this section, the reactions intended to effect substitution of sulfide for chloride in $W_6Cl_8{}^{4+}$ with the use of $NaSH$ and $NaOBu^n$ in pyridine are first listed and described. Then the ligand exchange reactions of the completely sulfide-substituted hexatungsten cluster complexes are described.

In a typical sulfidation reaction, the appropriate stoichiometric amounts of the W_6Cl_{12} cluster, the sulfiding agent $NaSH$, and the proton acceptor $NaOBu^n$ were placed into a reaction flask with a stirring bar and the flask connected to the vacuum line. For example, a reaction of 1:8:4 stoichiometry means that one mole of W_6Cl_{12} is reacted with eight moles of $NaSH$ and four moles of $NaOBu^n$, while a reaction of 1:2 means that one mole of cluster is reacted with two moles of $NaSH$. Then dry pyridine was either vacuum-distilled or syringed on top of the reactants. The mixture then could be stirred either at room temperature or heated to reflux for a certain reaction time.

Reaction in 1:2 stoichiometry

α-Tungsten(II) chloride (1.5 grams, 1.0 mmoles) and sodium hydrosulfide (0.11 grams, 2.0 mmoles) were placed into a 100 mL reaction flask followed by syringe of 40 mL pyridine. A dark yellow solution immediately formed. It was heated to reflux for one day and then filtered hot. The filtrate, which contained most of the product, was dark yellow. A trace of brown solid remained on the filter when pumped dry. Infrared spectra were obtained for this solid.

The filtrate was stripped of pyridine and pumped dry, leaving a dark yellow solid. The color was so dark that it looked almost black, but when the solid was ground, the yellow color appearred. Infrared spectra were obtained for this yellow solid. It was

further treated with *ca.* 30 mL of a 1M $HCl - CH_3OH$ solution whereupon most of the solid was solubilized. When solvent was stripped off the methanol filtrate and pumped dry, the product was a dark yellow solid. Infrared spectra and a chlorine analysis were obtained for this product. Anal. Calculated for $(pyH)_2[(W_6Cl_8)Cl_6]$: Cl, 28.2. Found: 28.0.

Reaction in 1:6 stoichiometry

α-Tungsten(II) chloride (0.5 gram, 0.33 mmole) and sodium hydrosulfide (0.11 gram, 2.0 mmole) were placed into a 100 mL reaction flask followed by vacuum distillation of *ca.* 40 mL pyridine. The mixture was then refluxed for four days. After cooling, a brown solid and a dark solution were separated by filtration. The filtrate was stripped of pyridine and the residue was dried under vacuum. Yields of 0.44 grams of soluble material and 0.23 grams for insoluble material (including the sodium salts) were obtained. Infrared spectra as well as tungsten and chlorine analyses were obtained for the soluble part, which was the major fraction. Anal. Found: $W, 51.5; Cl, 13.3; Cl/W_6$, 8.0.

Reaction in 1:8 stoichiometry

The reaction mixture of α-tungsten(II) chloride (0.5 gram, 0.33 mmole), sodium hydrosulfide (0.15 gram, 2.7 mmole) and pyridine was assembled in the identical manner to the above 1:6 reaction and was refluxed for three days. The subsequent work-up was also identical to the above 1:6 reaction except that the brown solid in the insoluble fraction was washed with methanol thoroughly in an extractor to remove the by-product of sodium chloride and then dried. The yield was 0.20 grams of the soluble material and 0.36 grams of the red solid remaining after methanol washing.

Infrared spectra were obtained for both parts. Analysis for the soluble material: Found: $W, 47.6; Cl, 13.2; Cl/W_6$, 8.6. Analysis for the insoluble material: Found: $W, 58.9; Cl, 3.3, Cl/W_6$, 1.7. Anal. Calcd. for $W_6S_{6.3}Cl_{1.7}(py)_6$: $W, 59.95; Cl$, 3.3.

Reaction in 1:8:4 stoichiometry

The reaction mixture of α-tungsten(II) chloride (1.53 gram, 1.0 mmole), sodium hydrosulfide (0.45 gram, 8.0 mmole) and sodium n-butoxide (0.38 gram, 4.0 mmole) was assembled in the usual manner, followed by vacuum distillation of *ca*. 40 mL pyridine. The mixture was refluxed for five days, and the subsequent process was also identical to the above 1:8 reaction. From the pyridine filtrate solution, a yield of 0.3 grams dark yellow solid was recovered after removal of solvent. In the insoluble fraction the by-product of sodium chloride was removed by thoroughly washing with methanol. The red solid, obtained as the major product in this way, was dried under vacuum. The yield was 1.3 grams. Infrared spectra were recorded for this major product. Anal. Calcd. for $W_6S_6Cl_2(py)_6$: Cl, 3.4. Found: Cl, 3.9.

A portion of this red solid was reacted with more sodium hydrosulfide in pyridine. The amount of sodium hydrosulfide used was double that calculated for replacement of the chlorine in this solid. The mixture was refluxed for one day, filtered after cooling, and the red insoluble major fraction was then washed with methanol and dried. A chlorine analysis showed the absence of any chlorine in the product. The pyridine filtrate solution was stripped of pyridine and pumped dry, leaving a dark yellow minor product. Infrared spectra were recorded for both parts.

Reaction in 1:12:6 stoichiometry

The reaction mixture of α-tungsten(II) chloride (1.67 gram, 1.09 mmole), sodium

hydrosulfide (0.73 gram, 13.0 mmole) and sodium n-butoxide (0.65 gram, 6.77 mmole) was assembled in the usual manner, followed by vacuum distillation of *ca.* 50 mL pyridine. The mixture was refluxed for two days. Unlike the above reactions, the pyridine filtrate in this case was light orange and gave almost nothing when pumped dry.[2] At the same time, a very dark colored solid was obtained. In order to remove sodium chloride and unreacted or excess sodium hydrosulfide, this dark solid was thoroughly washed with methanol in an extractor. The methanol solution was very intensely colored, unlike the light orange color resulting for the methanol extracts of the previous reactions. After drying under vacuum the product was a dark red powder. Infrared spectra were recorded. A chlorine analysis showed that no chlorine remained in the powder. Anal. Calcd for $W_6S_8(py)_6$: *W*, 60.2; *S*, 13.98; *N*, 4.58; *C*, 19.64; *H*, 1.65. Found: *W*, 60.0; *S*, 12.98; *N*, 4.36; *C*, 19.03; *H*, 1.70.

A 0.1 gram sample of the product was put into a 15-cm-long, 15-mm. o.d. Pyrex tube equipped with a balljoint. The tube was then attached to a vacuum line and pyridine was vacuum distilled into the tube until it was about one-fourth full. Then the tube was sealed with a torch so that pyridine occupied about half of the remaining volume, and was put into a furnace in a vertical position. The temperature was slowly raised to 200°C at the bottom of the tube and kept constant for 5 days, and then slowly returned to 25°C. Black single crystals were attached to the walls of the tube just above the surface of the still almost colorless liquid pyridine, while the major portion of the product was obtained as a black, finely crystalline powder at the bottom of the tube.

[2]For all of the previous sulfidation reactions, a dark yellow filtrate was always obtained, indicating that some cluster species were still in solution.

All of the above substitution reactions were conducted in refluxing pyridine. Pyridine served not only as solvent, but also as reagent in such a way that it occupied the terminal positions of the cluster once the terminal chloride ligands left during the substitution. The final products of the above substitution reactions are all pyridine molecular adducts. Unfortunately these highly substituted clusters, including the completely substituted one, are very insoluble. The solids also usually give very poor x-ray powder diffraction patterns. The following reactions are intended to solubilize the cluster species by replacement of terminal ligands with another organic ligand.

Reaction of $W_6S_8(py)_6$ with triethylphosphine

A 0.34 gram sample of the pyridine compound $W_6S_8(py)_6$ was put into a 100-mL reaction flask. The flask was attached to a vacuum line and *ca*. 40 mL of toluene was vacuum distilled into it. Then the flask was filled with nitrogen gas and 0.50 mL of triethylphosphine was transferred in by syringe. No obvious change happened upon stirring at room temperature, as the red solid did not react with the colorless solution. However, after the mixture was refluxed over night, all of the solid dissolved with formation of a greenish-yellow solution. After filtering this solution the solvent and excess triethylphosphine were stripped away under vacuum. Infrared spectra, powder diffraction pattern and magnetic susceptibility measurement were obtained for the dark yellow solid. ^{31}P NMR spectra were also recorded.

A portion of this solid was dissolved in dichloromethane to form a greenish yellow solution. The solution was allowed to stand at room temperature for several days. Dark green crystals were deposited and isolated.

Reaction of $W_6S_6Cl_2(py)_6$ with triethylphosphine

The starting material was taken from the 1:8:4 reaction described above. The reaction procedures were exactly the same as the above reaction. No obvious change happened when the mixture was stirred at room temperature, as the red solid did not react with the colorless solution. However, after the mixture was refluxed over night, the solid dissolved with formation of a greenish- yellow solution. After filtering this solution the solvent and excess triethylphosphine were stripped away under vacuum. Infrared spectra were obtained for the dark yellow solid. ^{31}P NMR spectra were also recorded. Anal. Calcd. for $W_6S_6Cl_2(PEt_3)_6$: *Cl*, 3.4. Found: *Cl*, 3.8.

Reaction of $W_6S_8(py)_6$ with tetrahydrothiophene

A 0.40 gram sample of the pyridine compound $W_6S_8(py)_6$ which was prepared from a 1:12:6 reaction was put into a 100-mL reaction flask. Then *ca*. 50 mL tetrahydrothiophene was vacuum distilled onto the pyridine compound. Stirring at room temperature did not solubilize the solid. However, after the mixture was refluxed for three days, the majority dissolved to form a dark yellowish-red solution. After filtering and stripping a little solvent under vacuum, the solution was left to stand at room temperature over several days. Single crystals grew out of the solution. If the solution was stripped of solvent and pumped under vacuum, an oily material was obtained. Ether was distilled in to break the oil and the powdered product was filtered and dried under vacuum. Infrared spectral data were recorded for both crystalline and powdered products.

Reaction of $W_6S_8(PEt_3)_6$ with pyridine

A portion of $W_6S_8(PEt_3)_6$ compound, which was made by ligand exchange of

triethylphosphine for pyridine described earlier, was put into a 100-mL reaction flask followed by addition of pyridine. A dark yellow solution was formed immediately. The solution was heated and brought to reflux for a couple of days. No solid was formed. Upon stripping pyridine from the solution under vacuum an oily product resulted, which was not characterized further.

Reaction of $W_6S_8(THT)_6$ with pyridine

A portion of $W_6S_8(THT)_6$ compound, which was made by ligand exchange of tetrahydrothiophene for pyridine described earlier, was put into a 100-mL reaction flask followed by addition of pyridine. A dark yellow solution was formed immediately. The solution was stirred at room temperature over night. A very fine red powder came out of solution slowly. The mixture was then heated, brought to reflux for one day, and filtered. A red powder was recovered and dried under vacuum. Infrared spectra were taken for the product.

X-ray Structure Determinations

Structure determination for $W_6S_8(py)_6$

Single crystals were grown from pyridine in a sealed tube at 200°C, as indicated in the earlier synthetic part. These single crystals appeared to be black and irregularly shaped. A relatively large single crystal was quickly selected and immediately mounted on the diffractometer in the low temperature nitrogen stream (-70°C), after the tube was opened in air. The crystal selected, with dimensions 0.2 x 0.1 x 0.1 mm, was mounted on a glass fiber. Data were collected with an Enraf-Nonius CAD4 diffractometer at low temperature. Graphite-monochromated $Mo\ K\alpha$ radiation was employed to collect data with $4^\circ < 2\theta < 55^\circ$, using the $\theta - 2\theta$ scan technique. Three

standard reflections, monitored every 300 reflections, showed no intensity variation during the data collection, indicating that there was no significant crystal or instrument instability. A total of 4621 unique reflections were collected and 3754 of them were considered as observed with $F_o^2 > 3\sigma(F_o^2)$. The absorption coefficient for Mo $K\alpha$ is $\mu = 178.04$ cm^{-1}. An empirical absorption correction was applied, using a ϕ scan technique.

Twenty-five orientation reflections were automatically indexed to indicate a triclinic crystal symmetry. The unit cell parameters are a = 10.624 (2) Å, b = 11.932 (3) Å, c = 9.397 (2) Å, α = 88.81 (2)°, β = 108.88 (1)°, γ = 65.72 (1)° and Z = 1. These cell parameters were very close to those of $Mo_6S_6Cl_2(py)_6$ [13]. So the structure actually was not directly solved by any program, rather, the position parameters of the three unique Mo atoms in $Mo_6S_6Cl_2(py)_6$ were used as those of three W atoms, and directly put into least-square refinements in the space group $P\bar{1}$ with the CAD4-SDP program [74]. At this stage all of the 3754 observed reflections were used in refinements. A single digit percent R factor was produced immediately after the initial four least-square refinements. The positional parameters for sulfur atoms were found from the Fourier difference map, which was produced by subsequent Fourier synthesis, and put into further refinement. By using this combination of least-square refinements and Fourier synthesis techniques, all non-hydrogen atoms were located and refined anisotropically to residuals of $R = 0.034$, $Rw = 0.042$. Idealized hydrogen positions were then calculated and put into refinements, but their positional parameters and isotropic B values were held constant throughout the remainder of the refinements. The structure was refined finally to $R = 0.0267$, $Rw = 0.0359$, after deleting three reflections with large $\Delta F/\sigma F$ values. The final electron

Table 2: Summary of crystal data, intensity collection, and structure refinement

compound	**1**	**2**	**3**
formula	$W_6S_8(py)_6$	$W_6S_8(PEt_3)_6 \cdot 1.44C'H_2C'l_2$	$W_6S_8(THT)_6$
formula weight	1834.30	2190.85	1888.58
space group	$P\bar{1}$	$R\bar{3}$	$Ia3$
a, Å	10.624 (2)	17.305 (1)	20.246 (8)
b, Å	11.932 (3)	17.305 (1)	20.246 (8)
c, Å	9.397 (2)	19.640 (3)	20.246 (8)
α, deg	88.81 (2)	90	90
β, deg	108.88 (1)	90	90
γ, deg	65.72 (1)	120	90
V, Å^3	1010.9 (4)	5094 (1)	8298 (6)
Z	1	3	8
calcd density, g/cm^3	3.02	2.14	3.02
$\mu(Mo\ K\alpha)$, cm^{-1}	178.04	108.65	176.27
λ, Å	0.71073	0.71073	0.71069
takeoff angle, deg	4	4	6
2θ limit, deg	55	45	50
no. of unique data	4621	1991	1346
no. of data observed[a]	3754	1394	527
no. of para. refined	227	92	67
data/parameter	16.5	15.2	7.8
Trans. factors	0.6335–0.9962	0.6549–0.9986	0.84–1.00
[b]R	0.0267	0.0257	0.047
[c]Rw	0.0359	0.0361	0.048

[a]Reflections are considered as observed with ${F_o}^2 > 3\sigma({F_o}^2)$.
[b]$R = \Sigma||F_o| - |F_c||/\Sigma|F_o|$.
[c]$Rw = [\Sigma\omega(|F_o| - |F_c|)^2/\Sigma\omega|F_o|^2]^{1/2}$; $\omega = 1/\sigma^2(|F_o|)$.

Table 3: Positional parameters and equivalent-isotropic thermal parameters ($Å^2$) of non-hydrogen atoms for $W_6S_8(py)_6$

Atom	X	Y	Z	$^aB_{eq}$, $Å^2$
$W(1)$	0.45353 (3)	0.37434 (2)	0.55952 (3)	1.111 (5)
$W(2)$	0.62958 (3)	0.38581 (2)	0.41813 (3)	1.036 (5)
$W(3)$	0.65627 (3)	0.45502 (2)	0.68993 (3)	1.069 (5)
$S(1)$	0.4807 (2)	0.4470 (2)	0.8035 (2)	1.46 (3)
$S(2)$	0.1919 (2)	0.5337 (2)	0.4552 (2)	1.53 (3)
$S(3)$	0.7230 (2)	0.2375 (1)	0.6556 (2)	1.57 (3)
$S(4)$	0.4336 (2)	0.3208 (1)	0.3042 (2)	1.65 (3)
$N(1)$	0.4004 (6)	0.2230 (5)	0.6346 (7)	2.0 (1)
$N(2)$	0.7778 (6)	0.2476 (5)	0.3137 (6)	1.8 (1)
$N(3)$	0.8406 (6)	0.4056 (5)	0.9172 (6)	1.7 (1)
$C(1)$	0.281 (1)	0.2472 (8)	0.669 (1)	4.0 (2)
$C(2)$	0.248 (1)	0.156 (1)	0.719 (1)	5.3 (3)
$C(3)$	0.347 (1)	0.0308 (9)	0.736 (1)	5.8 (3)
$C(4)$	0.465 (1)	0.0056 (9)	0.693 (2)	7.2 (4)
$C(5)$	0.488 (1)	0.1034 (8)	0.646 (1)	4.9 (3)
$C(6)$	0.7266 (8)	0.2419 (6)	0.1641 (7)	1.8 (2)
$C(7)$	0.8152 (9)	0.1598 (8)	0.0965 (8)	2.9 (2)
$C(8)$	0.957 (1)	0.0777 (8)	0.1815 (9)	3.4 (2)
$C(9)$	1.012 (1)	0.0815 (9)	0.3351 (9)	3.4 (2)
$C(10)$	0.9186 (8)	0.1683 (7)	0.3955 (8)	2.3 (2)
$C(11)$	0.8148 (8)	0.4500 (7)	1.0411 (8)	2.3 (2)
$C(12)$	0.9258 (9)	0.4184 (7)	1.1820 (8)	2.5 (2)
$C(13)$	1.0686 (8)	0.3460 (8)	1.1989 (9)	2.7 (2)
$C(14)$	1.0992 (9)	0.3011 (9)	1.074 (1)	3.1 (2)
$C(15)$	0.9823 (8)	0.3321 (8)	0.9354 (8)	2.6 (2)

$^aB_{eq} = (4/3)[B_{11}a^2 + B_{22}b^2 + B_{33}c^2 + B_{12}ab(\cos\gamma) + B_{13}ac(\cos\beta) + B_{23}bc(\cos\alpha)]$.

Table 4: Anisotropic thermal parameters[a] (x 10^2, $Å^2$) of non-hydrogen atoms for $W_6S_8(py)_6$

Atom	U_{11}	U_{22}	U_{33}	U_{12}	U_{13}	U_{23}
W(1)	1.448 (8)	0.895 (9)	1.865 (9)	-0.320 (7)	0.846 (7)	-0.275 (8)
W(2)	1.199 (8)	0.886 (9)	1.632 (9)	-0.099 (7)	0.721 (7)	-0.309 (8)
W(3)	1.166 (8)	1.092 (9)	1.548 (9)	-0.190 (7)	0.588 (7)	-0.260 (8)
S(1)	1.92 (6)	1.57 (6)	1.93 (6)	-0.40 (5)	1.03 (5)	-0.15 (5)
S(2)	1.45 (6)	1.91 (6)	2.44 (7)	-0.59 (5)	0.92 (5)	-0.46 (6)
S(3)	1.91 (6)	0.99 (6)	2.38 (6)	0.12 (5)	0.98 (5)	-0.01 (6)
S(4)	2.25 (6)	1.55 (6)	2.50 (7)	-0.78 (5)	0.96 (5)	-0.89 (5)
N(1)	2.8 (2)	1.7 (2)	3.6 (3)	-1.0 (2)	1.6 (2)	-0.2 (2)
N(2)	2.5 (2)	1.7 (2)	3.0 (2)	-0.7 (2)	1.8 (2)	-1.0 (2)
N(3)	2.0 (2)	2.5 (2)	1.7 (2)	-0.8 (2)	0.6 (2)	-0.4 (2)
C(1)	5.9 (4)	3.1 (4)	8.1 (5)	-2.3 (3)	4.3 (3)	-1.3 (4)
C(2)	8.9 (4)	6.3 (5)	9.8 (5)	-5.0 (3)	7.1 (3)	-3.2 (4)
C(3)	9.9 (5)	5.3 (4)	10.9 (7)	-5.7 (3)	5.7 (4)	-1.6 (5)
C(4)	6.9 (5)	2.4 (4)	19 (1)	-2.7 (3)	5.2 (6)	-1.1 (6)
C(5)	6.5 (4)	3.5 (3)	11.7 (7)	-3.3 (3)	5.5 (4)	-2.3 (4)
C(6)	2.2 (3)	1.8 (3)	2.0 (3)	0.0 (2)	0.9 (2)	-0.3 (2)
C(7)	5.0 (3)	3.5 (4)	3.4 (3)	-1.8 (3)	2.9 (2)	-1.3 (3)
C(8)	4.7 (4)	2.5 (4)	4.6 (3)	0.8 (3)	3.3 (3)	-0.5 (3)
C(9)	3.7 (4)	3.4 (4)	4.1 (3)	0.7 (4)	2.5 (3)	-0.4 (3)
C(10)	2.3 (3)	2.3 (3)	2.9 (3)	0.3 (3)	1.3 (2)	0.0 (3)
C(11)	2.5 (3)	3.7 (4)	2.3 (3)	-1.0 (2)	1.2 (2)	-0.6 (3)
C(12)	4.2 (3)	3.5 (3)	2.5 (3)	-2.4 (2)	1.1 (3)	-1.2 (3)
C(13)	3.3 (3)	4.9 (4)	3.0 (3)	-2.5 (2)	1.1 (3)	-1.4 (3)
C(14)	1.9 (3)	4.9 (4)	3.8 (4)	-0.7 (3)	0.7 (3)	-0.7 (3)
C(15)	2.1 (3)	4.6 (4)	2.4 (3)	-1.0 (3)	0.7 (2)	-0.8 (3)

[a]The general temperature factor expression is: $\exp[-2\pi^2(U_{11}h^2a^{*2} + U_{22}k^2b^{*2} + U_{33}l^2c^{*2} + 2U_{12}hka^*b^* + 2U_{13}hla^*c^* + 2U_{23}klb^*c^*)]$.

density difference map showed the largest peak of 2.33 e/Å^3 and several peaks over 1.0 e/Å^3. In all cases these peaks were located near the tungsten atoms and were considered to be artifacts caused by Fourier series termination errors. The crystallographic data are summarized in Table 2; atomic positions and equivalent-isotropic thermal parameters of non-hydrogen atoms are given in Table 3; the anisotropical thermal parameters of non-hydrogen atoms are given in Table 4.

Structure determination for $W_6S_8(PEt_3)_6 \cdot 1.44CH_2Cl_2$

Single crystals were grown from dichloromethane solution of $W_6S_8(PEt_3)_6$ by standing at room temperature. They were regularly shaped in the form of cubes. They are not stable in air as they lose solvent and become polycrystalline quickly. A single crystal with dimensions 0.2 x 0.2 x 0.3 mm was chosen and taken directly out of solution, and rapidly mounted on the CAD-4 diffractometer with the use of a glass fiber. The low temperature nitrogen stream (−70°C) was immediately used to freeze the single crystal to avoid solvent loss.

Data were collected with an Enraf-Nonius CAD4 diffractometer at low temperature. Graphite-monochromated $Mo\ K\alpha$ radiation was employed to collect data with $4^\circ < 2\theta < 45^\circ$. The $\theta - 2\theta$ scan method was used. 1991 unique reflections were collected and 1394 of them were considered as observed with $F_o^2 > 3\sigma(F_o^2)$. The absorption coefficient for $Mo\ K\alpha$ is $\mu = 108.65$ cm-1. Three standard reflections, monitored every 300 reflections, showed no intensity variation during the data collection. An empirical absorption correction was applied, using a ϕ scan technique.

The space group was unambiguously chosen as $R\bar{3}$ based on the systematic extinctions. The structure was solved by Direct methods (SHELXS-86) [75] and refined

Table 5: Positional parameters and equivalent-isotropic thermal parameters ($Å^2$) of non-hydrogen atoms for $W_6S_8(PEt_3)_6 \cdot 1.44CH_2Cl_2$

Atom	X	Y	Z	$^a B_{eq}(Å^2)$
W	0.03461 (2)	0.10143 (2)	0.05542 (2)	1.531 (6)
S(1)	0	0	0.1526 (2)	1.97 (5)
S(2)	0.062 4(1)	0.1851 (1)	−0.0513 (1)	1.97 (4)
P	0.0862 (1)	0.2392 (1)	0.1267 (1)	2.22 (5)
C(1)	0.1624 (5)	0.2472 (5)	0.1961 (5)	2.7 (2)
C(2)	0.1996 (7)	0.3341 (7)	0.2409 (5)	4.4 (3)
C(3)	0.1443 (6)	0.3457 (5)	0.0801 (5)	3.1 (2)
C(4)	0.2349 (6)	0.3632 (6)	0.0481 (6)	3.6 (2)
C(5)	−0.0033 (5)	0.2517 (5)	0.1677 (5)	3.2 (2)
C(6)	−0.0559 (6)	0.1781 (6)	0.2211 (5)	3.7 (2)
^{b}Cl	0.1060 (5)	0.0634 (5)	0.6228 (5)	7.3 (2)
^{b}C(7)	0	0	0.661 (2)	7.0 (8)

$^a B_{eq} = (4/3)[B_{11}a^2 + B_{22}b^2 + B_{33}c^2 + B_{12}ab(\cos\gamma) + B_{13}ac(\cos\beta) + B_{23}bc(\cos\alpha)]$.

^{b}Cl and C(7) atoms were refined isotropically.

Table 6: Anisotropic thermal parameters[a] (x 10^2, Å^2) of non-hydrogen atoms for $W_6S_8(PEt_3)_6$ in $W_6S_8(PEt_3)_6 \cdot 1.44CH_2Cl_2$

Atom	U_{11}	U_{22}	U_{33}	U_{12}	U_{13}	U_{23}
W	1.96 (1)	1.87 (1)	2.00 (2)	0.969 (7)	-0.05 (1)	-0.12 (1)
S(1)	2.8 (1)	2.8	2.8	1.8 (2)	1.8	1.8
S(2)	2.46 (8)	2.12 (7)	2.8 (1)	1.09 (5)	0.02 (8)	0.37 (8)
P	3.08 (8)	2.61 (8)	2.8 (1)	1.45 (6)	-0.29 (9)	-0.75 (8)
C(1)	3.5 (3)	3.9 (4)	2.9 (5)	1.9 (2)	-0.7 (4)	-0.6 (4)
C(2)	5.6 (5)	6.0 (5)	4.0 (5)	2.1 (4)	-2.1 (5)	-3.0 (5)
C(3)	4.6 (4)	1.7 (3)	4.8 (6)	0.9 (3)	-0.5 (4)	-0.6 (4)
C(4)	3.2 (4)	4.4 (4)	5.1 (6)	1.4 (3)	0.2 (4)	1.4 (4)
C(5)	4.0 (3)	5.2 (4)	4.0 (5)	3.2 (2)	-0.1 (4)	-1.9 (4)
C(6)	3.9 (4)	5.3 (5)	4.6 (6)	2.0 (3)	0.6 (4)	-0.9 (5)

[a]The general temperature factor expression is: $\exp[-2\pi^2(U_{11}h^2a^{*2} + U_{22}k^2b^{*2} + U_{33}l^2c^{*2} + 2U_{12}hka^*b^* + 2U_{13}hla^*c^* + 2U_{23}klb^*c^*)]$.

with the CAD4-SDP program using the combination of least-square refinements and Fourier synthesis techniques. All the non-hydrogen atoms were refined anisotropically, except the carbon and chlorine atoms in dichloromethane solvent. The positions of hydrogen atoms were calculated and put into the refinement, but their position parameters and isotropic temperature factors were held constant throughout the refinements. The structure was refined to $R = 0.0257$, $Rw = 0.0361$ after deleting three reflections with large $\Delta F/\sigma F$ values. The crystallographic data are also summarized in Table 2; atomic positions and equivalent-isotropical thermal parameters of non-hydrogen atoms are given in Table 5, and anisotropic thermal parameters are given in Table 6.

Structure determination for $W_6S_8(THT)_6$

Single crystals were grown in neat tetrahydrothiophene solution by standing at room temperature. These purple single crystals were regularly shaped cubes, which is similar to $W_6S_8(PEt_3)_6 \cdot 1.44CH_2Cl_2$. But unlike the phosphine complex, these single crystals are much more stable in air. Crystals were mounted on glass fibers, and were given preliminary examination with rotation diffraction photographs. Those with best diffraction pattern were chosen for single crystal analysis.

Several sets of data were collected, all on a Rigaku AFC6R four-circle diffractometer with a rotating anode source from Molecular Structure Corporation. The first set was collected at room temperature. 25 reflections with $14^\circ < 2\theta < 35^\circ$ were searched and indexed to give an initial orientation matrix, lattice parameters and cell scalars. After a run of Delaunay and Laue programs, a body centered cubic cell was suggested. A half-hemisphere ($\pm$h,k,l) of reflections was collected, excluding

Table 7: Positional parameters and equivalent-isotropic thermal parameters ($Å^2$) of non-hydrogen atoms for $W_6S_8(THT)_6$

atom	X	Y	Z	$^aB_{eq}(Å^2)$
W	0.70844 (7)	0.17181 (6)	0.22268 (7)	2.09 (6)
$S(1)$	0.6652 (4)	0.6652	0.6652	2.732 (4)
$S(2)$	0.7591 (4)	0.1927 (4)	0.1146 (4)	2.6 (4)
$S(3)$	0.6505 (5)	0.0667 (4)	0.1849 (5)	3.7 (5)
$C(1)$	0.711 (2)	0.012 (2)	0.151 (2)	5 (2)
$C(2)$	0.692 (3)	0.006 (3)	0.079 (2)	9 (3)
$C(3)$	0.639 (4)	0.035 (3)	0.059 (3)	16 (6)
$C(4)$	0.608 (2)	0.076 (2)	0.109 (2)	6 (3)

$^aB_{eq} = (4/3)[B_{11}a^2 + B_{22}b^2 + B_{33}c^2 + B_{12}ab(\cos\gamma) + B_{13}ac(\cos\beta) + B_{23}bc(\cos\alpha)]$.

Table 8: Anisotropic thermal parameters[a] (x 10^2, $Å^2$) of non-hydrogen atoms for $W_6S_8(THT)_6$

atom	U_{11}	U_{22}	U_{33}	U_{12}	U_{13}	U_{23}
W	2.83 (8)	2.34 (7)	2.78 (7)	-0.28 (6)	0.15 (7)	0.19(7)
S(1)	3.460 (4)	3.460	3.460	-0.2 (4)	-0.2	-0.2
S(2)	3.4 (5)	3.8 (5)	2.5 (5)	-0.6 (4)	0.2 (4)	-0.2 (4)
S(3)	5.9 (7)	3.2 (5)	4.7 (6)	-1.4 (5)	1.3 (5)	-0.2 (4)
C(1)	6 (3)	5 (2)	8 (3)	-1 (2)	-1 (3)	-0 (2)
C(2)	16 (6)	11 (4)	7 (3)	10 (4)	6 (4)	0 (3)
C(3)	40 (10)	15 (6)	10 (4)	17 (7)	-14 (6)	-10 (4)
C(4)	11 (4)	3 (2)	9 (4)	-1 (3)	-7 (3)	2(2)

[a]The general temperature factor expression is: $\exp[-2\pi^2(U_{11}h^2a^{*2} + U_{22}k^2b^{*2} + U_{33}l^2c^{*2} + 2U_{12}hka^*b^* + 2U_{13}hla^*c^* + 2U_{23}klb^*c^*)]$.

those reflections expected to be systematically extinct. Three strong reflections used as standards were checked every 150 reflections and very little deviation in intensity was seen. A total of 3610 (unaveraged) reflections with $4^\circ < 2\theta < 50^\circ$ was collected, with the use of the $2\theta - \omega$ scans technique. Of these reflections, 936 were observed. The data set was worked up using the TEXSAN [76] software package. MITHRIL [77], a direct methods program, was used to determine the position of the unique W atom and the other atoms were located from the Fourier difference map. A partial structure was solved in $Ia3$ space group with the R-factor down to 7%. However, many of the non-heavy atoms (including one sulfur atom) could not be refined anisotropically. It was believed to be caused by inadequate data, which was in turn caused by the poor quality of the crystal chosen.

The best set of data was collected at -65°C. The quality of the crystal was the best among those chosen as evidenced by the peak profile of the 25 reflections searched before data collection. For most of the crystals of this tetrahydrothiophene complex, it was common that the peak profile of reflections was frequently broad or with shoulder, indicating poor quality of the crystals. With the improvement of the crystal quality, the structure was refined down to $R = 0.052$, $Rw = 0.056$ by using the same procedures as those of the first data set. At this stage, two carbon atoms in the tetrahydrothiophene ligand still could not be refined anisotropically. After four reflections with large $\Delta F/\sigma F$ values were deleted, all of the non-hydrogen atoms were refined anisotropically. Finally, idealized hydrogen positions were calculated and put into the refinements (with their positional parameters and isotropical thermal factors held constant), and the structure was refined down to $R = 0.047$, $R_w = 0.048$. The crystallographic data are included in Table 2; atomic positions and equivalent-

isotropic thermal parameterss of non-hydrogen atoms are listed in Table 7; anisotropic thermal parameters of non-hydrogen atoms in the cluster are given in Table 8.

RESULTS AND DISCUSSION

Syntheses

Sulfidation reactions

In the ideal but still unknown "tungsten Chevrel phases" "W_6S_8" and "$M_xW_6S_8$", the essential cluster units W_6S_8 of the framework should consist of an octahedron of bonded W atoms, with a bridging S atom capping each face of the octahedron. These cluster units are almost identical to those of the well-known α-tungsten(II) halides $(W_6X_8)X_4$, except in the latter case, halides cap the faces of the octahedron instead of sulfides. Thus it should be possible to start with the α-tungsten(II) halides and substitute the bridging halides by sulfides to form the desired W_6S_8 cluster, providing that the cluster units are sufficiently robust to survive the reaction conditions.

Substitution of sulfide for chloride in $Mo_6Cl_8{}^{4+}$, the molybdenum analogue of $W_6Cl_8{}^{4+}$, has been extensively investigated earlier in this research group. Previous workers have found that sodium hydrosulfide is a decent sulfiding agent for the $Mo_6Cl_8{}^{4+}$ cluster compound. Michel demonstrated the first sulfide-substituted hexamolybdenum cluster $Mo_6Cl_7S^{3+}$ by reacting two moles of $NaSH$ per mole of $Mo_6Cl_8{}^{4+}$ in refluxing pyridine [12], as well as an extensively substituted cluster $Mo_6S_6Cl_2(py)_6$ by reacting eight moles of $NaSH$ per mole of $Mo_6Cl_8{}^{4+}$ at higher temperature (200°C) in pyridine in a sealed Pyrex ampoule [13]. Later Laughlin systematically studied the reactions between $Mo_6Cl_8{}^{4+}$ and $NaSH$ at different stoichiometries, with or without presence of $NaOBu^n$ [14].

So sodium hydrosulfide was chosen as the sulfiding agent for the studies of sulfidation of $W_6Cl_8{}^{4+}$. The first reaction studied was that with the 1:2 stoichiometry

(i.e., two moles of hydrosulfide per mole of cluster unit) in refluxing pyridine for one day. The reaction conditions and procedures were similar to the synthesis of the first sulfided hexamolybdenum cluster $Mo_6Cl_7S^{3+}$, and the initial target was indeed $W_6Cl_7S^{3+}$. However, all of the subsequent efforts (similar to the molybdenum case) to isolate any yield of $W_6Cl_7S^{3+}$ from the pyridine filtrate solution failed. It was found later that the material from the pyridine solution was the simple pyridine adduct of W_6Cl_{12} by the comparison of the infrared spectra. This was also supported by the chlorine analysis of the product isolated from the HCl methanol solution extraction. At this stage it was questioned whether any sulfidation ever happened. In the earlier runs of this 1:2 reaction, repeated efforts had been put into "isolation of $W_6Cl_7S^{3+}$ from pyridine solution" and no attention was paid to the insoluble solid separated from the pyridine solution by filtration of the reaction mixture. It was observed that this solid was in extremely small amount and was thought to be sodium chloride and/or sodium hydrosulfide which are not very soluble in pyridine. It was much later that infrared spectra were obtained for this solid, and the result was surprising. The far-infrared of this solid, as shown in Figure 6, clearly showed a broad band around 380 cm^{-1}, which was obviously out of the $W-Cl$ stretching range between 320 and 280 cm^{-1}. This band was believed to arise from $W-S$ stretching in a much more extensively sulfided cluster. The small amount of highly substituted cluster would also agree with the small amount of the sulfiding agent used. But analytical data of this trace of brown solid could not be obtained.

The studies of sulfidation reactions with higher $NaSH$/cluster ratios provide much more information. For the 1:6 reaction, the major product was still soluble in pyridine solution while the insoluble part was still in extremely small amount.

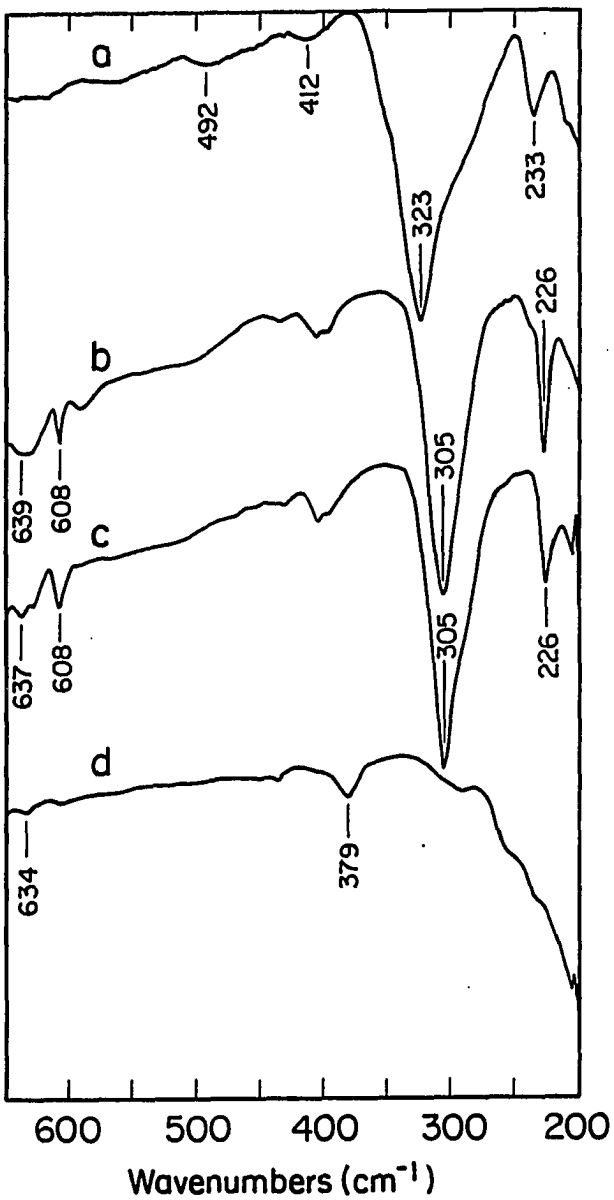

Figure 6: Far-infrared spectra of α-tungsten(II) chloride (a), pyridine adduct of α-tungsten(II) chloride (b), soluble product (c) and insoluble product of the 1:2 reaction (d)

Characterization of the major product indicated that substitution of sulfide into the bridging positions of the cluster does indeed occur. Analytical data gave molar ratios of $Cl/W_6 = 8.0$ for this pyridine soluble product, which was a dark yellow solid obtained after stripping of pyridine and drying under vacuum. So four chlorides per $W_6Cl_8Cl_4$ had been removed. Assuming chlorides were substituted by sulfides, the formula could be written as $(W_6Cl_6S_2)Cl_2(py)_n$. It must be pointed out that this formula does not necessarily mean that only one species is formed, as the material could be and probably was a mixture of sulfide-chloride clusters with average Cl/W_6 ratio of 8.0. The far-infrared spectrum of the major product is shown in Figure 8.[3] The strong broad band at 284 cm^{-1} falls right into the range of $W - Cl$ stretching vibration, indicating that there was still a dominate amount of chlorides in the cluster. Meanwhile, a weak band at 399 cm^{-1} emerged roughly at the same position as the strongest band in the far-infrared spectrum of the insoluble solid of the 1:2 reaction. This band is assigned as a vibration of primarily $W - S$ stretching, and its weak intensity relative to the intensity of the $W - Cl$ vibration corresponds well with the formula in which there are six bridged chlorides and two terminal chlorides *vs* only two bridged sulfides. Characterization of the insoluble minor product was not achieved due to the extremely small amount of the material.

The 1:8 reaction yielded less pyridine soluble product and more insoluble product. For the soluble part, a formula of $(W_6S_{1.7}Cl_{6.3})Cl_{2.3}(py)_n$ was deduced from the analytical data. The far-infrared spectrum of this material, as shown in Figure 8, was almost identical to that of $(W_6S_2Cl_6)Cl_2(py)_n$, featuring a strong band from

[3] All of the figures showing infrared spectra, except Figure 6, are included in the discussion of infrared spectra, which comes next.

the $W-Cl$ stretching vibration *vs* a weak band from the $W-S$ stretching vibration. The major product of this reaction was a red powder obtained from the pyridine insoluble material after removal of sodium chloride by methanol extraction. Analytical data indicated that its formula was close to $W_6S_{6.3}Cl_{1.7}(py)_6$. The far-infrared spectrum, as shown in Figure 9, indicated a much stronger $W-S$ stretching band than $W-Cl$ stretching band.

These results are slightly different from those of sulfidation reactions of Mo_6Cl_{12} with $NaSH$. First the solid products contain more deeply sulfided clusters compared to the molybdenum cases. In the latter cases, 1:6 reaction in refluxing pyridine/butanol solution produces fine powders of $Mo_6S_{3+x}Cl_{6-2x}(py)n$ $(0.1 < x < 0.5)$ [14], and the highly sulfided cluster $Mo_6S_6Cl_2(py)_6$ is only obtainable at much higher temperature [13]. Secondly the sulfidation of the soluble products was realized only when large amounts of $NaSH$ were used. It seems that subsequent sulfidation is promoted by introduction of initial sulfide into the W_6X_8 cluster during the substitution process, until the formation of a highly sulfided cluster like $W_6S_6Cl_2(py)_6$ is removed from the reaction process by precipitation.

The complete understanding of the mechanisms of the sulfidation process are impossible at this stage, however, multi-step reactions are probably involved. To best explain the results obtained for the paticular reactions performed, the following equations are proposed:

$$W_6Cl_{12} + 4NaSH \rightleftharpoons (W_6S_2Cl_6)Cl_2 + 4NaCl + 2H_2S \quad (14)$$

$$(W_6S_2Cl_6)Cl_2 + 4NaSH \rightleftharpoons W_6S_4Cl_4 + 4NaCl + 2H_2S \quad (15)$$

$$W_6S_4Cl_4 + 2NaSH \longrightarrow W_6S_6Cl_2 + 2NaCl + H_2 \quad (16)$$

For the reason of simplification the cluster cores are used in these equations, but actually all of them should be molecular derivatives with coordinated pyridine. For the same reason H_2S stands for pyridinium hydrosulfide here. Equations 14 and 15 describe the exchange of sulfides and chlorides among the 24 electron clusters. They contain $NaSH$ and H_2S on the left and right sides of the equations respectively. Equation 16 represents the oxidation of a 24 electron cluster to a 22 electron cluster, and involves only $NaSH$ as a reactant. Generally speaking, the sulfidation process tends to the formation of a highly sulfided cluster like $W_6S_6Cl_2$ no matter how much $NaSH$ is used. In the case of a 1:2 reaction, a small amount of highly sulfided material accounted for almost all of the sulfidation while any intermediate sulfide-chloride clusters were completely masked by the large amount of simple pyridine adduct of the starting material W_6Cl_{12}. When a 1:6 ratio was applied, the build-up of by-product H_2S during the sulfidation helped to sustain the intermediate cluster like $W_6S_2Cl_6$ as shown in equations 14 and 15. If more $NaSH$ was used like in the 1:8 reaction, the reinforcement of $NaSH$ helped the sulfidation to go further so that highly sulfided cluster became the major product.

Based on the proposed reaction routes, a better option to increase the extent of sulfidation would be removal of by-product H_2S so that the equilibriums expressed in equations 14 and 15 could shift to the right side. Addition of $NaOBu^n$ as proton acceptor had been used and proved to be successful. The 1:8:4 reaction gave a high yield of highly sulfided cluster with the formula close to $W_6S_6Cl_2(py)_6$. The following reactions are given as illustrative steps in the sulfidation process:

$$W_6Cl_{12} + 2NaSH + 2NaOBu^n \longrightarrow (W_6S_2Cl_6)Cl_2 + 4NaCl + 2HOBu^n \quad (17)$$

$$(W_6S_2Cl_6)Cl_2 + 2NaSH + 2NaOBu^n \longrightarrow W_6S_4Cl_4 + 4NaCl + 2HOBu^n \quad (18)$$

$$W_6S_4Cl_4 + 2NaSH \longrightarrow W_6S_6Cl_2 + 2NaCl + H_2$$

The overall reaction is illustrated in equation 19:

$$W_6Cl_{12} + 6NaSH + 4NaOBu^n \longrightarrow W_6S_6Cl_2 + 10NaCl + 4HOBu^n + H_2 \quad (19)$$

By calculation there should be about two moles of $NaSH$ per mole of cluster left, and ideally the sulfidation could continue with concommitant oxidation of the cluster to a 20 electron cluster unit:

$$W_6S_6Cl_2 + 2NaSH \longrightarrow W_6S_8 + 2NaCl + H_2 \quad (20)$$

But apparently little of this complete sulfidation actually occurred. In a separate reaction which followed the 1:8:4 reaction, $W_6S_6Cl_2(py)_6$ was treated with four moles of $NaSH$ in refluxing pyridine and $W_6S_8(py)_6$ was obtained as the major product. The minor product, which was recovered from the pyridine solution, indicated a surprisingly new far-infrared spectrum as shown in Figure 10. The strong broad

band at 466 cm^{-1} can not be from either $W-S$ or $W-Cl$ vibrations in a W_6X_8 cluster. Although the identity of this minor product is not understood, it is evident that complete sulfidation can be achieved when $W_6S_6Cl_2(py)_6$ is further treated with an excess amount of $NaSH$ in refluxing pyridine.

The complete sulfidation of the cluster was also successfully achieved in a one step reaction of 1:12:6 stoichiometry. The pyridine filtrate from the reaction mixture was almost colorless, which indicated that the solid product was obtained essentially in quantitative yield. Chlorine analysis confirmed the complete removal of the chlorides in the final product after methanol extraction washed away the inorganic salts like sodium chloride, sodium n-butoxide and sodium hydrosulfide. The complete analytical data of W, S, N, C and H indicated that the product had a formula of $W_6S_8(py)_6$. In its far-infrared spectrum the $W-S$ stretching vibration was manifested as the strong band at 378 cm^{-1}, while there was an absence of any $W-Cl$ vibration. The overall reaction is illustrated in equation 21:

$$W_6Cl_{12} + 8NaSH + 4NaOBu^n + 6py \longrightarrow W_6S_8(py)_6 + 12NaCl + 4HOBu^n + 2H_2 \qquad (21)$$

$W_6S_8(py)_6$ is a red, relatively air stable compound. It has extremely low solubility in organic solvents including pyridine. Its powder diffraction pattern shows only several weak lines, indicating that the material is poorly crystalline. Crystalline $W_6S_8(py)_6$ is obtained by heating the mixture of powder and pyridine at 200°C in a sealed Pyrex ampoule over at least several days. At such high temperature the solubility of $W_6S_8(py)_6$ in pyridine is believed to be increased. By applying a small

temperature gradient, $W_6S_8(py)_6$ slowly crystallizes out of pyridine solution at the site of lower temperature because of the solubility difference. The low solubility of the cluster is reflected by the still colorless pyridine liquid when the mixture is returned to room temperature. This sealed ampoule technique was first used by Michel in his synthesis of $Mo_6S_6Cl_2(py)_6$ [13]. An important safety note is that at such elevated temperature the vapor pressure of pyridine is really high, so in order to avoid explosion one must manipulate the temperatures carefully.

Ligand exchange reactions

Once the complete substitution of sulfide for chloride was established in the novel complex $W_6S_8(py)_6$, as the first example of the $W_6S_8L_6$ molecular derivatives, it became important to establish more molecular derivatives of this type and study their chemistry. Ligand exchange reactions not only can lead to the discovery of more new cluster derivatives and give an understanding of their ligand exchange properties, but also may bring the $W_6S_8L_6$ clusters into solution by choosing suitable coordinated ligands. While the importance of the former is obvious, the latter is particularly important in such ways that crystalline cluster complexes may be obtained and structurally characterized to confirm the presence of the hexatungsten cluster core. Studies of the soluble molecular derivatives could be essential in order to establish them as the molecular precursors to the still unknown ternary tungsten sulfides $M_xW_6S_8$.

The studies were focused on the completely sulfided clusters $W_6S_8L_6$, and the pyridine adduct was the initial starting complex simply because it was the first established one. But before concentrating on $W_6S_8L_6$, it's worthwhile to briefly discuss

the result of the reaction between $W_6S_6Cl_2(py)_6$ and triethylphosphine. At the early stage of studies of sulfidation on W_6Cl_{12}, there once remained questions or uncertainties about the removal of sodium chloride by-product from the highly sulfided clusters by methanol extraction. Although methanol should dissolve all the sodium chloride and other inorganic salts, because the methanol extraction took several days, it was questioned whether or not a complete removal of sodium chloride had succeeded. If not, the chlorine analysis would give higher chlorine content and thus misguide the calculation of the cluster sulfidation. Particularly for the 1:8:4 reaction, the product was formulated as $W_6S_6Cl_2(py)_6$ based on chlorine analysis. Subsequent treatment of this product with excess triethylphosphine in refluxing toluene led to the formation of a soluble cluster complex, and any possible sodium chloride was separated by filtration. Chlorine analysis of the dark yellow solid recovered from the filtrate solution indicated that its formula was close to $W_6S_6Cl_2(PEt_3)_6$. The result of this simple reaction confirms not only the still incomplete sulfidation by the 1:8:4 reaction but also the complete removal of sodium chloride by methanol extraction. However, interpretation of the ^{31}P NMR spectrum of this triethylphosphine complex is uncertain. Only one resonance was observed at the same chemical shift value as that for $W_6S_8(PEt_3)_6$, discussed below. It is believed that this compound is present as one component of a mixture. The species $W_6S_6Cl_2(PEt_3)_6$ should be paramagnetic and its resonance may be broadened so much that it can not be seen under ordinary conditions.

When $W_6S_8(py)_6$ was stirred with excess triethylphosphine in toluene at room temperature, no ligand displacement occurred as the red powder remained unchanged in the colorless solution. But when the mixture was brought to reflux, almost ev-

erything dissolved to form a greenish-yellow solution within several hours. A dark yellow solid was recovered from the filtrate solution by stripping of the solvent and excess triethylphosphine under vacuum. The infrared spectra of this product indicated the complete disappearance of bands arising from coordinated pyridine and the appearance of bands characteristic of coordinated triethylphosphine. One band with little change from that of the pyridine adduct is the strong band at 387 cm^{-1}, characteristic of the $W-S$ stretching vibration in the hexatungsten cluster. Apparently the complete substitution of phosphine for pyridine was achieved, as illustrated in equation 22:

$$W_6S_8(py)_6 + 6PEt_3 \quad \text{—} \quad W_6S_8(PEt_3)_6 + 6py \tag{22}$$

Unlike the pyridine adduct, the phosphine adduct is quite soluble in many organic solvents like dichloromethane, tetrahydrofuran, and of course toluene. It thus became possible for the first time to study the cluster in solution. The proton decoupled ^{31}P NMR spectrum was obtained and shown in Figure 7. The appearance of a single phosphorus signal strongly supports the existence of an undistorted octahedral cluster in solution, and clearly demonstrates the survival of the hexatungsten cluster through the earlier sulfidation reaction and the ligand exchange of phosphine for pyridine in $W_6S_8(py)_6$.

Identical results have been achieved in studies of the ligand exchange of phosphine for pyridine in the analogous hexamolybdenum sulfide cluster $Mo_6S_8(py)n$ $(3 < n < 5)$ by other researchers in this group [17]. Meanwhile, Saito and coworkers have established the same compound $W_6S_8(PEt_3)_6$ through another unrelated synthetic pathway at the same time as this work [78], as well as $Mo_6S_8(PEt_3)_6$

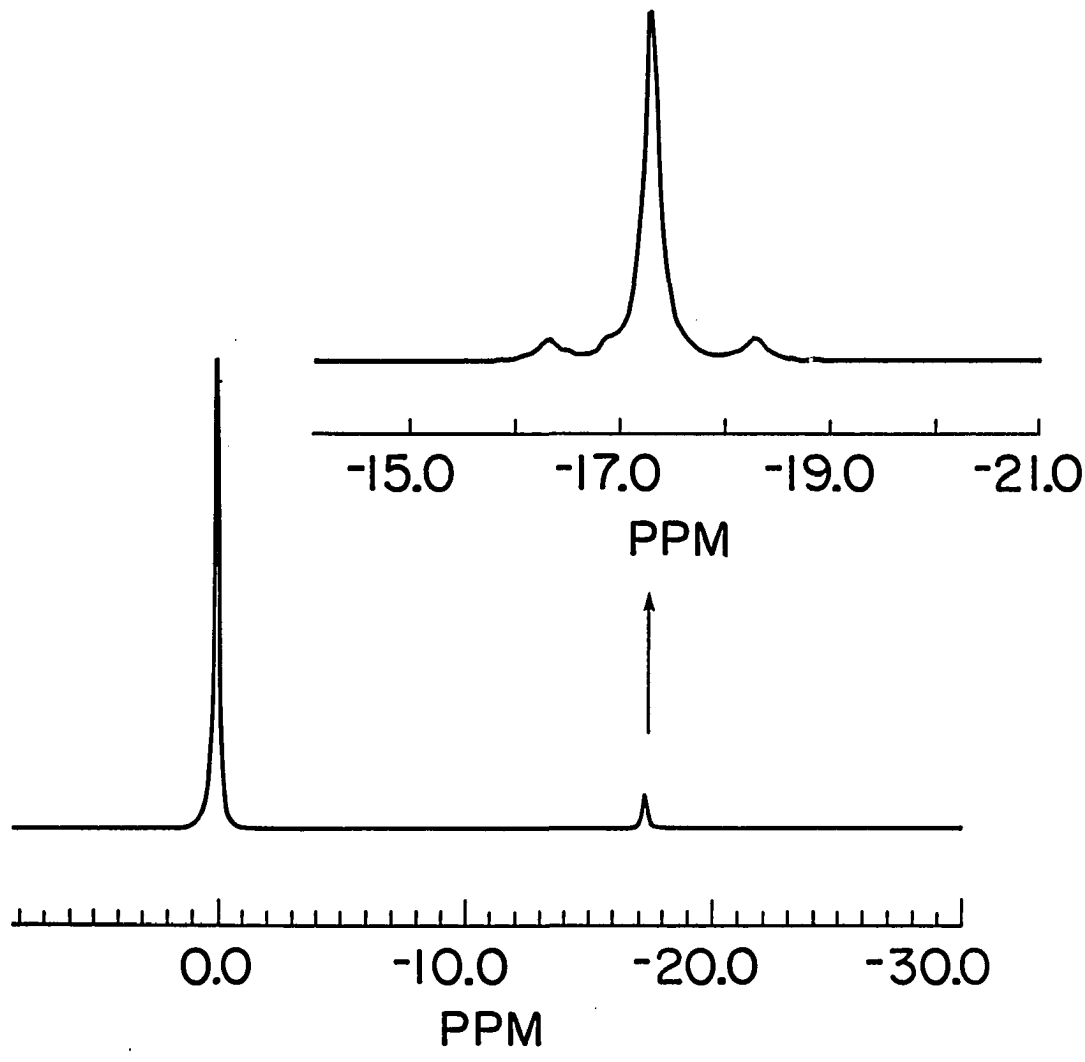

Figure 7: Proton decoupled ^{31}P nuclear magnetic resonance spectrum of $W_6S_8(PEt_3)_6$

a little earlier [19]. In their studies single crystal diffraction analysis was used to characterize the existence of $W_6S_8(PEt_3)_6$,[4] and information about its electronic spectroscopy as well as electrochemistry was also included. Their synthetic route includes the interesting and quite unique reductive dimerization of trimeric tungsten cluster, which was prepared from reaction of W_6Cl_{12} with elemental sulfur. After separation of the $W_6S_8(PEt_3)_6$ by column chromatography the net yield was very low at 10%. The synthetic route in this dissertation has the advantage that the hexatungsten cluster core from the starting material W_6Cl_{12} has been utilized, and thus a high yield of single product is available through relatively mild reaction and easy separation conditions.

The ligand displacement of tetrahydrothiophene for pyridine in $W_6S_8(py)_6$ was also achieved, by refluxing the pyridine adduct and neat tetrahydrothiophene overnight. As in the case of reaction with phosphine, heating was necessary to overcome the bonding between coordinated pyridine and the cluster otherwise ligand displacement could not occur at a convenient rate. The overall process is given in equation 23:

$$W_6S_8(py)_6 + 6THT \quad \text{---} \quad W_6S_8(THT)_6 + 6py \tag{23}$$

The tetrahydrothiophene adduct was soluble in the solution. The product was recovered by either stripping of the solvent followed by treatment with ether to break the resulting oil, or reducing the volume of the solution followed by crystallization at room temperature for several days. Infrared spectra confirmed the complete removal

[4]The result from structure determination will be compared with that of $W_6S_8(PEt_3)_6 \cdot 1.44CH_2Cl_2$ established in this dissertation in the discussion of crystal structures later.

of coordinated pyridine and the preservation of the $W-S$ vibration in the cluster as a strong band at 384 cm^{-1}. $W_6S_8(THT)_6$ is air stable. The dark purple crystals, after exposure to air for weeks, still give strong x-ray diffraction photographs. But unlike the phosphine adduct, this material is much less soluble in other organic solvents like dichloromethane, toluene and tetrahydrofuran.

Conversion from $W_6S_8(PEt_3)_6$ back to $W_6S_8(py)_6$ in liquid pyridine has been tried but found to be unsuccessful. The phosphine adduct was immediately solubilized when pyridine was introduced to form a dark yellow solution. But the insoluble pyridine complex was not obtained even when the solution was refluxed for several days. The resulting solution appeared no different from the initial solution. Stripping of the solvent under vacuum led to an oily residue which was not further characterized. It's unclear whether any phosphine was replaced by pyridine, beyond the fact that $W_6S_8(py)_6$ was not precipitated even at reflux condition in neat pyridine. The phosphine adduct seems at least kinetically more stable than the pyridine adduct.

Conversion from $W_6S_8(THT)_6$ back to pyridine has also been tried in neat pyridine. Like the phosphine case, a dark yellow solution was formed when pyridine was introduced to $W_6S_8(THT)_6$. But when the solution was stirred at room temperature, an extremely fine red powder gradually precipitated out of solution. This powder was so fine that filtering did not separate any solid from the filtrate. This pyridine mixture was then brought to reflux for one day. A red powder was separated from a still yellow solution by filtering and then dried. Infrared spectra, which constitute a powerful characterization tool for many of the discussed clusters, indicated that the cluster is apparently still preserved based on the strong $W-S$ vibration at 379 cm^{-1}. Appearance of coordinated pyridine bands supports the ligand

displacement of pyridine for tetrahydrothiophine. But some bands characteristic of coordinated tetrahydrothiophene, although extremely weak, are still present. So the complete ligand displacement may not be achieved.

These results suggest a relative stability order of the molecular derivatives of the W_6S_8 cluster unit, at least kinetically. The triethylphosphine adduct is the most stable one, while the tetrahydrothiophene adduct is about the same as, or slightly more stable than the pyridine adduct. In other words, the bondings between the hexatungsten cluster and the organic ligands appear to have the following order: $PEt_3 > THT \geq py$.

Infrared Spectra

All infrared spectra were collected using a paraffin oil mull of the sample between two cesium iodide pressed plates. Samples were prepared in the drybox and were temporarily stored under nitrogen before being placed into the sample chamber of the instrument which was constantly purged with nitrogen. Spectra were recorded separately in the mid-infrared (4000–400 cm^{-1}) and far-infrared (650–200 cm^{-1}) regions. These infrared spectra have proved to be a powerful characterization method, as the molecular cluster derivatives have bands characteristic of tungsten-chloride stretching, tungsten-sulfide stretching, and coordinated organic ligands.

The far-infrared spectra of the hexatungsten chloride clusters contain strong absorption bands below 350 cm^{-1}. Amorphous α-tungsten(II) chloride, according to the studies of R. D. Hogue and R. E. McCarley, shows a very strong band at 321 cm^{-1}, a shoulder at 294 cm^{-1} and a medium band at 233 cm^{-1} [50]. These three bands are assigned as internal W_6Cl_8 stretching modes, and the tungsten-terminal

chloride stretching is also contained in that strong band at 321 cm^{-1}. The far-infrared spectrum of the $\alpha - WCl_2$ recorded in this study barely contains that (very weak) shoulder, but does contain a very strong band at 323 cm^{-1} and a medium band at 233 cm^{-1} (see Figure 5). The pyridine adduct of this chloride cluster shows a strong band at 306 cm^{-1} and a medium band at 227 cm^{-1}. In spite of the mixing among the internal stretching modes in W_6Cl_8, the bands at 300 cm^{-1} region might be attributed to tungsten-chloride stretchings (including tungsten-internal chloride and tungsten-terminal chloride) and the bands at 230 cm^{-1} region might be attributed to tungsten-tungsten stretchings. Substitution of sulfide into the W_6Cl_8 cluster unit always decreases the intensities of the bands in the tungsten-chloride region, while new bands appear in the 380–410 cm^{-1} region. Apparently the new bands are to high to be considered as tungsten-chloride stretchings, and they are generally regarded as tungsten-sulfide stretching modes of the cluster despite the possible mixing of the W_6X_8 internal modes. The bands at 230 cm^{-1} region usually change little, a indication that the hexatungsten cluster unit is preserved.

While the tungsten-chloride, tungsten-sulfide and tungsten-tungsten stretching bands are located in the far-infrared region, bands characteristic of coordinated organic ligands are over both the mid- and far-infrared regions. For example, the pyridine adducts show a set of peaks (see Table 9) from 1600 to 690 cm^{-1}, as well as two bands below 650 cm^{-1}. It has been thoroughly studied and well recognized that the majority of infrared bands which originate in the internal vibrations of pyridine recur on an approximately band-for-band basis in the spectra of pyridine complexes [79]. Generally speaking, the bands shown in the mid-infrared region are either carbon-carbon (ring modes) or carbon-hydrogen modes. The distinction between the two

Table 9: Absorption frequencies (cm^{-1}), found in the infrared spectra of pyridine derivatives

Free py^a	Coord. py^a	py adduct of W_6Cl_{12}	$W_6S_8(py)_6$
1627 (w,b)[b]		1634 (vw)	
1578 (s,sh)	1598 (s)	1599 (w)	1597 (m)
1570 (w)		1537 (vw)	1564 (vw)
			1350 (w)
	1240 (w)	1261 (w)	1231 (vw)
1217 (w)	1217 (w)	1217 (w)	1213 (s)
1145 (w)	1145 (w)	1163 (vw)	1148 (m)
1067 (w)	1070 (w)	1067 (w)	1067 (s)
1031 (w)	1031 (w)	1038 (w)	1040 (m)
991 (w)	990 (w)	1005 (w)	1009 (vw)
			937 (vw)
		868 (w)	870 (vw)
		806 (w)	
	750 (w)	752 (m)	756 (s)
	691 (w)	690 (w)	687 (s)
		677 (w)	
601 (s)	625 (m)	639 (vw)	634 (w)
		608 (w)	
403 (m)	420 (m)	406 (vw)	435 (w)
		306 (vs)	378 (vs)
		227 (m)	232 (ms)

[a] Literature values [79].

[b] Relative intensities given in the parentheses: s = strong, m = medium, w = weak, v = very, sh = shoulder, b = broad.

groups has been clear since the studies of the infrared spectra of normal and deuterated molecules of numerous heterocyclic nitrogenous ligands and their complexes by Thornton and coworkers [80]. But it's beyond the purpose of this dissertation to specify the actual assignments of these bands. The two bands in the far-infrared spectra occur at 600 cm^{-1} (in-plane ring bend) and 400 cm^{-1} (out-of-plane ring bend) regions. These bands, especially the two in far-infrared region, are very characteristic of coordinated pyridine in the cluster complexes. The triethylphosphine and tetrahydrothiophene adducts also have their own characteristic bands from the coordinated ligands.

The spectra of the cluster species recovered from pyridine solutions of the W_6Cl_{12} and $NaSH$ reactions are similar to each other (see Table 10). The bands of the 1:2 reaction product are essentially identical to those of the pyridine adduct of W_6Cl_{12}. For the 1:6 and 1:8 reaction products, pyridine bands at 1634, 1605, 1533, 1252, 1217, 1155, 1069, 1043, 1003, 754, and 685 cm^{-1} in the mid-infrared region are almost identical to those of the W_6Cl_{12} pyridine adduct. In the far-infrared spectra (also shown in Figure 8), two bands over 600 cm^{-1}, which are considered as in-plane ring bends, are also very similar to those of the unsulfided pyridine adduct. In the cases examined the band at 608 cm^{-1} is always stronger than that at 639 cm^{-1}. The possible reason for this double appearance of in-plane ring bend might be that there is a lot of free pyridine in these pyridine soluble clusters, all of which are obtained as glassy solids by pumping the pyridine solutions to dryness. A material containing more than the expected number of coordinated pyridines is indicated by the tungsten and chlorine analyses. It is known that free pyridine shows the in-plane ring bend near 601 cm^{-1} [79]. One notable difference is the shifting of the out-of-plane ring

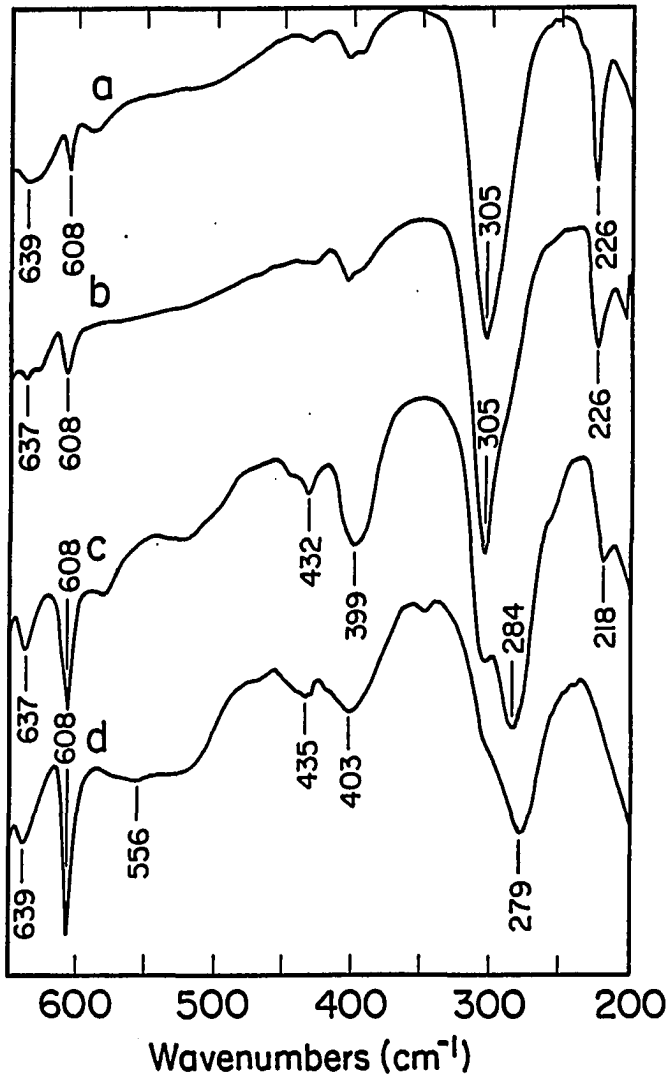

Figure 8: Far-infrared spectra of simple pyridine adduct of W_6Cl_{12} (a), soluble product of the 1:2 reaction (b), 1:6 reaction (c), and 1:8 reaction (d)

Table 10: Absorption frequencies (cm^{-1}), found in the infrared spectra of the soluble clusters from sulfidation reactions

py adduct of W_6Cl_{12}	1:2	1:6	1:8
1634 (vw)[a]	1633 (vw)	1633 (vw)	1634 (vw)
1599 (w)	1605 (w)	1607 (w)	1605 (m)
1537 (vw)	1535 (vw)	1537 (w)	1533 (w)
1261 (w)		1252 (w)	1252 (vw)
1217 (w)	1215(w)	1217 (w)	1217 (m)
1163 (vw)	1155 (vw)	1155 (vw)	1155 (vw)
1067 (w)	1067 (w)	1067 (w)	1069 (m)
1038 (w)	1043 (w)	1043 (w)	1043 (w)
1005 (w)	1005 (w)	1005 (w)	1005 (w)
			943 (vw)
868 (vw)			
806 (vw)			
752 (m)	750 (m)	752 (ms)	754 (ms)
690 (w)			685 (ms)
677 (w)	677 (w)	679 (m)	
639 (vw)	637 (vw)	637 (vw)	639 (vw)
609 (w)	608 (w)	608 (m)	608 (m)
406 (vw)	406 (vw)	432 (w)	435 (w)
		399 (m)	403 (w)
306 (vs)	305 (vs)	310 (sh)	310 (sh)
	. .	284 (vs)	279 (vs)
227 (m)	226 (m)	218 (w)	

[a]Relative intensities given in the parentheses: s = strong, m = medium, w = weak, v = very, sh = shoulder, b = broad.

bend to 432 and 435 cm^{-1}, respectively, for 1:6 and 1:8 products, from 403 cm^{-1} of the W_6Cl_{12} pyridine adduct. The bands falling into the range of tungsten-chloride stretching vibrations, at 284 and 279 cm^{-1}, are strong and broad (often with shoulders), for 1:6 and 1:8 cases, respectively, with some change of intensity and shape from that of the unsulfided cluster adduct. The significant difference is that these two lightly sulfided clusters show weak and broad bands at 399 and 403 cm^{-1}, respectively, which are recognized as coming from tungsten-sulfide stretching modes. The relative intensities of these tungsten-chloride and tungsten-sulfide stretching bands agree well with the extent of sulfidation of the cluster species.

The spectra of the cluster species recovered from the pyridine insoluble powders of the sulfidation reactions are close to each other in a similar way (see Table 11). For these 1:2, 1:8, 1:8:4 and 1:12:6 products, the coordinated pyridine bands in the mid-infrared spectra have little difference from those of the soluble pyridine cluster species. But only two pyridine bands are found in the far-infrared spectra (also shown in Figure 9), at 635 and 435 cm^{-1} (it is usually true that the highly sulfided clusters generally have about six pyridine in the molecules and thus no free pyridine). The strong bands in the far-infrared region belong to those of tungsten-sulfide stretching at 380 cm^{-1}. The band positions shift a little to lower frequencies and their intensities increase a lot as the degree of sulfidation increases, compared to the soluble sulfided clusters discussed above. Bands arising from tungsten-chloride stretching are completely absent in the spectra of the 1:12:6 product, but visible in the other cases. The far-infrared spectrum of $W_6S_8(py)_6$ from the 1:12:6 reaction is extremely simple with sharp bands attributable to tungsten-sulfide and tungsten-tungsten stretching modes, and pyridine ring bends, as expected for this highly symmetric cluster. The

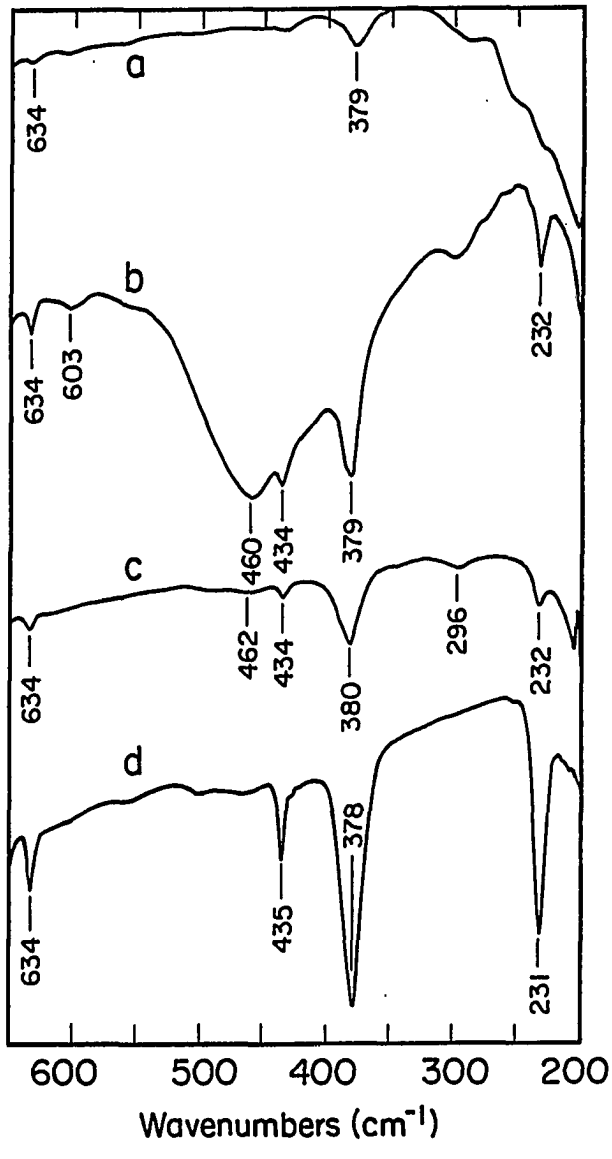

Figure 9: Far-infrared spectra of insoluble product of the 1:2 reaction (a), 1:8 reaction (b), 1:8:4 reaction (c), and 1:12:6 reaction (d)

Table 11: Absorption frequencies (cm^{-1}), found in the infrared spectra of the insoluble clusters from sulfidation reactions

1:2	1:8	1:8:4	1:12:6
1599 (w)[a]	1597 (w)	1599 (w)	1597 (m)
			1564 (vw)
	1350 (vw)	1350 (vw)	1350 (vw)
			1231 (vw)
1213 (w)	1213 (m)	1213 (m)	1213 (s)
1151 (w)	1148 (w)	1148 (w)	1148 (m)
1067 (w)	1067 (w)	1067 (w)	1067 (s)
1042 (vw)	1040 (w)	1040 (w)	1040 (m)
970 (vw)			937 (vw)
			870 (vw)
754 (w)	756 (m)	754 (m)	756 (s)
690 (w)	690 (m)	687 (m)	687 (s)
634 (vw)	634 (w)	634 (w)	634 (w)
	460 (s,b)		
	434 (w)	434 (w)	435 (w)
379 (m)	379 (s)	380 (s)	378 (vs)
290 (vw)	300 (w)	296 (w)	
	232 (m)	232 (w)	231 (s)

[a]Relative intensities given in the parentheses: s = strong, m = medium, w = weak, v = very, sh = shoulder, b = broad.

spectrum of the 1:8 product is not completely understood, because of a strong and broad band at 460 cm^{-1}. This band is sometimes visible in other highly sulfided pyridine-insoluble cluster products, usually as a weak but broad band. It was once thought to arise from WS_2 impurity produced by cluster decomposition. But crystalline WS_2 shows the strong and sharp band at 356 cm^{-1} as the only strong band by a later infrared examination.

It might just be a coincidence, but there is one pyridine-soluble product which also shows a band in the 460 cm^{-1} region. $W_6S_6Cl_2(py)_6$ from the 1:8:4 reaction was treated with more sodium hydrosulfide in refluxing pyridine at a $NaSH$/cluster ratio of four. The major product of this reaction was the completely sulfided cluster $W_6S_8(py)_6$, but the minor species recovered from pyridine solution showed a surprising spectrum as shown in Figure 10. All of the bands in the mid-infrared region are bands characteristic of pyridine. In the far-infrared spectrum, two weak bands are present at 611 cm^{-1} and 409 cm^{-1}, which are from the in-plane and out-of-plane ring bends, respectively, along with a very strong band at 466 cm^{-1}. The bands arising from tungsten-sulfide and tungsten-chloride stretching modes in W_6X_8 are not present at all. Possibly the pyridine of a new tungsten sulfide is formed for this particular case, but the origin of the band at 466 cm^{-1} is not known.

The spectra of the triethylphosphine adduct of W_6S_8 (see Table 12) show that the bands characteristic of coordinated pyridine are absent. This demonstrates that the replacement of pyridine was complete when $W_6S_8(py)_6$ was treated with excess triethylphosphine in refluxing toluene. In the mid-infrared spectrum as shown in Figure 11, bands are seen at 1416, 1261, 1096, 1032, 999, 804, 762, 717, and 667 cm^{-1}. Excluding bands at 1416, 1096 and 804 cm^{-1}, the positions and intensities of

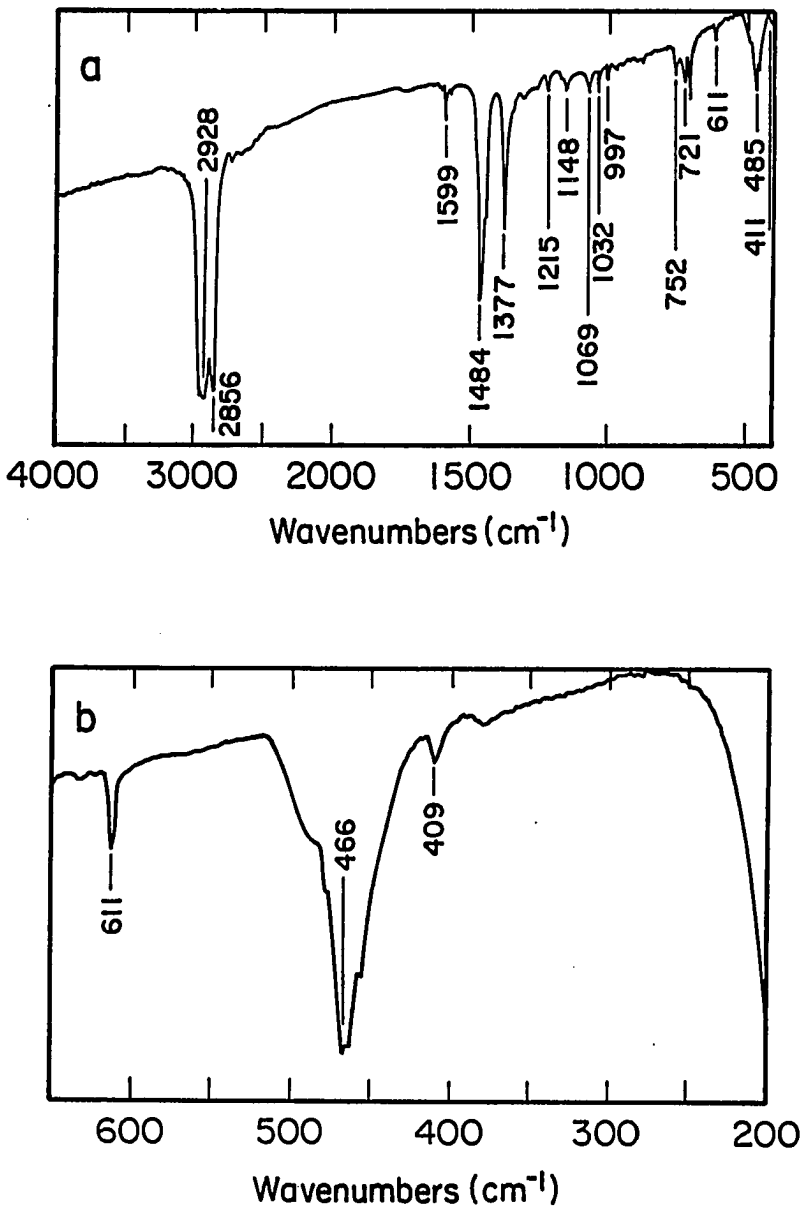

Figure 10: Mid-infrared (a) and far-infrared (b) spectra of the soluble product of the reaction between $W_6S_6Cl_2(py)_6$ and $NaSH$ (1:4)

the other bands are in good agreement with those of coordinated triethylphosphine cited in the literature [81]. The three extra bands are also present in the spectra of $Mo_6S_8(PEt_3)_6$ [16], indicating they must be associated with the coordinated triethylphosphine of these hexametal clusters, as the internal modes of M_6S_8 and $M-P$ stretching can not be at such high frequencies. The far-infrared spectrum (see Figure 12), showing peaks at 625, 464, 406, 387, 368, 335, and 231 cm^{-1}, is also dominated by the bands characteristic of coordinated triethylphosphine, especially the three medium to strong bands at 406, 368 and 335 cm^{-1} arising from δ(CCP) bending modes of triethylphosphine. With the strong band at 625 cm^{-1} also from triethylphosphine, there are only three bands left in the far-infrared region to be assigned. The medium to strong band at 387 cm^{-1} is attributed to tungsten-sulfide stretching in the hexatungsten cluster, and the weak band at 231 cm^{-1} is primarily tungsten-tungsten stretching in the cluster. These two bands are less intense compared to the corresponding bands in the pyridine cluster adduct, probably because the bands from coordinated ligand are relatively stronger in the triethylphosphine case. The final band is an extremely weak one at 464 cm^{-1}. This band is not recorded in the literature for coordinated triethylphosphine but is also found as a weak band in the triethylphosphine adducts of hexamolybdenum sulfide clusters [16] as shown in Table 13.

The infrared data (see Table 12) also indicate that no pyridine remains bound to the cluster upon reaction of $W_6S_8(py)_6$ with tetrahydrothiophene, as none of the characteristic pyridine bands remains in the spectrum of the product. Distinct peaks at 1306, 1269, 1254, 1130, 1070, 1034, 957, 879, and 809 cm^{-1} in the mid-infrared spectrum (see Figure 11) all correlate with those for coordinated tetrahydrothiophene

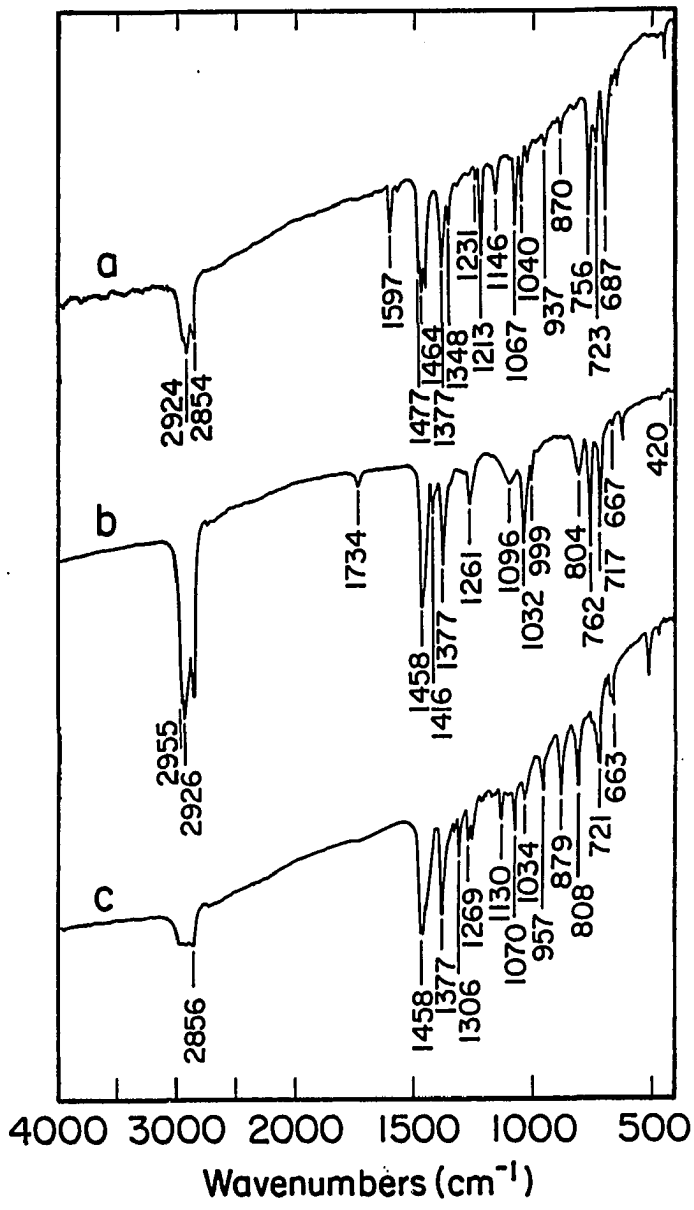

Figure 11: Mid-infrared spectra of $W_6S_8(py)_6$ (a), $W_6S_8(PEt_3)_6$ (b), and $W_6S_8(THT)_6$ (c)

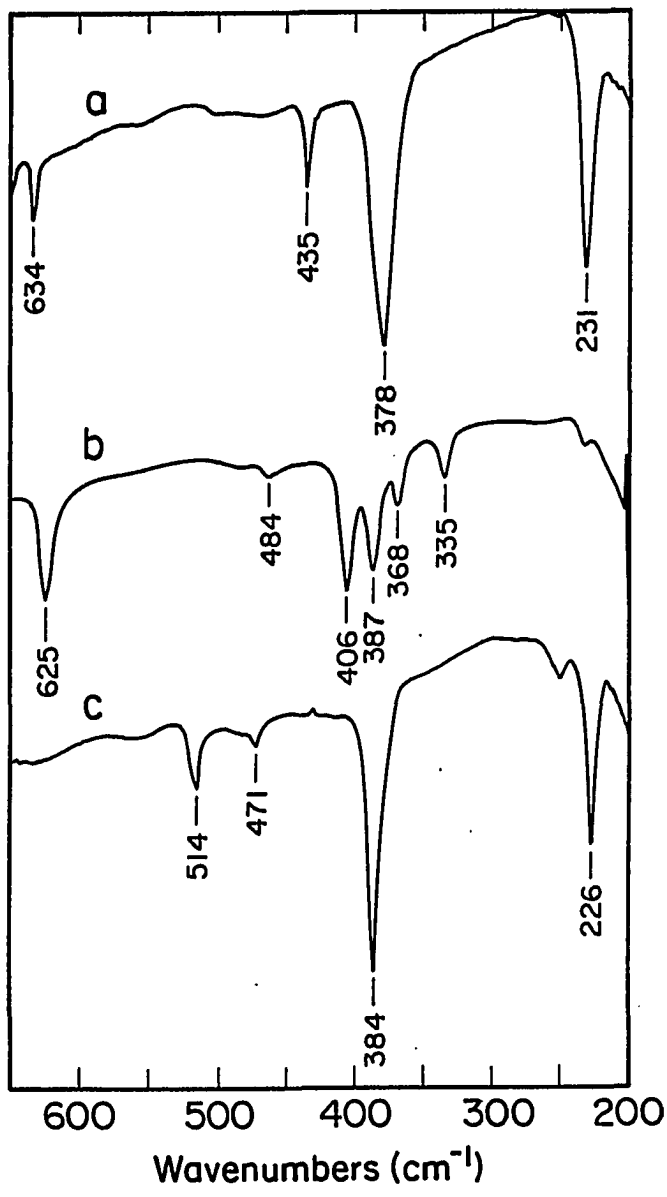

Figure 12: Far-infrared spectra of $W_6S_8(py)_6$ (a), $W_6S_8(PEt_3)_6$ (b), and $W_6S_8(THT)_6$ (c)

Table 12: Absorption frequencies (cm^{-1}), found in the infrared spectra of the molecular cluster complexes $W_6S_8L_6$

$W_6S_8(py)_6$	$W_6S_8(PEt_3)_6$	coord. PEt_3[a]	$W_6S_8(THT)_6$	coord. THT[b]
1597 (m)[c]				
1564 (vw)				
1350 (w)	1416 (w)		1306 (m)	1310 (m)
	1261 (w)	1255 (w)	1269 (m)	1275 (m)
1231 (vw)			1254 (m)	1259 (s)
1213 (s)				1210 (mw)
				1200 (mw)
1148 (m)			1130 (m)	1132 (mw)
1067 (s)	1096 (w)		1070 (ms)	1076 (w)
1040 (m)	1032 (s)	1033 (s)	1034 (w)	
1009 (vw)	999 (vw)	1005 (w)		
937 (vw)		980 (vw)	957 (m)	947 (m)
870 (vw)			879 (s)	876 (ms)
	804 (w)		808 (s)	806 (ms)
756 (s)	762 (s)	765 (s)		
		733 (s)		
	717 (m)	710 (m)		
687 (s)	667 (w)	680 (w)	663 (w)	657 (m)
634 (w)	625 (s)	641 (m)	514 (m)	535 (s)
	464 (vw)		471 (w)	476 (sh)
435 (w)	406 (s)	413 (m)		
378 (vs)	387 (s)		384 (vs)	
	368 (m)	365 (m)		
	335 (m)	335 (m)	249 (w)	
232 (ms)	231 (w)		226 (s)	

[a]Literature values [81].

[b]Literature values [82].

[c]Relative intensities given in the parentheses: s = strong, m = medium, w = weak, v = very, sh = shoulder, b = broad.

reported in the literature [82]. The far-infrared spectrum (see Figure 12) is simple and dominated by two sharp bands from W_6S_8, like the pyridine adduct of W_6S_8. The very strong band at 384 cm^{-1} is due to tungsten-sulfide stretching and the strong band at 226 cm^{-1} is of primarily tungsten-tungsten stretching mode. These two bands have been constantly observed for the molecular adducts of W_6S_8. Besides these two, there are also a medium band at 514 cm^{-1}, and two very weak bands at 471 and 249 cm^{-1}, respectively.

The comparison of the infrared spectra data among the molecular complexes of the completely sulfided W_6S_8 cluster is given in Table 12. The mid-infrared and far-infrared spectra are shown in Figures 11 and 12, respectively. Additionally, each member of these hexatungsten cluster complexes shows almost identical infrared spectra to that of the particular member of the analogous hexamolybdenum cluster complexes. For the comparison, the infrared spectra data for these hexamolybdenum cluster complexes is given in Table 13.

When the tetrahydrothiophene adduct was treated with refluxing pyridine, a red powder product was obtained and separated. The infrared spectra (shown in Figure 13) of this red powder indicate that pyridine is the primary ligand bound to the still intact cluster. All of the bands seen in $W_6S_8(py)_6$ are repeated in exact positions with identical intensities. But there are additional very weak bands at 1306, 1261 (doublet), 870, and 808 cm^{-1} in the mid-infrared region, which are characteristic of tetrahydrothiophene. It seems less likely that the ligand replacement of tetrahydrothiophene fell short of completion before the compound precipitated, than that some free tetrahydrothiophene was adsorbed on the surface of the fine powders.

These results demonstrate the usefulness of infrared spectra to monitor the ex-

Table 13: Absorption frequencies (cm^{-1}), found in the infrared spectra of the molecular complexes of the analogous Mo_6S_8 cluster

$Mo_6S_8(py)n$	$Mo_6S_8(PEt_3)_6$	$Mo_6S_8(THT)_6$
1589 (m)[a]		
1570 (vw)		
	1416 (mw)	
		1306 (ms)
	1261 (m)	1269 (m)
		1254 (m)
1211 (m)		
1148 (w)		1130 (m)
1067 (m)	1097 (mw,b)	1070 (ms)
1036 (m)	1032 (ms)	1035 (vw)
1009 (vw)		1023 (vw)
		957 (m)
		879 (ms)
	802 (m,b)	808 (m)
750 (ms)	760 (m)	
692 (m)		673 (w)
		665 (vw)
628 (w)	624 (m)	
612 (w)		
	559 (w,b)	
		515 (m)
	478 (w,b)	466 (w,b)
431 (w)	404 (ms)	
377 (vs)	391 (s)	388 (vs)
	365 (w)	
	334 (w)	
271 (w)		279 (w)
240 (w)		272 (m)

[a]Relative intensities given in the parentheses: s = strong, m = medium, w = weak, v = very, sh = shoulder, b = broad.

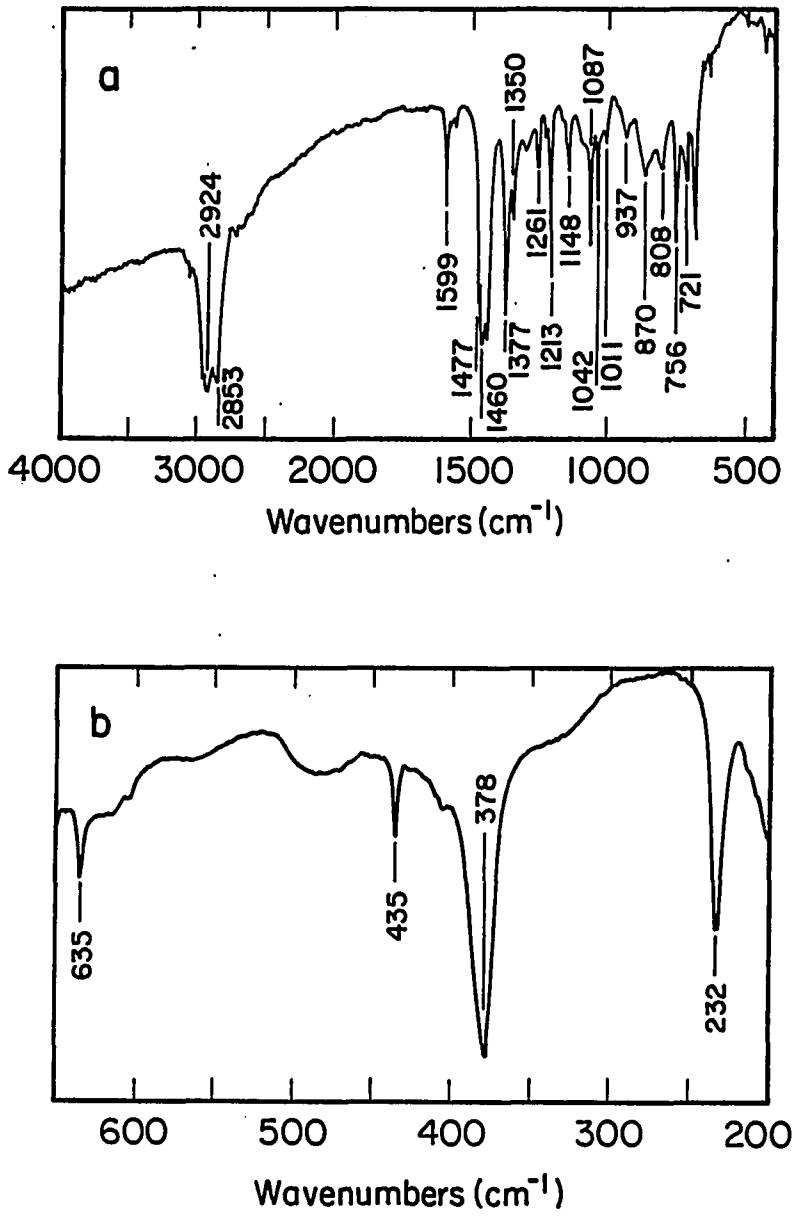

Figure 13: Mid-infrared (a) and far-infrared (b) spectra of the insoluble product of the reaction between $W_6S_8(THT)_6$ and pyridine

tent of sulfidation and coordinated ligand exchange of the hexatungsten clusters. The cluster unit has always been apparently intact and preserved through these reactions, as the W_6X_8 internal modes are always observed. The constant bands at 230 cm^{-1} region are attributed primarily to tungsten-tungsten stretchings. Substitutions of sulfide for chloride in W_6X_8 always decrease the intensities of bands in the tungsten-chloride region (320–280 cm^{-1}), and increase the intensities of bands in the tungsten-sulfide region (400–380 cm^{-1}).

Crystal Structures

All of the molecular complexes prepared in this work contain the hexatungsten cluster unit which is shown in Figure 1. The cluster can be considered as an octahedron of tungsten atoms with eight sulfur atoms capping the faces of the octahedron, or alternatively it may be viewed as a cube of eight sulfur atoms with six tungsten atoms over (slightly out of) each face of the cube. Each tungsten atom has an additional coordination position at each vertex of the octahedron, which is occupied by a nitrogen atom in pyridine, or a phosphorus atom in triethylphosphine, or a sulfur atom in tetrahydrothiophene, for each case of $W_6S_8(py)_6$, $W_6S_8(PEt_3)_6 \cdot 1.44CH_2Cl_2$, and $W_6S_8(THT)_6$, respectively. The cluster unit can be written as $W_6S^i{}_8L^a{}_6$.

$W_6S_8(py)_6$ (1) crystallizes in the space group $P\bar{1}$ with one molecule per cell. The cluster is located at the center of inversion so there is only one-half of a cluster unit (three W atoms, four S atoms, three N atoms and fifteen C atoms) in the asymmetric unit. Tables 14 and 15 give selected bond distances and angles of the cluster. The average $W - W$ bond distance of the six unique $W - W$ bonds in the cluster is 2.6617 (2) Å with the maximum $W - W$ bond distance difference of 0.0135

Table 14: Selected bond distances (Å) in $W_6S_8(py)_6$

$W(1)-W(2)$	2.6634 (4)	$W(1)-S(1)$	2.440 (2)
$W(1)-W(2')$	2.6610 (4)	$W(1)-S(2)$	2.473 (1)
$W(1)-W(3)$	2.6671 (4)	$W(1)-S(3)$	2.469 (2)
$W(1)-W(3')$	2.6608 (3)	$W(1)-S(4)$	2.461 (2)
$W(2)-W(3)$	2.6641 (4)	$W(2)-S(1')$	2.453 (2)
$W(2)-W(3')$	2.6536 (3)	$W(2)-S(2')$	2.453 (2)
av $W-W$	2.6617 (2)	$W(2)-S(3)$	2.461 (2)
$W(1)-N(1)$	2.263 (8)	$W(2)-S(4)$	2.450 (2)
$W(2)-N(2)$	2.257 (6)	$W(3)-S(1)$	2.462 (2)
$W(3)-N(3)$	2.244 (5)	$W(3)-S(2')$	2.465 (2)
av $W-N$	2.255 (5)	$W(3)-S(3)$	2.452 (2)
		$W(3)-S(4')$	2.452 (2)
		av $W-S$	2.458 (3)

Table 15: Selected bond angles (deg) in $W_6S_8(py)_6$

$W(2)-W(1)-W(3)$	59.97 (1)	$S(1)-W(1)-S(2)$	89.42 (5)
$W(2)-W(1)-W(3')$	59.79 (1)	$S(1)-W(1)-S(3)$	89.64 (5)
$W(2')-W(1)-W(3)$	59.741 (9)	$S(2)-W(1)-S(4)$	90.17 (5)
$W(2')-W(1)-W(3')$	60.080 (9)	$S(3)-W(1)-S(4)$	89.86 (5)
$W(1)-W(2)-W(3)$	60.08 (1)	$S(1')-W(2)-S(2')$	89.56 (6)
$W(1)-W(2)-W(3')$	60.06 (1)	$S(1')-W(2)-S(4)$	90.31 (6)
$W(1')-W(2)-W(3)$	59.956 (9)	$S(2')-W(2)-S(3)$	89.07 (6)
$W(1')-W(2)-W(3')$	60.245 (9)	$S(3)-W(2)-S(4)$	90.31 (6)
$W(1)-W(3)-W(2)$	59.94 (1)	$S(1)-W(3)-S(3)$	89.52 (7)
$W(1)-W(3)-W(2')$	60.104 (9)	$S(1)-W(3)-S(4')$	90.08 (6)
$W(1')-W(3)-W(2)$	59.964 (9)	$S(2')-W(3)-S(3)$	89.00 (7)
$W(1')-W(3)-W(2')$	60.15 (1)	$S(2')-W(3)-S(4')$	90.58 (7)
av $W-W-W$	60.01	av $S-W-S$	89.79
$W(1)-S(1)-W(2')$	65.89 (4)	$S(1)-W(1)-N(1)$	92.5 (2)
$W(1)-S(1)-W(3)$	65.94 (5)	$S(2)-W(1)-N(1)$	94.3 (1)
$W(2')-S(1)-W(3)$	65.36 (5)	$S(3)-W(1)-N(1)$	93.3 (1)
$W(1)-S(2)-W(2')$	65.40 (4)	$S(4)-W(1)-N(1)$	94.4 (2)
$W(1)-S(2)-W(3')$	65.22 (4)	$S(1')-W(2)-N(2)$	93.0 (1)
$W(2')-S(2)-W(3')$	65.60 (5)	$S(2')-W(2)-N(2)$	95.1 (2)
$W(1)-S(3)-W(2)$	65.40 (3)	$S(3)-W(2)-N(2)$	94.0 (1)
$W(1)-S(3)-W(3)$	65.63 (4)	$S(4)-W(2)-N(2)$	91.0 (2)
$W(2)-S(3)-W(3)$	65.67 (4)	$S(1)-W(3)-N(3)$	93.6 (2)
$W(1)-S(4)-W(2)$	65.67 (5)	$S(2')-W(3)-N(3)$	93.6 (2)
$W(1)-S(4)-W(3')$	65.58 (4)	$S(3)-W(3)-N(3)$	94.5 (2)
$W(2)-S(4)-W(3')$	65.55 (5)	$S(4')-W(3)-N(3)$	92.1 (2)
av $W-S-W$	65.58	av $S-W-N$	93.5
$W(2)-W(1)-W(2')$	89.78 (1)	$S(1)-W(1)-S(4)$	173.09 (7)
$W(3)-W(1)-W(3')$	89.86 (1)	$S(2)-W(1)-S(3)$	172.42 (7)
$W(1)-W(2)-W(1')$	90.22 (1)	$S(1')-W(2)-S(3)$	172.98 (6)
$W(3)-W(2)-W(3')$	90.08 (1)	$S(2')-W(2)-S(4)$	173.83 (6)
$W(1)-W(3)-W(1')$	90.14 (1)	$S(1)-W(3)-S(2')$	172.77 (5)
$W(2)-W(3)-W(2')$	89.923 (9)	$S(3)-W(3)-S(4')$	173.44 (5)
av $W-W-W$	90.00	av $S-W-S$	173.09

Å. The average $W - S$ distance of the twelve unique $W - S$ bonds and the average $W - N$ distance of the three unique $W - N$ bonds are 2.458 (3) Å and 2.255 (5) Å, respectively.

$W_6S_8(PEt_3)_6 \cdot 1.44CH_2Cl_2$ (**2**) crystallizes in the space group $R\bar{3}$ with three molecules in its hexagonal cell. The cluster is centered on a site having $\bar{3}(S6)$ symmetry, with two of the eight bridging sulfur atoms on the 3-fold axis. There are only one W, two S, one P and six C atoms in the asymmetric unit (excluding the solvent). Tables 16 and 17 give selected bond distances and angles of the cluster unit. There are only two unique $W - W$ bonds in the cluster, with the average bond distance of 2.6732 (3) Å and the difference of 0.007 Å. The average $W - S$ bond distance of the four unique $W - S$ bonds is 2.452 (3) Å, and there is one unique $W - P$ bond of 2.513 (2) Å in the whole cluster. From reductive dimerization of trimeric cluster units Saito and coworkers had established the same cluster $W_6S_8(PEt_3)_6$. They reported the structure of $W_6S_8(PEt_3)_6$ which crystallized in space group $P\bar{1}$ with two independent cluster units in its unit cell [78]. The structure results for the triclinic form, including the bond distances and bond angles, are in good agreement with the results given here for the trigonal ($R\bar{3}$) form. For example, The $W - W, W - P$ and $W - S$ distances are 2.680 (1), 2.519 (7) and 2.46 (1) Å, respectively, from their structure work with $R = 0.058, Rw = 0.060$. However, the refinement (R factors) and standard deviations of bond distances and angles are far superior for the latter structure established in this study.

$W_6S_8(THT)_6$ (**3**) crystallizes in space group $Ia3$ with eight molecules per uint cell. This is the highest symmetry space group among these three molecular complexes. The local symmetry of the cluster is the same as the one in **2**. The selected

Table 16: Selected bond distances (Å) in $W_6S_8(PEt_3)_6 \cdot 1.44CH_2Cl_2$[a]

$W - W^{iii}$	2.6767 (6)	$W - S(1)$	2.456 (3)
$W - W^{ii}$	2.6696 (6)	$W - S(2)$	2.455 (2)
av $W - W$	2.6732 (3)	$W^{ii} - S(2)$	2.442 (2)
$W - P$	2.513 (2)	$W^{iii} - S(2)$	2.456 (2)
		av $W - S$	2.452 (3)

[a]Equivalent positions: (*ii*) x − y, x, −z; (*iii*) −y, x − y, z; (*iv*) −x, −y, −z; (*v*) −x + y, −x, z; (*vi*) y, −x + y, −z.

Table 17: Selected bond angles (deg) in $W_6S_8(PEt_3)_6 \cdot 1.44CH_2Cl_2$[a]

$W^{iii} - W - W^{v}$	60.000	$W - S(1) - W^{iii}$	66.04 (9)
$W^{ii} - W - W^{iii}$	59.912 (9)	$W - S(2) - W^{iii}$	65.87 (6)
$W^{ii} - W - W^{vi}$	60.18 (2)	$W - S(2) - W^{ii}$	66.07 (6)
av $W - W - W$	60.00	$W^{ii} - S(2) - Wiii$	66.25 (6)
$S(1) - W - S(2)$	89.64 (6)	av $W - S - W$	66.06
$S(1) - W - S(2)^{v}$	89.33 (6)	$P - W - S(1)$	95.09 (8)
$S(2) - W - S(2)^{vi}$	90.19 (6)	$P - W - S(2)$	92.57 (8)
$S(2)^{v} - W - S(2)^{vi}$	89.87 (6)	$P - W - S(2)^{vi}$	91.69 (8)
av $S - W - S$	89.76	$P - W - S(2)^{v}$	95.64 (8)
		av $P - W - S$	93.75

[a]Equivalent positions: (*ii*) x − y, x, −z; (*iii*) −y, x − y, z; (*iv*) −x, −y, −z; (*v*) −x + y, −x, z; (*vi*) y, −x + y, −z.

bond distances and angles of the cluster are summarized in Tables 18 and 19.

The average $W - W$ bond distance is 2.6617 (2) Å in **1**, 2.6732 (3) Å in **2**, and 2.653 (3) Å in **3**. Compared to the $W - W$ distance 2.626 Å in $W_6Cl_{12}(PBu_3)_2$ [83], the distances found here are a little longer, in accordance with the fact that W_6S_8 is a 20 electron cluster while the chloride cluster unit $W_6Cl_8{}^{4+}$ has 24 electrons for $W - W$ bonding. By using the Pauling bond order equation [31] and the $W - W$ single bond distance d(1) = 2.630 Å [60], the $W - W$ bond distance is estimated at 2.677 Å for a 20 electron cluster with bond order n = 0.833, generally in good agreement with the observed values. It is statistically and perhaps chemically significant that the $W - W$ distance is shorter in **1** and **3** than in **2**, by 0.012 and 0.020 Å, respectively.

Unlike the trigonally distorted cluster units found in most of the Chevrel phases, these isolated molecular clusters in **1**, **2** and **3** are almost regular octahedra. In the former compounds the octahedra are elongated along the 3-fold axis, that is, the metal-metal bonds in the triangles perpendicular to the 3-fold axis are shorter than the bonds between these triangles, by as little as 0.022 Å in $Cu_{3.66}Mo_6S_8$ to as large as 0.164 Å in Mo_6S_8 [3,4]. This distortion is directly related to the weak intercluster metal-metal bonding which results from the close approach of cluster units in the Chevrel phases. As a general trend, the weaker this intercluster metal-metal bonding is, the less distorted or more regular the octahedral clusters will be.[5] $Cu_{3.66}Mo_6S_8$ (almost 24 electrons) has an intercluster $Mo - Mo$ distance of 3.389 Å whereas in Mo_6S_8 (20 electrons) this distance is only 3.084 Å. For the isolated $W_6S_8L_6$ clusters where no such intercluster bonding exists, regular octahedra are expected in these

[5] For compounds where the electron count is 21, 22 or 23 the distortion may also be enhanced by Jahn-Teller effects.

Table 18: Selected bond distances (Å) in $W_6S_8(THT)_6$[a]

$W - W^{iii}$	2.656 (3)	$W - S(1)$	2.44 (1)
$W - W^{ii}$	2.650 (3)	$W - S(2)$	2.454 (8)
av $W - W$	2.653 (3)	$W^{ii} - S(2)$	2.436 (8)
$W - S^a$	2.548 (9)	$W^{iii} - S(2)$	2.428 (8)
		av $W - S$	2.440 (6)

[a]Equivalent positions: (*ii*) x - y, x, -z; (*iii*) -y, x - y, z; (*iv*) -x, -y, -z; (*v*) -x + y, -x, z; (*vi*) y, -x + y, -z.

Table 19: Selected bond angles (deg) in $W_6S_8(THT)_6$[a]

$W^{iii} - W - W^v$	60.00	$W - S(1) - W^{iii}$	66.1 (3)
$W^{ii} - W - W^{iii}$	59.92 (3)	$W - S(2) - W^{iii}$	65.6 (2)
$W^{ii} - W - W^{vi}$	60.17 (7)	$W - S(2) - W^{ii}$	65.7 (2)
av $W - W - W$	60.00	$W^{ii} - S(2) - Wiii$	66.2 (2)
$S(1) - W - S(2)$	89.2 (2)	av $W - S - W$	65.9
$S(1) - W - S(2)^v$	89.0 (2)	$S(1) - W - S(3)$	93.9 (3)
$S(2) - W - S(2)^{vi}$	90.5 (2)	$S(2) - W - S(3)$	93.9 (3)
$S(2)^v - W - S(2)^{vi}$	90.3 (2)	$S(2)^{vi} - W - S(3)$	92.6 (3)
av $S - W - S$	89.75	$S(2)^v - W - S(3)$	94.1 (3)
		av $S - W - S(3)$	93.6

[a]Equivalent positions: (*ii*) x - y, x, -z; (*iii*) -y, x - y, z; (*iv*) -x, -y, -z; (*v*) -x + y, -x, z; (*vi*) y, -x + y, -z.

20 electrons clusters. For **2** the $W - W$ bonds in the triangles perpendicular to the 3-fold axis are only 0.007 Å longer (not shorter) than that between these triangles. For **3** this distance difference is 0.006 Å. For **1** where the site symmetry is much lower it is more difficult to make conclusions about distortions. However the minimal distortion of the W_6 octahedron is reflected by the small difference of only 0.013 Å between the longest and the shortest of the $W - W$ bonds.

The average $W - S$ bond distances are essentially identical in these compounds after considering the statistical errors. However the strength of the $W - L$ bonding between cluster and coordinated organic ligand is significantly different for different terminal ligands. The average $W - N$ distance is 2.255 (3) Å in **1** and the unique $W - S^a$ ($S^a = S$ in tetrahydrothiophene ligand) bond distance is 2.548 (9) Å in **3**, while the unique $W - P$ distance is 2.513 (2) Å in **2**. Based upon the Pauling covalent radii of 0.70, 1.04 and 1.10 Å, respectively, for N, S and P, and an estimated radius of 1.41 Å for W,[6] calculated bond distances for $W - N, W - S$ and $W - P$, respectively, are 2.11, 2.45 and 2.51 Å. As shown in Table 20, the observed and calculated $W - P$ bond distances are in good agreement, but the observed $W - N$ and $W - S^a$ distances are 0.15, 0.10 Å, respectively, longer than the calculated values. Thus it is concluded that the $W - N$ and $W - S^a$ bonding are much weaker than the $W - P$ bonding. This agrees well with the experimental results of the ligand exchange reactions of these cluster adducts. While the easy replacement of pyridine by triethylphosphine occurs during synthesis of $W_6S_8(PEt_3)_6$, the reverse substitution is not observed, even upon refluxing of the phosphine complex in liquid pyridine. Meanwhile, the

[6]The estimated radius for W is derived from the average $W - S$ distance 2.45 Å in the cluster units and the Pauling covalent radius of 1.04 Å for S.

Table 20: Bond distances (Å) and bond orders of $W-W$ and $W-L$ in $W_6S_8L_6$

formula	$W_6S_8(py)_6$	$W_6S_8(PEt_3)_6 \cdot 1.44CHCl_2$	$W_6S_8(THT)_6$
$W-W$	2.6617 (2)	2.6732 (3)	2.653 (3)
[a]est $W-W$	2.677	2.677	2.677
$W-S$	2.458 (3)	2.452 (3)	2.440 (6)
$W-L$	2.255 (5)	2.513 (2)	2.548 (9)
[b]est $W-L$	2.11	2.51	2.45
$\Delta(W-L)$	0.15	0.00	0.10
[c]BO $(W-L)$	0.56	1.00	0.68

[a]Estimated bond distance from Pauling bond order equation, d(n) = d(1) − 0.6log n, d(1) = 2.630 Å for $W-W$ single bond, n = 20/24 = 0.833 for W_6S_8.

[b]Estimated single bond distance from Pauling covalent radius r(N), r(P), r(S), and the calculated covalent radius of tungsten atom r(W) = d($W-S$)− r(S), where d($W-S$) is the average $W-S$ distance 2.45 Å in these clusters.

[c]Estimated bond order from Pauling bond order equation , d(n) = d(1) − 0.6log n, where d(n) is observed $W-L$ distance and d(1) is estimated $W-L$ single bond distance.

tetrahydrothiophene and the pyridine adducts can be interconverted.

The stronger $W-L$ bonding in **2** also correlates with the slightly longer $W-W$ bond in this compound than in **1** and **3** (see table 20). The difference in $W-W$ distances may be expected based on the nature of the donor ligand. The cluster orbitals that are oriented toward the terminal ligands are somewhat antibonding with respect to the $W-W$ bonds of the cluster. Increased donation of electron density to these orbitals may have a $W-W$ bond lengthening effect. This explanation agrees well with the results given here for the three molecular complexes of W_6S_8.

As shown by data given in Table 21, studies of $Mo_6S_8(PEt_3)_6 \cdot 2CH_2Cl_2$ and $Mo_6S_8(THT)_6$ (THT = tetrahydrothiophene) reveal similar relations [16]. The $Mo-L$ bonding in $Mo_6S_8(PEt_3)_6 \cdot 2CH_2Cl_2$ is much stronger than that in $Mo_6S_8(THT)_6$. While the observed and calculated $Mo-P$ distances are in good agreement, the $Mo-S$ bond between Mo and tetrahydrothiophene ligand is actually 0.14 Å longer than the calculated value. Notably also the average $Mo-Mo$ distance in the phosphine complex is 2.6584 (5) Å, compared to that of 2.640 (4) Å in the tetrahydrothiophene complex.

It is also worthwhile to point out that $W_6S_8(py)_6$ is isomorphous with $Mo_6S_6Cl_2(py)_6$, $W_6S_8(PEt_3)_6 \cdot 1.44CH_2Cl_2$ is isomorphous with $Mo_6S_8(PEt_3)_6 \cdot 2CH_2Cl_2$, and $W_6S_8(THT)_6$ is isomorphous to $Mo_6S_8(THT)_6$. The comparisons between the triethylphosphine and tetrahydrothiophene complexes are more direct and meaningful as all of them are $M_6S_8L_6$ 20 electron clusters. For the triethylphosphine complexes, as shown in Table 22, the $W-W$ and $W-S$ distances are slightly longer than those of the Mo analogues, which is expected as the W atom radius is just slightly longer than that of the Mo atom. On the other hand, in these complexes the $W-P$ distance

Table 21: Bond distances (Å) and bond orders of $Mo-Mo$ and $Mo-L$ in analogous hexamolybdenum molecular clusters

formula	$Mo_6S_8(PEt_3)_6 \cdot 2CHCl_2$	$Mo_6S_8(THT)_6$	$Mo_6S_6Cl_2(py)_6$
$Mo-Mo$	2.6584 (5)	2.640 (4)	2.634 (2)
[a]est $Mo-Mo$	2.662	2.662	2.637
$Mo-S$	2.446 (1)	2.430 (8)	2.469 (3)
$Mo-L$	2.524 (1)	2.576 (8)	2.29
[b]est $Mo-L$	2.50	2.44	2.10
$\Delta(Mo-L)$	0.02	0.14	0.19
[c]BO ($Mo-L$)	0.93	0.58	0.48

[a]Estimated bond distance from Pauling bond order equation, d(n) = d(1) − 0.6log n, d(1) = 2.610 Å for $Mo-Mo$ single bond, n = 20/24 = 0.833 for Mo_6S_8, n = 22/24 = 0.917 for $Mo_6S_6Cl_2$.

[b]Estimated single bond distance from Pauling covalent radius r(N), r(P), r(S), and the calculated covalent radius of molybdenum atom r(Mo) = d($Mo-S$)− r(S), where d($Mo-S$) is the average $Mo-S$ distance 2.44 Å in the 20 electrons clusters.

[c]Estimated bond order from Pauling bond order equation , d(n) = d(1) − 0.6log n, where d(n) is observed $Mo-L$ distance and d(1) is estimated $W-L$ single bond distance.

Table 22: Comparison of bond distances in $M_6S_8L_6$

formula	$M_6S_8(THT)_6$	$M_6S_8(PEt_3)_6 \cdot nCH_2Cl_2$
$Mo-Mo$	2.640 (4)	2.6584 (5)
$W-W$	2.653 (3)	2.6732 (3)
$Mo-S$	2.430 (8)	2.446 (1)
$W-S$	2.440 (6)	2.452 (3)
$Mo-L$	2.576 (8)	2.524 (1)
$W-L$	2.548 (9)	2.513 (2)

is actually shorter than the $Mo-P$ distance. This indicates that the $W-L$ bonding is unusually stronger than the Mo-L bonding in the triethylphosphine case. Comparison of data for the tetrahydrothiophene complexes seems to give similar results but much less meaningful because of large statistical errors of the bond distances. The comparison between the pyridine complexes of M_6S_8 would be interesting and meaningful, but unfortunately it has not been possible to obtain structural data for $Mo_6S_8(py)_6$ because good crystals have not been grown.

Magnetic Properties

Magnetic susceptibility data for $W_6S_8(py)_6$ were collected over the range 5–350K at 5K intervals, as shown in Figure 14. A singlet ground state is reflected by the constant susceptibility χ_M of -59 x 10^{-6} emu per mole over the range 200–350K. Over the lower temperature range, a paramagnetic pattern is present, which reflects the presence of traces of paramagnetic impurity. The small bump near 60K is probably caused by the antiferromagnetic transition of O_2 which is absorbed on the surface of the sample.

Magnetic susceptibility measurements for $W_6S_8(PEt_3)_6$ over the range 5–300K gave similar results. The singlet ground state is also reflected by the constant susceptibility over the range 150–300K with a paramagnetic tail at lower temperatures and also a small bump from O_2.

The magnetic measurements confirm the complete substitution of sulfide for chloride in $W_6Cl_8{}^{4+}$. The singlet ground state is expected for the completely substituted product $W_6S_8L_6$. When passing from $W_6Cl_8{}^{4+}$ with 24 electrons to W_6S_8 with 20 electrons, the electron configuration changes from $E_g{}^4$ to $E_g{}^0$. Any incomplete

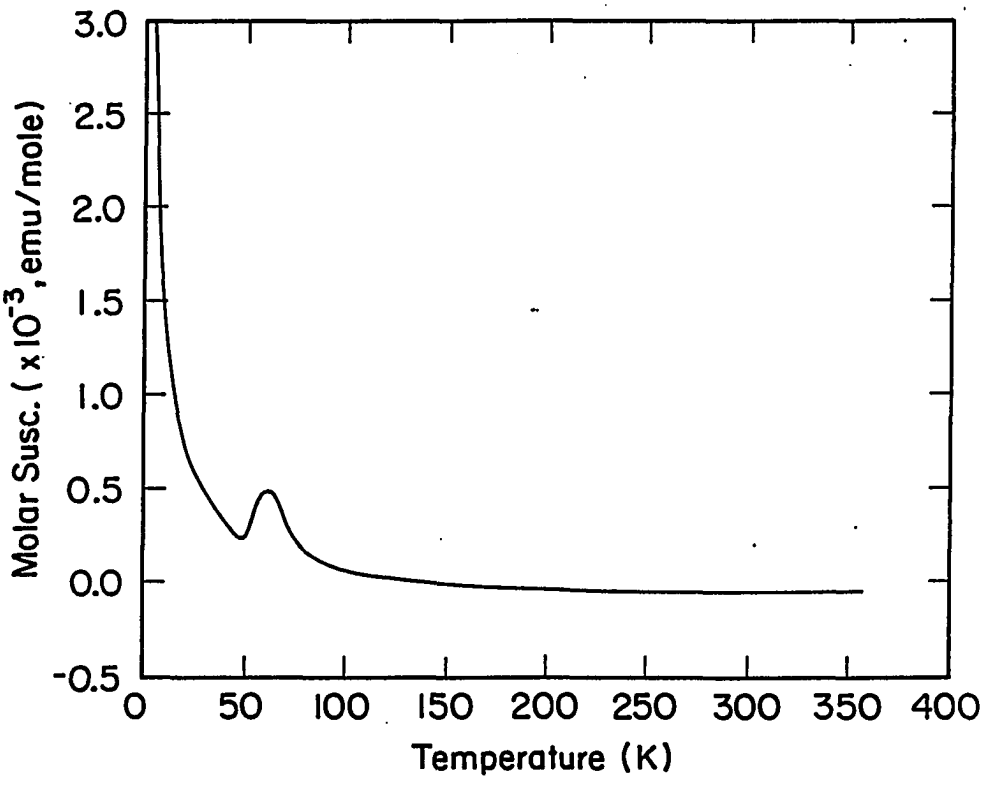

Figure 14: Molar susceptibility of $W_6S_8(py)_6$

substitution would lead to a product with one or more electrons in the E_g orbital (for example, ${E_g}^1$ for W_6S_7Cl), hence should result in degeneracy in the ground state of the product and consequent paramagnetism.

CONCLUSIONS

Through the sulfidation reaction studies it is found that sodium hydrosulfide is a good sulfiding reagent, especially in combination with the proton acceptor sodium n-butoxide. The discrete tungsten sulfide cluster W_6S_8 has been prepared by complete substitution of sulfide for chloride in W_6Cl_8 of α-tungsten(II) chloride. The W_6S_8 cluster is stabilized by coordination of ligands like pyridine, triethylphosphine and tetrahydrothiophene.

Structures for these molecular cluster complexes have been determined. The $W-W$ bond distances in the W_6S_8 clusters are longer than those in $W_6Cl_8{}^{4+}$, by an amount in agreement with a bond order of 0.833 in the former as compared to 1.0 in the latter, based on 20 and 24 electrons, respectively, for $W-W$ bonding. The nearly perfect octahedral symmetry of the cluster units, and their diamagnetic susceptibility, clearly indicate that there is no orbital degeneracy in the ground state of the complexes. This agrees with the assessment for the molybdenum clusters that on passing from $(M_6Cl_8)Cl_4$ to M_6S_8 the electron configuration changes from $E_g{}^4$ to $E_g{}^0$. The bond distance change clearly reflects removal of electrons from $M-M$ bonding orbitals in this process.

Substitution of coordinated pyridine ligands by triethylphosphine has been achieved but not the reverse. However, the pyridine and tetrahydrothiphine complexes can be interconverted. Based upon the comparison of $W-L$ bond distances, this is explained by strong $W-P$ bonding relative to weak $W-N$ and $W-S^a$ bonding. Thus it should be possible to form other molecular derivatives of the W_6S_8 cluster by displacement of the pyridine ligands.

PART III.

REMOVAL OF COORDINATED LIGANDS FROM THE MOLECULAR CLUSTER COMPLEXES

INTRODUCTION

The chemistry of Chevrel phases $M_x{}^{n+}Mo_6Y_8{}^{n-}$ ($Y = S, Se$ and Te) has been thoroughly studied and well established because of the interesting physical and chemical properties of these materials [3–7]. These properties are directly related to the structure of these phases, which consists of Mo_6Y_8 cluster units interlinked in three dimensions by intercluster $Mo - Mo$ and $Mo - Y$ bonds. These phases were usually prepared directly from the elements at high temperatures around 1000°C, or alternatively from reactions of the metal wanted in the ternary phase and the binary compounds Mo_6Y_8 at relatively lower temperatures. The binary compound Mo_6S_8 must be prepared indirectly, and is not thermodynamically stable towards disproportination into Mo and MoS_2 above 468°C [22,23].

The attempts to extract Mo_6S_8 cluster unit from the Chevrel phases into molecular complexes have not succeeded [84]. The molecular model complexes of Mo_6S_8 cluster unit found in these ternary and binary molybdenum sulfides had not been known until they were established through different routes more recently [16–20]. On the other hand, the attempts to convert the molecular model complexes into the Chevrel-related solid state phases have not yet been successful [15] and are still under investigation [66].

None of the tungsten analogues like $M_xW_6Y_8$ and W_6Y_8 has ever been established. The possible explanation is that the "tungsten Chevrel phases" are not thermodynamically stable at high temperatures where the Chevrel phases are usually synthesized. So low temperature routes could be essential to establish these phases. The establishment of the molecular cluster complexes makes them become potential molecular precursors for the ternary and binary tungsten sulfides $M_xW_6S_8$

and W_6S_8. If successful, this would lead to the establishment of the still unknown "tungsten Chevrel phases".

The preliminary studies concerned with attempts to remove the coordinated ligand from the molecular cluster complexes, which is essential in order to establish them as molecular precursors for the "tungsten Chevrel phases", are reported in this work.

EXPERIMENTAL

Materials

Unless otherwise indicated all materials and reaction mixtures were handled under dry inert atmospheres or on a high vacuum manifold. Solids were carefully handled in vials, water-cooled condenser-equipped reflux reaction flasks, and extractors. Solvents were generally vacuum-distilled or syringed against nitrogen/argon pressure.

Pyridine and toluene were dried by refluxing with CaH_2, distilled and stored under nitrogen over outgassed 4Å molecular sieves. Methanol was dried over sodium methoxide, followed by vacuum distillation onto outgassed 3Å molecular sieves for storage. Dichloromethane was dried by refluxing with phosphorous(V) oxide, followed by vacuum distillation onto outgassed 3Å molecular sieves. Acetonitrile was dried by refluxing with CaH_2 followed by distillation onto 3Å molecular sieves for storage.

Lead, zinc and sulfur powders were used as received. Aluminum chloride was purified by sublimation before use. Anhydrous zinc chloride, trifluoromethylsulfonic acid, and $Et_2O \cdot BF_3$ were used as received. The molecular adducts $W_6S_8L_6$ were prepared according to the procedures discussed in Part 2.

Analytical Procedures

Chlorine was determined by potentiometric titration of neutralized solutions with standard $AgNO_3$ solution using a $Ag/AgCl$ indicating electrode with a standard calomel electrode as the reference. Samples were first decomposed and oxidized in

$NaOH$ solutions with H_2O_2, and then the solution were neutralized with HNO_3. The end point was determined by the second derivative method.

Tungsten was determined by conventional gravimetric analyses. Samples were either decomposed and oxidized directly by concentrated HNO_3, or treated with NH_4OH and H_2O_2 first and then oxidized with concentrated HNO_3, in tared porcelain crucibles. Following ignition in a muffle furnace at 800°C for about 4 hours, the resulting WO_3 was weighed.

Physical Measurements

Infrared spectroscopy

Infrared spectra (4000–200 cm^{-1}) were obtained from an IR/98 Fourier Transform Infrared Spectrometer made by IBM Instruments, Inc. Samples were prepared as Nujol mulls. Data were collected for the mulls which were pressed between CsI plates, while the dry atmosphere was used as reference. The sample chamber was constantly purged with nitrogen. Mid-infrared (4000–400 cm^{-1}), and far-infrared (600–200 cm^{-1}) spectra were recorded separately.

X-ray powder diffraction

An Enraf Nonius Delft FR552 Guinier camera was used to obtain x-ray powder patterns. A General Electric XRD-5 generator with a Philips normal focus tube and a copper target was used to generate the x-rays. Air sensitive samples were ground thoroughly and then mounted between strips of cellophane tape in the drybox. Powdered NBS silicon was added to the samples and used as an internal standard.

Synthetic Procedures

The studies were focused on the pyridine adduct $W_6S_8(py)_6$. One reason to choose this complex is that pyridine is known to be a relative weak ligand for the cluster from the studies in Part 2, and thus might be easier to remove. Also, deligation of the triethylphosphine adduct of the Mo_6S_8 cluster was found to be extremely difficult and complete deligation was not realized [15]. Reactions designed to remove the pyridine ligands were pursued in both solid state reactions and reactions in organic solvents.

Thermal decomposition of $W_6S_8(py)_6$

The same reaction procedures were employed for thermal decomposition of $W_6S_8(py)_6$ at different temperatures. In a typical reaction, a portion of $W_6S_8(py)_6$ was put into a Pyrex ampule equipped with a standard balljoint and then connected to the vacuum line. This red powder was then heated in a working vacuum with the use of a furnace and the temperature was maintened constant at 250°C overnight. The product was a black powder amorphous to x-rays. Tungsten analysis and infrared spectra were obtained. Anal. Found: W, 69.6.

A portion of this black powder was reacted with refluxing pyridine for two days. The solution was still colorless and the solid was still a black powder. After filtering the solid was dried under vacuum and infrared spectra were obtained.

Other thermal decomposition reactions were performed at 300°C and 640°C. The products were always black powders. Tungsten analyses and infrared spectral data were obtained for each case. Anal. Found: W, 74.7 for 300°C product, 79.0 for 640°C product.

Reaction of $W_6S_8(py)_6$ with lead

0.40 grams $W_6S_8(py)_6$ (0.22 mmole), and 0.06 grams lead powder (0.3 mmole) were put into a Pyrex ampule with a standard balljoint and then connected to the vacuum line. This mixture was heated under vacuum in a furnace and the temperature was maintened constant at 250°C for one day. The existence of lead metal in the product mixture was obvious by the examination under a microscope, while the major part of the mixture was a black powder just like the thermally-decomposed products described above. Infrared spectra were collected for this product.

The mixture was reheated up to 350°C for two days. Upon returning to room temperature, the product was still a mixture of black powder and lead powder.

Reaction of $W_6S_8(py)_6$ with aluminum chloride

0.18 grams $W_6S_8(py)_6$ (0.10 mmole), and 0.08 grams unhydrous $AlCl_3$ (0.6 mmole) were put into a Pyrex ampoule with a standard balljoint. It was then connected to the vacuum line and sealed under vacuum. The ampoule was put into a furnace and maintained at 225°C for five days. Then the $AlCl_3$ and its pyridine adduct were sublimed away by keeping one end of the ampoule in air while heating the mixture at the other end to 200°C. The resulting product was obtained as a black powder in a yield of 0.15 grams. Infrared spectra were collected for this product.

Reaction of $W_6S_8(py)_6$ with zinc and zinc chloride

0.50 grams $W_6S_8(py)_6$ and an excess amount of Zn and $ZnCl_2$ were mixed and put into a reaction tube equipped with a standard adaptor. The tube was connected to the vacuum line and then evacuated. The mixture was heated in *vacuo* at 200°C for one day. Infrared spectra were collected for the resulting black powder.

Reaction of $W_6S_8(py)_6$ with trifluoromethylsulfonic acid

0.50 grams $W_6S_8(py)_6$ (0.27 mmole) was loaded into a 100-mL reaction flask in the drybox followed by vacuum distillation of *ca*. 50 mL acetonitrile. Upon stirring overnight under nitrogen atmosphere, no change was observed as the solid remained insoluble in the colorless solution. Immediately after 0.30 mL trifluoromethylsulfanic acid (excess) was added into the mixture by syringe under the blanket of nitrogen gas, the solid became solubilized and the color of the solution turned into dark greenish-yellow. The solution was stirred overnight although it appearred that the reaction was finished shortly after the addition of the acid. No solid product was obtained when the solution was filtered.

Then the solvent was stripped from the filtrate solution under vacuum, leaving a dark oily material which could not be dried. The oily substance remained after the addition of ca. 20 mL ether by vacuum distillation, but was redissolved in acetonitrile added by distillation after the ether was stripped away. All efforts to isolate any cluster compounds from the solution failed, as the product either was completely soluble in solution or formed as an oily material in another solvent.

Reaction of $W_6S_8(py)_6$ with trifluoromethylsulfonic acid in methanol

0.44 grams $W_6S_8(py)_6$ (0.24 mmole) was loaded into a 100-mL reaction flask in the drybox followed by vacuum distillation of ca. 20 mL methanol, and addition of 0.13 mL trifluoromethylsulfonic acid (1.44 mmole) under the blanket of argon gas. Stirring at room temperature overnight did not bring any change to the red solid and colorless solution. The mixture was then heated and brought to reflux for two days. After cooling, a black solid was separated from the dark green filtrate solution by

filtering and dried under vacuum. Infrared spectra were recorded for this powdered product obtained in a yield of 0.34 grams. Anal. Found: W, 66.4.

A portion of this black powder was reacted with refluxing pyridine for two days. After cooling, a black solid was separated from a dark yellow filtrate solution and dried under vacuum. The filtrate was stripped of pyridine and also dried under vacuum to result in a dark yellow solid. Infrared spectral data were recorded for both parts.

Reaction of $W_6S_8(py)_6$ with $Et_2O \cdot BF_3$

0.30 grams $W_6S_8(py)_6$ (0.16 mmole) was loaded into a 100-mL reaction flask in the drybox followed by the addition of ca. 20 mL toluene under the blanket of argon gas. Then 1.2 mL $Et_2O \cdot BF_3$ (excess) was added into the mixture under the blanket of argon gas, and the mixture was stirred at room temperature over night. The color of the mixture gradually turned darker during this period. Then the solid was separated by filtering from the still almost colorless filtrate solution and dried under vacuum. The yield for this powdered product, which gave a yellow color when ground in a mortar, was 0.32 grams. Infrared spectra were obtained for this product.

This powdered product was reloaded into a 100-mL reaction flask followed by addition of ca. 20 mL toluene and 0.6 mL $Et_2O \cdot BF_3$. The mixture was heated and brought to reflux overnight. After cooling, the mixture was filtered to remove the solid from the colorless solution. The solid was dried and infrared spectra were obtained.

RESULTS AND DISCUSSION

Thermal Decomposition

One way to break the bond between the coordinated organic ligands and the metal centers in organometallic compounds and cluster compounds is by thermal deligation. Assuming that pyridine was liberated as a result of bond cleavage upon heating $W_6S_8(py)_6$, that would leave open positions at the terminal cordination sites of the cluster. Then the bridging sulfides in a neighboring cluster could occupy these open positions. The reverse would also occur for the bridging sulfides of this cluster and the open positions of the neighboring cluster. In such a way, the clusters would be no longer isolated as they were in the molecular complex, but rather, would become cross-linked to the neighboring clusters. Ideally, if this occurred for the pyridine adduct $W_6S_8(py)_6$ without disrupting the cluster, it would lead to the formation of "W_6S_8":

$$W_6S_8(py)_6 \longrightarrow W_6S_8 + 6py \tag{24}$$

The pyridine complex was heated in *vacuo* at different temperatures. Each heating resulted in a black, powdered product, at the same time pyridine was lost.[7] These black powders did not recombine with pyridine even with prolonged refluxing in neat pyridine. These results suggest that cross-linking between the neighboring clusters occurred during the heating. But one should be cautious here because there was no direct evidence of the preservation of the cluster. The infrared spectra showed

[7] Lost pyridine was collected in the cold trap at liquid nitrogen temperature but not analyzed.

two weak and broad bands at 460 and 400 cm^{-1} in the lower frequency region for the products obtained at 250°C and 300°C. For the product obtained at 640°C, the band at 460 cm^{-1} remained while the 400 cm^{-1} band disappeared and a weak but sharp band appeared at 360 cm^{-1}. This new band is characteristic of $W - S$ stretching vibrations in WS_2 (see Figure 15). So the infrared spectra may suggest that the cluster is preserved below 300°C, with the characteristic $W - S$ vibration of the cluster at 400 cm^{-1}.

The results of tungsten analyses for the products obtained at lower temperatures were lower than the calculated 81.2% for "W_6S_8". Assuming that the clusters were preserved and some pyridine was still bound to the cluster, the two products could be formulated as $W_6S_8(py)_3$ and $W_6S_8(py)_2$, respectively, based on tungsten analyses of 69.6% and 74.7% for the products obtained at 250°C and 300°C. The infrared spectra in the mid-infrared region showed extremely small signals or residues of bands. The positions of these bands, though, are in good agreement with those of the coordinated pyridine of the molecular complexes. The product obtained at 640°C has a tungsten content of 79.0%, which is close to that of the "W_6S_8". The mid-infrared spectrum is devoid of the bands of pyridine, but the far-infrared spectrum suggested that decomposition of the cluster to form WS_2 had occurred.

All of these black powders were amorphous to x-ray diffraction. This is understandable considering the low temperatures employed in these reactions. Even for the possible formation of tungsten sulfide (WS_2) and tungsten metal, the reaction temperatures are not high enough to form crystalline materials. X-ray diffuse scattering data for these powders were measured, and the product obtained at 640°C shows a different pattern from those of products obtained at lower temperatures. Accord-

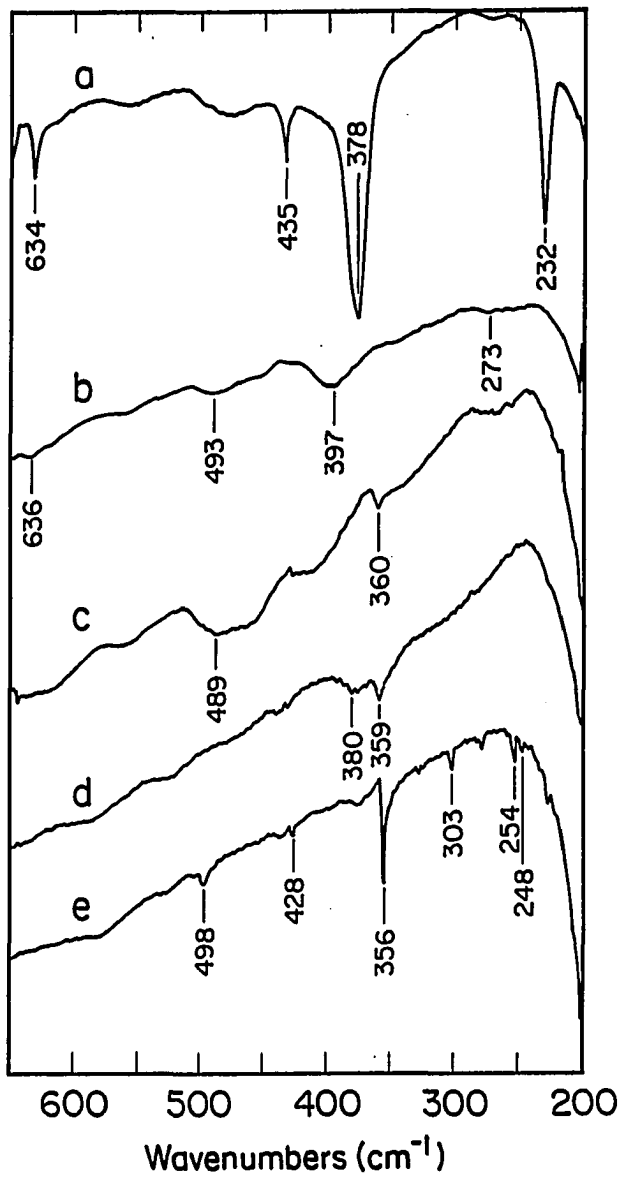

Figure 15: Far-infrared spectra of $W_6S_8(py)_6$ (a), the thermal-decomposition product at 250°C (b), at 640°C (c), residue of TGA for $W_6S_8(THT)_6$ (d), and WS_2 (e)

ing to Goldman [85], the pattern shows the character of layered compounds. This supports the cluster decomposition in the reaction at 640°C, because the expected product WS_2 is indeed a layered compound.

In order to better understand the thermal decomposition of $W_6S_8(py)_6$, a TGA (thermal gravimetric analysis) study was pursued for this pyridine complex. Several repeated measurements confirmed that the loss of weight is a multistep process, which is shown in the Figure 16. It is clear from this figure that heating at lower temperatures (up to 550°C) under argon or helium does not remove pyridine completely, which agrees well with the results obtained from the thermal decomposition. Above 550°C, another weight loss occurrs, but it may be different from the result of the thermal decomposition in *vacuo* at 640°C. The residue after the TGA analysis is a yellow solid, which shows a powder pattern similar to that of WO_3 by x-ray diffraction. Even with the use of an oxygen trap for the argon or helium flow, and substantial purge of the sample holder before running the TGA, the yellow solid is always the residue obtained. This result suggests that the final weight loss corresponds to the oxidization of cluster to WO_3, which is a thermodynamically preferred compound if oxygen is present.

A TGA study was also applied to the analogous tetrahydrothiophene complex. The result is also shown in Figure 16. The weight loss is also a multistep process, but is more sharp compared to that of the pyridine adduct. The first step starts at 200°C, and is very sharp with 16% weight loss. The second step starts at 300°C with an additional 4% weight loss. The weight is then relatively stable over 400°C. This indicates that loss of weight occurs much faster for the tetrahydrothiophene complex at relatively lower temperature. The residue after the TGA analysis is a black solid

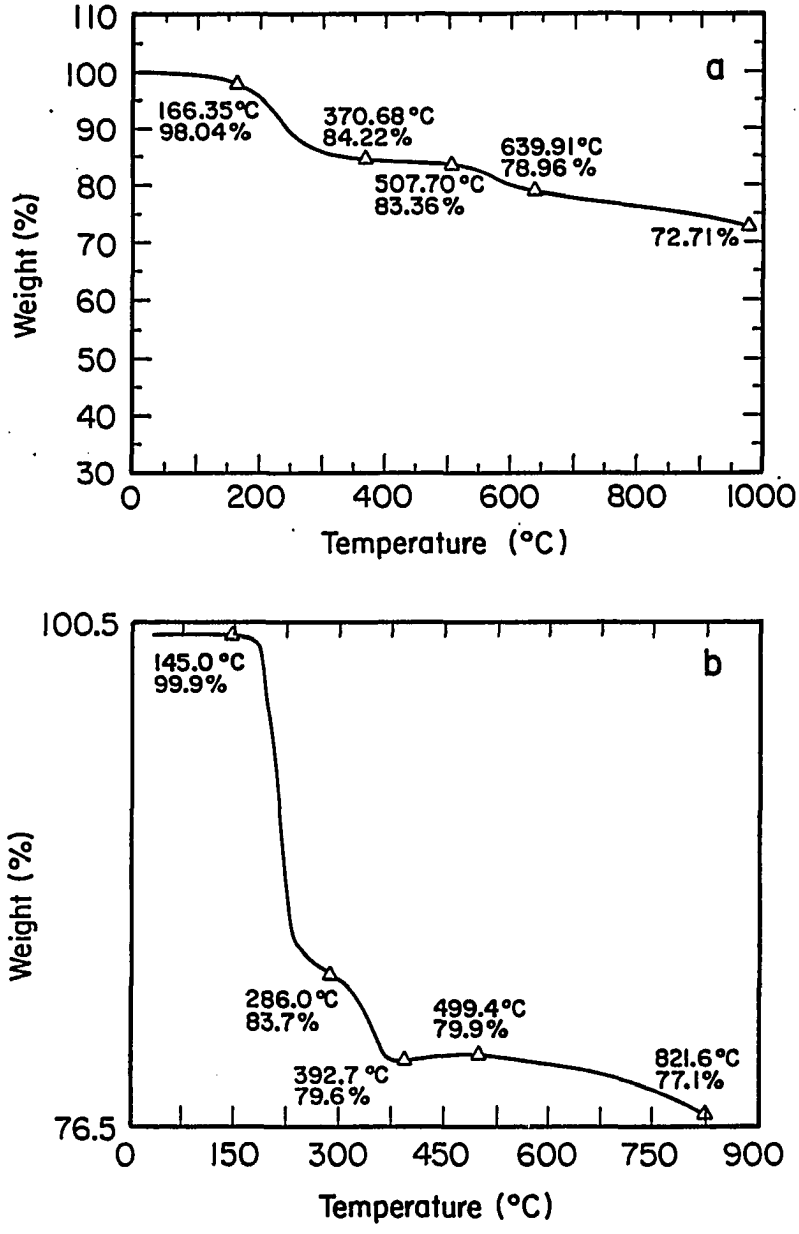

Figure 16: TGA analysis for $W_6S_8(py)_6$ (a) and $W_6S_8(THT)_6$ (b)

which almost retained the morphology of the starting crystalline tetrahydrothiophene complex. The far-infrared spectrum of this residue showed two bands at 380 and 359 cm^{-1} (see Figure 15). These bands may indicate a mixture of some cluster and some WS_2. So the tetrahydrothiophene complex evidently behaves differently from the pyridine complex. Structurally this result might be expected because the ligand bonded to the cluster is an organic sulfur atom. Upon decomposition the sulfur atom may remain bonded to the metal while hydrocarbon molecules are lost. This is likely especially when it is considered that the clusters of the solid state Chevrel phases are known to have hydrodesulfurization activities [6]. While this may suggest some new chemistry of the tetrahydrothiophene adduct of W_6S_8, it also indicates that this adduct may tend to form WS_2 which is not a prefered result.

Solid State Reactions

From the results of thermal decomposition and TGA studies it is realized that thermal deligation of $W_6S_8(py)_6$ cannot be complete at lower temperatures. It is also realized that raising the temperature to facilitate this process probably results in cluster decomposition. One way to avoid such a conflict might be the use of a "pyridine-philic" agent. $AlCl_3$ would be such an agent as it is a strong Lewis acid and combines with pyridine strongly. Ideally it might help to remove pyridine completely from the cluster at lower temperature, as shown in the following equation:

$$W_6S_8(py)_6 + 6AlCl_3 \longrightarrow W_6S_8 + 6py \cdot AlCl_3 \qquad (25)$$

The reaction was tried in a sealed Pyrex tube and the temperature was set at 225°C as a upper limit in fear of a potential explosion caused by the high vapor

pressure of $AlCl_3$. The result was a mixture of black powdered product and some white material, which was removed by sublimation at 200°C. The infrared spectral data suggested that this material was similar to the simple thermal decomposition reaction products at 250°C and 300°C. There remained a residue of coordinated pyridine bands in the mid-infrared region. The far-infrared spectrum showed that bands of coordinated pyridine disappeared but one broad band remained at 400 cm^{-1}, which might suggest the retention of the cluster. No tungsten analytical data were obtained, but based on the yield of the reaction there remained at least two pyridine per cluster. So the initial hope of using Lewis acid $AlCl_3$ to combine and completely remove pyridine from the cluster at low temperature was not recognized experimentally.

Other options that were considered included the use of ternary metal, and the combination of ternary metal and metal chloride (Lewis acid). It was thought that ternary hexatungsten sulfides might be more thermally stable than the binary sulfide, and would be easier to make. It is known from the studies of Chevrel phases that insertion of ternary metal cations stabilized the ternary phases, especially for the sulfide phases. Mo_6S_8 cannot be prepared directly, and undergoes disproportionation into molybdenum metal and molybdenum disulfide above 468°C. The stablility of the analogous binary tungsten phase is probably even lower. So by using the ternary metal it was hoped that reduction of cluster would help to deligate the coordinated pyridine:

$$W_6S_8(py)_6 + Pb \longrightarrow PbW_6S_8 + 6py \tag{26}$$

$$W_6S_8(py)_6 + Zn + ZnCl_2 \longrightarrow ZnW_6S_8 + Zn(py)_2Cl_2 + 4py \tag{27}$$

The results of the two reactions undertaken in *vacuo* did not suggest that the ternary phases were obtained. The metal powders were still present in mixtures with black powdered products. The infrared spectral data indicated that the black powdered products were very similar to the thermal decomposition products obtained at lower temperatures and the product of the reaction with $AlCl_3$. It is very likely that kinetic barriers hamper the intended effect of ternary metal and metal chloride. At the temperatures employed here in these solid state reactions, the thermal energy was just not enough to promote diffusion of the solid state reactants. Even for the reaction with lead where the temperature was over its melting point, such a kinetic barrier apparently could not be overcome. For all of the solid state reactions tested in this preliminary study, the idealized process of utilizing ternary metal and/or metal chloride (Lewis acid) to remove pyridine ligands was not experimentally realized.

Reactions in Solutions

The reactions in solution have the advantage that those kinetic barriers in solid state reactions are minimized or removed. Thus the removal of coordinated pyridine from the molecular cluster complex was also undertaken in solutions. The option of using acids to deligate pyridine complex was chosen in the studies here. Particularly, $HOSO_2CF_3$ is a strong Bronsted acid, and it was hoped that protonation of pyridine into pyridinium cation would lead to naked "W_6S_8" in non-coordinating solvents, or a labile molecular complex in a solvent with weak coordinating ability.

The reaction of the molecular cluster pyridine complex and excess $HOSO_2CF_3$ was first tried in acetonitrile, which is a weakly coordinating ligand. Without addition of the acid, the mixture of the pyridine complex and acetonitrile did not change

even at reflux condition. At room temperature, as soon as the acid was introduced into the mixture, reaction immediately occurred as all solid dissolved and colorless solvent turned into dark yellowish-green solution. The reaction was observed to be done in several minutes. Unfortunately, no product could be isolated from the solution. Stripping of the solvent led to an oily material, which could not be dried and susequently analyzed. The oily material was either completely soluble in solvents like acetonitrile, propylamine, or remained as an oily material in solvents like ether. It is not understood what occurred in this reaction as no subsequent isolation of any product was possible.

The reaction of the molecular pyridine complex and a stoichiometric amount of the acid was repeated, but in methanol instead of acetonitrile. Methanol is known to have extremely weak coordinating ability, and idealy would not coordinate to the cluster when the pyridine is protonated:

$$W_6S_8(py)_6 + 6H^+ \longrightarrow W_6S_8 + 6pyH^+ \qquad (28)$$

The reaction was first tried at room temperature. But unlike the reaction in acetonitrile, no change occurred as red pyridine complex remained insoluble in the colorless solvent. When the mixture was heated and brought to reflux, reaction gradually occurred as the mixture turned darker. A black powdered product was obtained by filtration from a dark green solution after the reaction was finished and cooled down. Infrared spectra of this powdered product are shown in Figure 17. The mid-infrared spectrum confirmed the removal of pyridine ligands as all of the bands of coordinated pyridine disappearred. The spectrum also indicated that methanol was not present in the product. In the far-infrared region, three bands were seen

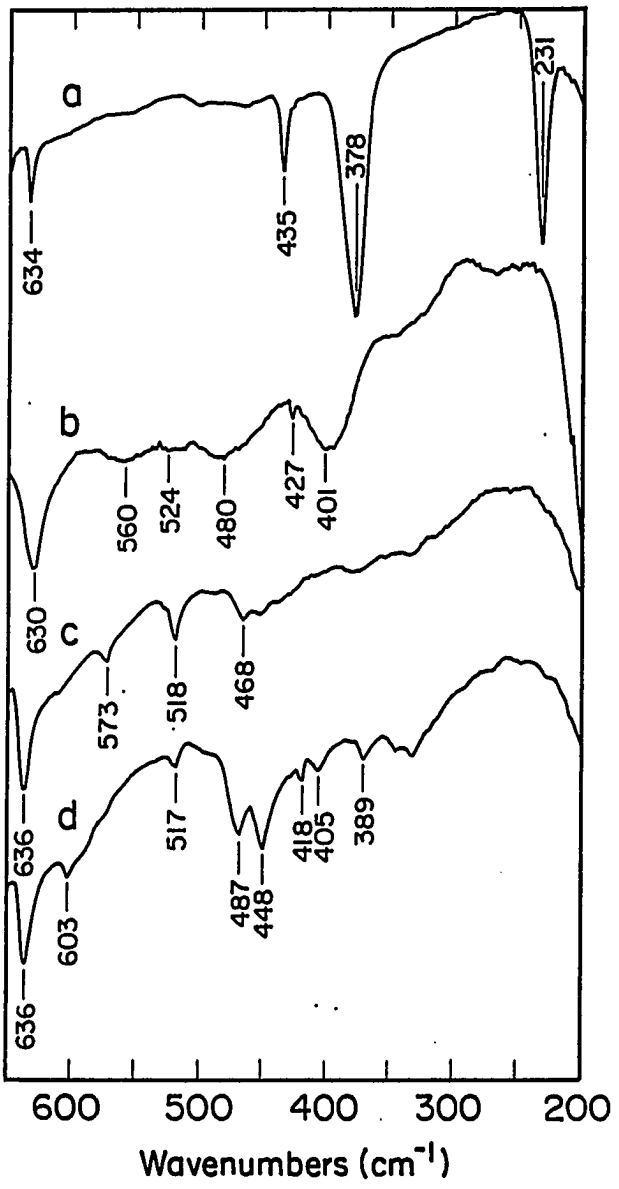

Figure 17: Far-infrared spectra of $W_6S_8(py)_6$ (a), the product of the reaction between $W_6S_8(py)_6$ and $HOSO_2CF_3$ in methanol (b), the insoluble product of the subsequent pyridine reaction (c), and soluble product of the same reaction (d)

at 630, 460 and 400 cm^{-1}. The tungsten analysis, 66.4% W, indicated that this product could not be "W_6S_8".

In order to verify whether the cluster was still preserved, a portion of this product was reacted with pyridine at reflux condition. No pyridine adduct of W_6S_8 was recovered from this reaction. Rather, the reaction resulted in a black solid and a dark yellow solution from which a dark yellow solid was obtained by stripping of the solvent. Far-infrared spectra for both parts were shown in Figure 17. Although the spectra were not fully understood, they clearly indicated that the hexatungsten cluster was not preserved as the bands characteristic of W_6S_8 cluster were no longer present. Apparentely the cluster was broken in this acid reaction in methanol. In the studies of analogous hexamolybdenum molecular complexes, it was found that the cluster was preserved in such a reaction [66]. But for the tungsten cluster, the stability against probable oxidation by $HOSO_2CF_3$ is just not enough.

Reaction of the pyridine complex with Lewis acid in solution was also pursued. The ether adduct of boron trifluoride was chosen as the source of Lewis acid BF_3. In a non-coordinating solvent, "W_6S_8" would be obtained ideally:

$$W_6S_8(py)_6 + 6Et_2O \cdot BF_3 \longrightarrow W_6S_8 + 6py \cdot BF_3 + 6Et_2O \qquad (29)$$

The reaction between the pyridine complex and excess amount of $Et_2O \cdot BF_3$ was first tried at room temperature in toluene. The solid gradually turned from red to dark colored while the solution remained almost colorless. The dark yellow solid product obtained weighted more than the starting pyridine complex. The infrared spectra of this product are shown in Figures 18 and 19. In the mid-infrared region, bands from pyridine could still be recognized. In the far-infrared region, bands were

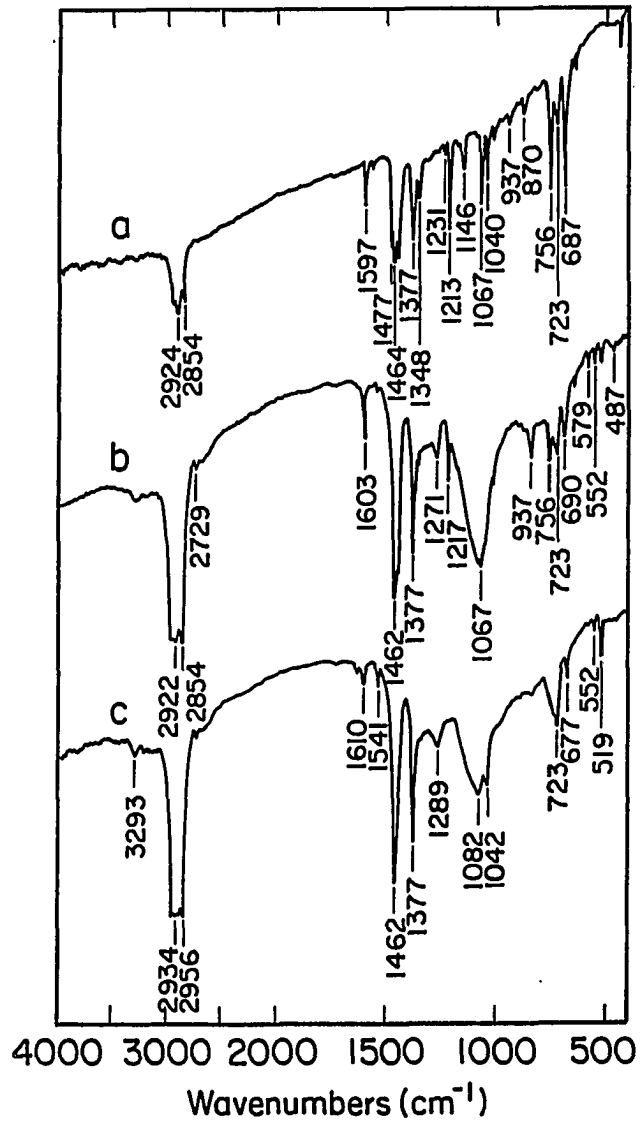

Figure 18: Mid-infrared spectra of $W_6S_8(py)_6$ (a), the product of the reaction between $W_6S_8(py)_6$ and $Et_2O \cdot BF_3$ at room temperature (b), and at reflux condition (c)

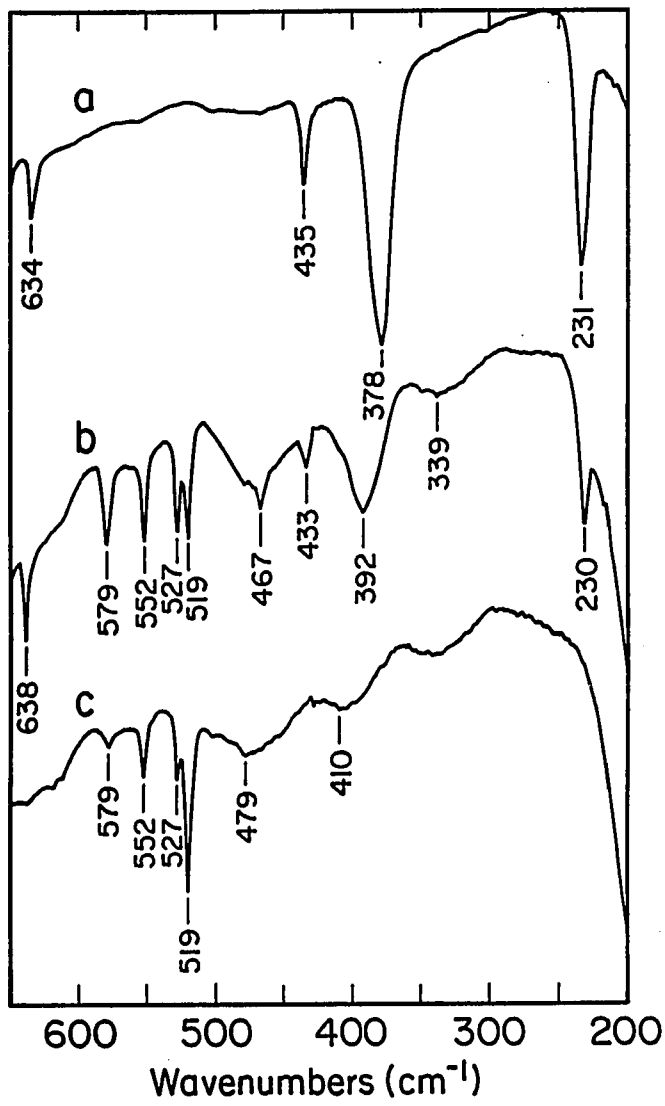

Figure 19: Far-infrared spectra of $W_6S_8(py)_6$ (a), the product of the reaction between $W_6S_8(py)_6$ and $Et_2O \cdot BF_3$ at room temperature (b), and at reflux condition (c)

seen at 638, 579, 552, 527, 519, 467, 433, 392, and 230 cm^{-1}. While bands similar to those of a molecular pyridine complex were also present, new bands appearred at 579, 552, 527, and 519 cm^{-1}. It is very likely that BF_3 was just attached to the molecular pyridine cluster in this product while the cluster was still isolated and intact. Presumably, such attachment occurred through bridging sulfur atoms in the cluster unit as the sulfur atoms have an extra lone pair of electrons.

This dark yellow solid was further reacted with more $Et_2O \cdot BF_3$ in toluene at reflux. Infrared spectra of the resulting product, also shown in Figure 18 and 19, indicated little pyridine (if any at all) was left. At the same time, a weak and broad band at 410 cm^{-1} replaced the bands attributed to the internal modes of the molecular W_6S_8 cluster. It is not clear whether the cluster was still intact or disrupted after the apparent reaction promoted by the enhanced temperature.

CONCLUSIONS

It appears from the work here that thermal deligation of the molecular pyridine adduct of W_6S_8 cluster cannot be complete at the temperatures where the clusters are preserved. At elevated temperature, however, the cluster appears to decompose into disproportionation products. The additions of ternary metal and/or ternary metal chloride is found to have little effect towards promoting the deligation at the temperatures (200°C to 350°C) used in these solid state reactions.

The attempts to remove pyridine ligands by reactions with strong acids in solutions failed to proceed with the preservation of the cluster, W_6S_8. Further studies should include the reductions with active metals in solutions in the hope that ternary tungsten sulfide phases "$M_xW_6S_8$" would be mole stable and easier to obtain.

SUMMARY AND FUTURE WORK

The aim of this dissertation has been to explore the chemistry of hexanuclear tungsten cluster compounds, of which much less was known in the literature compared to the chemistry of hexamolybdenum cluster compounds. Particularly, a rich chemistry has been known for the ternary and binary molybdenum chalcogenides or Chevrel phases, $M_xMo_6Y_8$ and Mo_6Y_8 (M = ternary metal cation; $Y = S, Se$ and Te). However, no such tungsten analogues have ever been synthesized. A great deal of chemistry was discovered and progress was made in this work towards the establishment of the ideal "tungsten Chevrel phases".

The synthetic route chosen in this work was a low temperature one, as the absence of the "tungsten Chevrel phases" is probably attributed to their thermodynamic instability. α-Tungsten(II) chloride, which contains hexatungsten cluster unit $W_6Cl_8{}^{4+}$, was chosen as the starting material based on its structural similarity to the ideal W_6S_8 cluster unit. Although the chemistry of α-tungsten(II) chloride was well-developed, a convenient and relatively efficient synthesis of this compound was not available in the literature. The reduction of tungsten(IV) chloride with metals was studied in this work, and reduction with iron metal at 500°C proved to be a good synthetic method, with a yield of 60% in a reaction period of two or three days.

Sulfidation of α-tungsten chloride or W_6Cl_{12} was studied, with the use of sodium

hydrosulfide and sodium n-butoxide in pyridine. Incomplete and complete sulfidation occurred depending on the amount of sodium hydrosulfide and sodium n-butoxide used. With the stoichiometry of six to eight moles of sodium hydrosulfide per mole of cluster, lightly sulfided cluster with an average composition of approximately $(W_6S_2Cl_6)Cl_2(py)_n$ was obtained as a soluble product from the pyridine solution, while the extensively sulfided cluster like $W_6S_6Cl_2(py)_6$ was obtained as an insoluble powdered product. The compositions given here were deduced from elemental analyses, and were believed to be averaged values of mixture of clusters with differening compositions. Future study of isolation and purification of mixed sulfide-chloride clusters with a single stoichiometry is needed to understand the trends of the entire series, $W_6S_{8-x}Cl_x$.

With the use of an excess amount of sodium hydrosulfide and sodium n-butoxide (for example, twelve moles of sodium hydrosulfide and six moles of sodium n-butoxide per mole of cluster), the completely sulfided cluster $W_6S_8(py)_6$ was synthesized in almost quantitative yield. Through exchange of terminal ligands, $W_6S_8(PEt_3)_6$ and $W_6S_8(THT)_6$ were also established. The substitution of ligands in the terminal positions of the $W_6S_8L_6$ cluster was found to depend upon both the substituting ligand and the leaving ligand. Triethylphosphine was found to coordinate to the W_6S_8 cluster most strongly, while the pyridine and tetrahydrothiophene complexes could be interconverted. These results were supported by the study of the bonding between the cluster and the organic ligands, based upon x-ray structure determinations of these cluster complexes. Further research on ligand exchange reactions would uncover more complexes of the W_6S_8 cluster, of which the weakly-coordinated complexes and soluble complexes are of particularly interest.

In the last part of this work, the removal of the terminal ligands from $W_6S_8(py)_6$ was examined as a method of preparing the "tungsten Chevrel phases" from the potential molecular precursors. At lower temperatures like 250°C and 300°C, the thermal deligation of $W_6S_8(py)_6$ was incomplete as evidenced by elemental analysis. At 640°C, however, cluster disruption occurred as evidenced by the detection of WS_2 in the infrared spectrum. Information of the products of the thermal deligation was still limited as these materials are amorphous to x-ray diffraction. There was evidence from preliminary study by TEM (Transmission Electron Microscopy), however, that some of these material is crystalline to electron diffraction [86]. Further study of the products of the thermal deligation at various temperatures by TEM and SEM (Scanning Electron Microscopy) may be able to clarify questions like whether new phases were produced or at what temperature the cluster disruption occurred. Furthermore, growing single crystals and subsequently studying their structures and electronic structures may uncover interesting chemistry and provide insight into the nature of the intercluster bonding analogous to that found in the Chevrel phases.

It was also found in this work that the addition of lead, aluminum chloride, and zinc and zinc chloride had little effect towards promoting the deligation at the temperatures (200°C to 350°C) used in these solid state reactions. Reactions of acids with $W_6S_8(py)_6$ in solution intended to promote the deligation also failed to produce the ideal binary "tungsten Chevrel phases", W_6S_8. It is possible that acids attack the bridging sulfides of the cluster instead of the terminal ligands. Further study of reductive reactions of the molecular cluster in solution may provide an approach to the ideal ternary "tungsten Chevrel phases", $M_xW_6S_8$.

Finally, reactivity studies intended to remove the terminal ligands from other

molecular complexes of W_6S_8 may be useful, as only $W_6S_8(py)_6$ was studied in this work. With the establishment of more molecular complexes $W_6S_8L_6$, another interesting aspect is the study of controlled deligation. That is, trying to remove only one or two ligands per cluster at a time. The information obtained in such a study may be very useful in developing methods for the complete deligation, as well as providing insight into the nature of intercluster bonding of the cluster units.

REFERENCES

[1] Schäfer, H.; von Schnering, H.G.; Tillack, J.; Kuhnen, K.; Wohrle, H.; Baumann, H. *Z. Anorg. Allgem. Chem.* **1967**, *353*, 287.

[2] Hogue, R.D.; McCarley, R.E. *Inorg. Chem.* **1970**, *6*, 1354.

[3] Yvon, K. In *Current Topics in Materials Science*, 1st ed.; Kaldis, E., Ed.; North-Holland: New York, 1978; Vol. 3, Chapter 2.

[4] Chevrel, R.; Sergent, M. In *Topics in Current Physics*, Fischer, O. and Maple, M.B., Eds.; Springer-Verlag: Heidelberg, 1982; Vol. 32.

[5] Matthias, B.T.; Marezio, M.; Corenzwit, E.; Cooper, A.S.; Barz, H.E. *Science* **1972**, *175*, 1465.

[6] McCarty, K.F.; Schrader, G.L. *Ind. Eng. Chem. Prod. Res. Dev.* **1984**, *23*, 519.

[7] Schöllhorn, R.; Kumpers, M.; Besenhard, J.O. *Mat. Res. Bull.* **1977**, *12*, 781.

[8] Perrin, C.; Sergent, M.; LeTraon, A. *J. Solid State Chem.* **1978**, *25*, 197.

[9] Perrin, C.; Sergent, M. *J. Chem. Res. (M)* **1983**, 449.

[10] Perrin, C.; Potel, M.; Sergent, M. *Acta Crystallogr.* **1983**, *C39*, 415.

[11] (a) Sergent M.; Fischer, O; DeCroux, U.; Perrin, C.; Chevrel, R. *J. Solid State Chem* **1978**, *22*, 87. (b) Perrin, C.; Chevrel, R.; Sergent, M.; Fischer, O. *Mat. Res. Bull.* **1979**, *14*, 1505.

[12] Michel, J.B.; McCarley, R.E. *Inorg. Chem.* **1982**, *21*, 1864.

[13] Michel, J.B. *Ph.D. Dissertation,* Iowa State University, Ames, IA, 1979.

[14] Laughlin, S.K. *M.S. Thesis,* Iowa State University, Ames, IA, 1986.

[15] Spink, D.A. *M.S. Thesis,* Iowa State University, Ames, IA, 1986.

[16] Spink, D.A. *Ph.D. Dissertation,* Iowa State University, Ames, IA, 1989.

[17] McCarley, R.E.; Laughlin, S.K.; Spink, D.A.; Hur, N. *Abstracts of Papers,* 3rd. North American Chemical Congress, Toronto, Ontario, Canada; American Chemical Society: Washington, D.C., 1988, INOR 575.

[18] McCarley, R.E.; Zhang, X.; Spink, D.A.; Hur, N. *Abstracts of Papers,* 199th National Meeting of the American Chemical Society; Boston, MA, 1990.

[19] Saito, T.; Yamamoto, N.; Yamagata, T.; Imoto, H. *J. Am. Chem. Soc.* **1988**, *110,* 1646.

[20] Saito, T.; Yamamoto, N.; Yamamoto, N.; Nagase, T.; Tsuboi, T.; Kobayashi, K.; Yamagata, T.; Imoto, H.; Unouram, K. *Inorg. Chem.* **1990**, *29,* 764.

[21] Chevrel, R.; Sergent, M.; Prigent, J. *J. Solid State Chem.* **1971**, *3,* 515.

[22] Chevrel, R.; Sergent, M.; Prigent, J. *Mat. Res. Bull.* **1974**, *9,* 1487.

[23] Schöllhorn, R.; Kumpers, M.; Plorin, D. *J. Less-Common Metals* **1978**, *58,* 55.

[24] Schöllhorn, R.; Kumpers, M.; Besenhard, J. *Mat. Res. Bull.* **1977**, *12*, 781.

[25] (a) Tarascon, J.M.; DiSalvo, F.J.; Murphy, D.W.; Hull, G.W.; Rietman, E.A.; Waszczak, J.V. *J. Solid State Chem.* **1984**, *54*, 204. (b) Behlok, R.J.; Kullberg, M.L.; Robinson, W.R. *Proceedings, 4th International Conference on Chemistry and Uses of Molybdenum,* Barry, H.F.; Mitchell, P.C.H., Eds.; Climax Molybdenum Co., Ann Arbor, Michigan, 1982, p 23.

[26] Andersen, O.; Klose, W.; Nohl, H. *Phys. Rev. B.* **1978**, *17*, 1209.

[27] Burdett, J.K.; Lin, J-H. *Inorg, Chem.* **1982**, *21*, 5.

[28] Nohl, J.; Klose, W.; Andersen, O. In *Topics in Current Physics;* Fischer, O. and Maple, M.B., Eds.; Springer-Verlag: Heidelberg, 1982; Vol. 32, Chapter 6.

[29] Hughbanks, T.; Hoffmann, R. *J. Am. Chem. Soc.* **1983**, *105*, 1150.

[30] Certain, D.; Lissillour, R. *Z. Phys. D.* **1986**, *3*, 411.

[31] Pauling, L. *Nature of the Chemical Bond,* 3rd.; Cornell University Press: Ithaca, New York, 1960; p 256.

[32] Perrin, A.; Sergent, M.; Fischer,O. *Mat. Res. Bull.* **1978**, *13*, 259.

[33] Perrin, A.; Perrin, C.; sergent, M. *J. Less-Common Metals* **1988**, *137*, 241.

[34] Perrin, C.; Sergent, M. *J. Less-Common Metals* **1986**, *123*, 117.

[35] Hill, J.B. *J. Am. Chem. Soc.* **1916**, *38*, 2383.

[36] Lindner, K. *Ber. dt. Chem. Ges.* **1922**, *55*, 1458.

[37] Lindner, K. *Z. Anorg. Chem.* **1927**, *162*, 203.

[38] Lindner, K.; Kohler, A. *Z. Anorg. Chem.* **1924**, *140*, 357.

[39] Lindner, K.; Hellwig, H. *Z. Anorg. Chem.* **1925**, *142*, 180.

[40] Lindner, K.; Heller, E.H.; Helwig, H. *Z. Anorg. Chem.* **1923**, *130*, 209.

[41] Sheldon, J.C. *Nature* **1959**, *184*, 1210.

[42] Sheldon, J.C. *J. Chem. Soc.* **1960**, 1007.

[43] Sheldon, J.C. *J. Chem. Soc.* **1960**, 3106.

[44] Sheldon, J.C. *J. Chem. Soc.* **1962**, 410.

[45] Mackay, R.A. *Ph.D. Dissertation,* State University of New York at Story Brook, Stony Brook, New York, 1966.

[46] Cotton, F.A.; Wing, R.M.; Zimmerman, R.H. *Inorg. Chem.* **1967**, *6*, 11.

[47] Clark, R.J.H.; Kepert, D.L.; Nyholm, R.J.; Rodley, G.A. *Spectrochim. Acta* **1966**, *22*, 1967.

[48] Hartley, D.; Ware, M.J. *Chem. Commun.* **1967**, 912.

[49] Opalovskii, A.A.; Samoilov, P.O. *Dokl. Akad. Nauk. SSSR* **1957**, *174*, 1109.

[50] Hogue, R.D. *Ph.D. Dissertation,* Iowa State University, Ames, IA, 1968.

[51] Mattes, R. *Z. Anorg. Allg. Chem.* **1968**, *357*, 30.

[52] Brosset, C. *Ark. Kemi. Miner. Geol.* **1945**, *20A*, No. 7.

[53] Brosset, C. *Ark. Kemi. Miner. Geol.* **1946**, *22A*, No. 11.

[54] Schäfer, H.; Schnering, H.G.; Tillack, J.; Kuhnen, F.; Wohrle, H.; Baumann, H. *Z. Anorg. Allg. Chem.* **1967**, *353*, 281.

[55] Siepmann, R.; Schnering, H.G. *Z. Anorg. Chem.* **1968**, *357*, 289.

[56] Brown, T.M. *Ph.D. Dissertation,* Iowa State University, Ames, IA, 1963.

[57] Murray, G.A. *M.S. Thesis,* Iowa State University, Ames, IA, 1965.

[58] Walton, R.A.; Edwards, D.A. *Spectrochim. Acta.* **1968**, *24A*, 833.

[59] Cotton, F.A.; Stanley, G.G. *Chem. Phys. Letters* **1978**, *58*, 450.

[60] McCarley, R.E. *Polyhedron* **1986**, *5*, 51.

[61] Baumann, H.; Plautz, H.; Schäfer, H. J. *Less-Common Metals* **1971**, *24*, 301.

[62] Schäfer, H.; Plautz, H.; Abel, H-J.; Lademann, D. *Z. Anorg. Allg. Chem.* **1985**, *526*, 168.

[63] Nannelli, P.; Block, H.P. *Inorg. Chem.* **1968**, *7*, 2423.

[64] Saito, T,; Nishida, M.; Yamagata, T.; Yamagata, Y.; Yamaguchi, Y. *Inorg. Chem.* **1986**, *25*, 1111.

[65] Lee, S.C.; Holm, R.H. *Angew. Chem. Int. Ed. Engl.* **1990**, *29*, 840.

[66] Hilsenbeck, S.; McCarley, R.E., Department of Chemistry, Iowa State University, unpublished results.

[67] Emeleus. J.; Gutman, V. *J. Chem. Soc.* **1950**, 2115.

[68] Dorman, W.C. *M.S. Thesis,* Iowa State University, Ames, IA, 1972.

[69] McCarley, R.E.; Brown, T.M. *Inorg. Chem.* **1964**, *3,* 1232.

[70] Shäfer, H.; Trenkel, M.; Brendel, C. *Mon. fur Chemie* **1971**, *102,* 1293.

[71] Schaefer, M. *Ph.D. Dissertation,* Iowa State University, Ames, IA, 1971.

[72] Brauer, G. *Handbuch der Preparativen Anorganischen Chemie,* Ferdinand Enke Verlag: Stuttgard, 1975; p 371.

[73] Galbraith Laboratories, Inc., Knoxville, Tennessee.

[74] B.A. Frenz & Associates, INC., College Station, Texas 77840, 1985.

[75] Sheldrick, G.M. In *Crystallographic Computing 3,* Eds., Sheldrick, G.M.; Kruger, C.; Goddard, R. Oxford University Press, 1985, p 175.

[76] *TEXSAN-TEXRAY Structure Analysis Package,* Molecular Structure Corporation, 1985.

[77] Gilmore, C.J. *J. Appl. Cryst.,* **1984**, *17,* 42.

[78] Saito, T; Yoshikawa, A; Yamagata, T.; Imoto, H.; Unoura, K. *Inorg. Chem.* **1989**, *28,* 3588.

[79] (a) Gill, N.S.; Nuttall, R.H.; Scaite, D.E.; Sharp, D.W. *J. Inorg. Nucl. Chem.* **1961**, *18,* p 79. (b) Thornton, D.A. *Coord. Chem. Rev.* **1990** *104,* 251.

[80] Foulds, G.A.; Hodgson, J.B.; Hutton, A.T.; Niven, M.L.; Percy, G.C.; Thornton, D.A. *Spectrosc. Lett.* **1979**, *12,* 25.

[81] (a) Goggin, P.J.; Goodfellow, R.J. *J. Chem. Soc.* **1966**, 1462. (b) Shobatake, K.; Nakamoto, K. *J. Am. Chem. Soc.* **1970**, *92*, 3332.

[82] Lewis, J.; Miller, J.R.; Richards, R.L.; Thompson, A. *J. Chem. Soc.* **1965**, 5850.

[83] Saito, T.; Manabe, H.; Yamagata, T.; Imoto, H. *Inorg. Chem.* **1987**, *26*, 1362.

[84] Tarascon, J.M; DiSalvo, F.J.; Chen, C.H.; Carrol, P.J.; Walsh, M.; Rupp, L. *J. Solid State Chem.* **1985**, *58*, 290.

[85] Goldman, A., Department of Physics, Iowa State University, private communication.

[86] Zhang, X.; McCarley, R.E., Department of Chemistry, Iowa State University, unpublished results.

ACKNOWLEDGEMENTS

I would like to express my sincere thanks to Professor Robert E. McCarley, for his guidance, enthusiasm and patience during the course of this research project, as well as his understanding, support and encouragement which helped me through many difficult times during my years at Iowa State.

I would like to thank members of this research group, from whom I learned a lot and with whom I had a lot of fun. I would also like to thank all of the professors and staff members at ISU and Ames Lab who assisted me with the various physical measurements reported in this dissertation, especially Dr. Lee M. Daniels and Professor Robert A. Jacobson for their valuable assistances in the x-ray single crystal structure determinations. I would like to take this opportunity to thank all the members of my committee.

I am grateful to the people that I have encountered and called friend throughout my stay here. I learned from them what friendship is really all about.

My deepest appreciation goes to my fiancee Jin Qian, for her love, encouragement and support. Finally, I would like to dedicate this dissertation to my parents. They not only raised me, but also had provided me the best environment of learning and education I could possibly get. Although they are tens of thousands of miles away from me at the other side of the earth, their love and encouragement have always

been nearby throughout my entire period of graduate study.

This work was supported by the U.S. Department of Energy (DOE Report IS-T-1392) under Contract W-7405-eng-82 and in part by a grant (CHE-8406822) from the National Science Foundation.